Plasticity of Dopamine-Releasing Central Brain Neurons Underlying Adaptational Feeding-Related Behavior in *Drosophila Melanogaster*

Dissertation

for the award of the degree

"Doctor rerum naturalium"

of the Georg-August-Universität Göttingen

within the doctoral program (Sensory and Motor Neuroscience)

of the Göttingen Graduate School for Neurosciences, Biophysics, and Molecular Biosciences (GGNB)

submitted by

Büşra Çoban-Poppinga

from

Gümüshane, Turkey

Göttingen 2020

PhD Committee Members:

Prof. Dr. André Fiala (Supervisor, Reviewer)
Dept. of Molecular Neurobiology of Behavior, Georg-August-University, Göttingen

Prof. Dr. Martin Göpfert (Reviewer)
Dept. of Cellular Neurobiology, Georg-August-University, Göttingen

Prof. Dr. Thomas Dresbach, PhD
Dept. of Anatomy and Embryology, University Medical Center, Göttingen

Members of the Examination Board:

Prof. Dr. André Fiala (Supervisor, Reviewer)
Dept. of Molecular Neurobiology of Behavior, Georg-August-University, Göttingen

Prof. Dr. Martin Göpfert (Reviewer)
Dept. of Cellular Neurobiology, Georg-August-University, Göttingen

Prof. Dr. Thomas Dresbach, PhD
Dept. of Anatomy and Embryology, University Medical Center, Göttingen

Additional Members of the Examination Board:

Dr. Jan Clemens
Neuronal Computation and Behavior, European Neuroscience Institute Göttingen (ENI), Göttingen

Prof. Dr. Carolin Wichmann
Molecular Architecture of Synapses Group Center for Biostructural Imaging of Neurodegeneration (BIN)
Institute for Auditory Neuroscience & Inner Ear Lab, University Medical Center, Göttingen

Prof. Dr. Ralf Heinrich
Dept. of Cellular Neurobiology, Georg-August-University, Göttingen

Thesis submission: February 21st, 2020

Dissertation: April 21st, 2020

Declaration of academic honesty:

I hereby declare that the doctoral thesis entitled "Plasticity of Dopamine-Releasing Central Brain Neurons Underlying Adaptational Feeding-Related Behavior in *Drosophila Melanogaster*" has been written independently and with no other sources and aids than quoted within the text, references and acknowledgements.

Büşra Çoban-Poppinga

Göttingen, February 21st, 2020

…dedicated to my soul mate and eternal love ***Haiko Poppinga***

Table of Contents

1 Introduction

1.1 Adaptation to internal states

Are the conditions of an environment the factors that make it habitable? Or is it the ability to adapt to a habitat that makes survival possible?

All conditions in a natural system are destined to change due to the constant flow of energy. Organisms living under these constantly changing conditions must adapt to these changes and, ultimately, have evolved an ability to adapt to survive. Hence, adaptation at various levels is one key component of the existence of an organism.

Natural selection has grinded basic mechanisms of adaptation in the nervous systems of animals. These mechanisms underlie behavioral strategies that depend on external and internal conditions in a similar and conserved way among animals (Hochachka and Somero, 2002; Symons, 1990).

Energy, i.e., food, is the "currency" for survival in all animals. Therefore, foraging and feeding behavior is one of the most prominent and indispensable behaviors under dynamic internal and external conditions (Biro and Stamps, 2010; Careau et al., 2008; Mobbs et al., 2018; Scholz et al., 2017).

This study aims at understanding mechanisms of the nervous system underpinning the adaptation to these dynamic conditions. As one pronounced adaptive behavior, feeding-related behavior was chosen as the subject of the study. Structural and functional adjustments in neuronal circuits leading to behavioral modifications are investigated using experimental, parametric changes in food conditions.

1.2 *Drosophila* as a model organism to study adaptation

In order to investigate behavioral and neuronal circuit adaptations, *Drosophila melanogaster* is used as a model organism in this study for numerous reasons. The first reason is the simple handling of *Drosophila.* Easy maintenance and handling of flies are advantageous when the behavioral read-out is tested. A large number of behaviors can be tested reliably and under changing food conditions,

including relatively complex, motivation-based behaviors (e.g. Edgecomb et al., 1994; Ja et al., 2007; Krashes et al., 2009; Tully and Quinn, 1985).

In fact, flies exhibit specific behavioral alterations based on the internal hunger state (the "hunger/satiation state" of the animal will be referred to as "internal state" in this study throughout). For instance, hunger causes robust alterations in state-dependent behaviors such as associative olfactory short- and long-term memory formation (Krashes and Waddell, 2008; Tempel et al., 1983), food uptake (Ja et al., 2007), proboscis extension reflex (PER; Dethier, 1976; Wang et al., 2004) or odor tracking (Root et al., 2011; Sayin et al., 2019).

However, the most important reasons making *Drosophila* suitable for this study are explained in detail in the following sections, i.e., the wide range of genetic tools and the evolutionary conservation of the mechanisms underlying feeding.

1.2.1 Evolutionarily conserved mechanisms of the modulation of internal states

The internal state of an animal is to a large degree regulated by the release of neuromodulators (Destexhe and Marder, 2004). The majority of these neuromodulators and their working principles are highly conserved. The peptide insulin is one example. Insulin is a highly conserved metabolic signal that regulates carbohydrate uptake of cells, but affects also behavior. It promotes food uptake in both vertebrates and *Drosophila* (Brogiolo et al., 2001; Rulifson et al., 2002). *Drosophila* insulin-like peptides (DILPs) are considered to be equivalents of the mammalian insulin (Brogiolo et al., 2001). A second example is norepinephrine (NE) in mammals and its *Drosophila* ortholog octopamine (OA). These neuromodulators convey information about the sweet taste and the nutritious value of sugar in a similar way from the gustatory sensory system and gustatory tract, respectively (Youn et al., 2018). They also influence the energy homeostasis through similar mechanisms (Berridge and Waterhouse, 2003; LeDue et al., 2016; Wang et al., 2004; Youn et al., 2018). As a final example, Neuropeptide Y (NPY) release promotes feeding in mammals (Barsh and Schwartz, 2002; Brown et al., 1999) in the same way as two homologs in *Drosophila*, neuropeptide F (NPF) and short neuropeptide F (sNPF) (Lee et al., 2004; Wu et al., 2003) do. Sensory processing is also adjusted in similar ways between rodents and *Drosophila* as a more peripheral step of a state-dependent behavioral modulation. For instance, hungry flies exhibit less sensitivity to repulsive odors as well as higher sensitivity to attractive odors (Krashes et al., 2009; Root et al., 2011; Ko et al., 2015). The sensitization/desensitization to different odors is also

observed in rodents (Murakami et al., 2005). Such state-dependent sensory adjustments are achieved by, e.g., a change in excitability of the olfactory receptor neurons (ORNs) through certain neuromodulators, including dopamine (DA) in both *Drosophila* and in vertebrates (Krashes et al., 2009; Root et al., 2011; Ko et al., 2015; Murakami et al., 2005). In conclusion, *Drosophila* is a suitable model organism when the evolutionary conservation between insects and vertebrates are taken into account. Additionally, *Drosophila* has a relatively compact nervous system compared to that of vertebrates. Thus, investigating the mechanisms of adaptations in *Drosophila* can provide a more straightforward understanding about how these adaptations occur.

1.2.2 Binary gene expression systems as a main approach

Despite of the fact that *Drosophila* have far fewer neurons when compared to vertebrates, they are capable of performing complex cognitive behaviors - such as learning and memory (Heisenberg, 2003; Hige, 2018; Pitman et al., 2009; Wolf et al., 1998). This ability is perhaps a result of the comparably more compact structuring in the brain, i.e., the circuitries involved in complex behaviors contain typically much smaller numbers of neurons. Even a single neuron in the *Drosophila* brain can orchestrate a complex behavior (Alekseyenko et al., 2013; Mann et al., 2013). Thus, almost each neuron in the central nervous system (CNS) of a fly can be individually identified and can be genetically targeted (Givon and Lazar, 2016; Shinomiya et al., 2011; Ukani et al., 2019). For that purpose, genetic tools can be utilized in *Drosophila* to label specific neuronal populations and to restrict the expression of certain genes spatially and temporally.

In order to express different genes explicitly in certain neurons, binary gene expression systems are typically used. In these systems, a cell specific promoter sequence is fused with a transcription factor (TF; transgenic “driver line”) that recognizes a specific sequence fused. The recognition sequence is expressed in a second fly, and it is fused with a desired genetic tool (“effector line”). Driver and effector transgenes become combined in one animal simply by crossing two transgene-containing animals and by collecting the filial generation. Upon this combination, restricted TF expression in the desired cell population drives the expression of the transgene. Thus, the expression of the genetic tool is restricted to, for example, particular neurons. Thereby, the generation of huge numbers of transgenic animals that contain different driver/effector combinations is not required.

The most common binary system used in *Drosophila* genetics, and also in this study, is the Gal4/UAS system (Brand and Perrimon, 1993; Fischer et al., 1988; Figure 1.1). In this system, spatial expression is achieved by the cell specific "driver" DNA sequence fused with a Gal4 sequence. The desired genetic tool is fused with the target sequence of Gal4, UAS (upstream activating sequence). As this binary system makes use of genes from yeast which are artificially implemented in the fly genome, the Gal4 expression does not target any other DNA sequence in the fly genome.

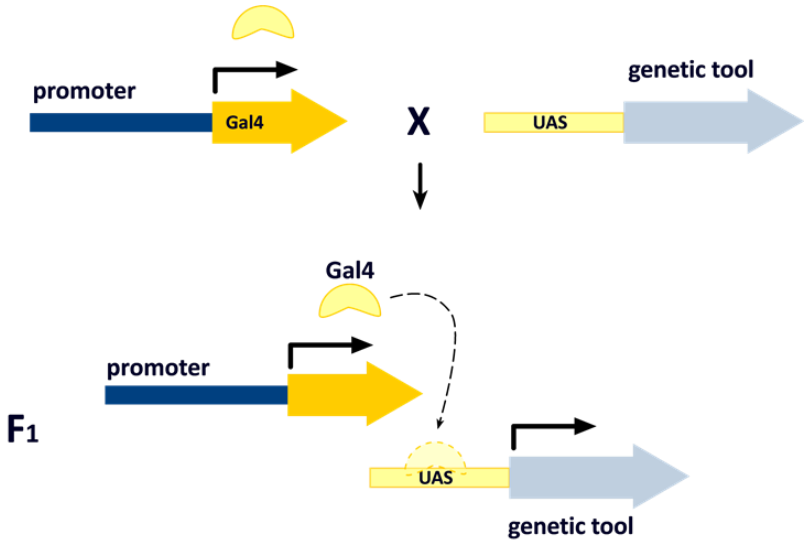

Figure 1.1 Working principle of the Gal4/UAS binary system. A cell-specific promoter fused with Gal4, and the Gal4 binding site (UAS) fused with genetic tool of choice are depicted. These genetic constructs are brought together in the F_1 generation of the crossed flies. The expression of Gal4 drives the expression of the interested genetic tool of inteerst in a cell specific manner.

There are two alternative, but similar binary gene expression systems, LexA/LexAop (Lai and Lee, 2006) and QF/QUAS (Potter et al., 2010). The working principle of these binary systems is the same as Gal4/UAS system. The combination of these alternative systems in one animal allows one to manipulate or visualize multiple separated cells independently.

1.2.3 Genetic tools to manipulate specific cell types in the brain

Drosophila is an extremely advantageous model organism because of the sophisticated techniques with which genetically modified animals can be created and the many tools with which neurons can be manipulated or visualized. Thanks to the small chromosome number (four) of *Drosophila* and the fact that the genome is entirely mapped, genetic tools can be relatively routinely implemented in the *Drosophila* (Rubin, 1985; del Valle Rodríguez et al., 2012). In recent years, genetic tools have been established that can be temporally switched on or off by heat or light (i.e., thermogenetic and

optogenetic tools, respectively) (Bernstein et al., 2012; Govorunova et al., 2015). These temporally restricted, reversible experimental modulations of neuronal activity allow drawing correlations between neuronal activity and a behavior. This approach is also employed in this study.

Genetic tools to inhibit neuronal activity or neuronal transmission that are utilized in this study, are, e.g., shibire^{ts} (Shi^{ts}) and gtACRI as a thermogenetic and optogenetic tool, respectively. Shibire^{ts} is a dominant negative mutant form of the *Drosophila* dynamin protein that is involved in vesicle recycling (Grigliatti et al., 1973). This mutant form is temperature-sensitive: If the temperature increases above 28°C, the mutant form of dynamin undergoes a conformational change such that the endocytosis of released vesicles is impaired. This situation leads to a block of further vesicle release (van der Bliek and Meyerowrtz, 1991; Grigliatti et al., 1973; Kitamoto, 2001). In this study, this tool is used to block synaptic output of a desired neuronal population during a behavioral experiment. Another inhibitory tool used in this study is the light-inducible anion channel g*t*ACRI. gtACR is an anion channel discovered in the alga *Guillardia theta* and it is largely Cl^- conductive (Govorunova et al., 2015). Light induction inhibits neuronal activity by hyperpolarizing the membrane potential (Govorunova et al., 2015; Mohammad et al., 2017). g*t*ACRI is utilized in this study as an inhibitory tool in order to eliminate any effect of high temperatures on behavior or possible leaky function of thermogenetic tools below 25°C.

In order to artificially activate neurons of interest in the behavioral experiments, two optogenetic tools are utilized, i.e., channelrhodopsin XXL (ChR-XXL) and csChrimson (Dawydow et al., 2014; Klapoetke et al., 2014). These two channelrhodopsins are light-sensitive cation channels that open upon light stimulation, which results in depolarization of the cell membranes (Dawydow et al., 2014; Klapoetke et al., 2014). ChR-XXL is a modified version of channelrhodopsin-2 (ChR-2). Even very low intensity of blue light is sufficient to evoke membrane depolarization and synaptic transmission (Dawydow et al., 2014; Nagel et al., 2003). CsChrimson, which is used as an additional excitatory optogenetic tool, is another artificial form which has a red-shifted activation spectrum (Klapoetke et al., 2014).

The final optogenetic tool employed in this study is a light-inducible adenylate cyclase called bPAC (Stierl et al., 2011). Activation of bPAC with blue light enables one to elevate the cyclic AMP (cAMP) level in the targeted cell. This tool is used to manipulate cAMP-dependent signaling rather than directly depolarize the cells.

1.2.4 Genetic tools to analyze structural synaptic plasticity

Beside the temporal and spatial manipulation of cell activity, *Drosophila* offers a variety of genetic tools to visualize and characterize the structure of neurons. Such tools are also utilized in this study to analyze how the structure of neurons of interest are modulated in dependence of external and internal conditions.

The most common strategy to visualize cells in *Drosophila* relies on a restricted expression of a fluorescent reporter protein such as GFP using the binary Gal4/UAS system (Yeh et al., 1995). This basic method allows us to visualize neurons and quantify the cellular structures such as branch numbers, volume, etc. However, concerning the structural analysis of a densely packed neuronal population, much more sophisticated tools for visualization are necessary.

Synaptically localized protein-fused reporters are employed for further characterization of the neurons and structurally modified synaptic sites. For instance, the dendritic trees of a neuronal population, can be visualized via a powerful tool called DenMark (Dendritic Marker) (Nicolaï et al., 2010). This tool is based on the expression of a dendritically localized mCherry reporter protein.

Similar to DenMark, many synaptically localized reporter proteins are created by fusing a reporter protein with either a complete or a short form of selected synaptic proteins. For instance, a GFP reporter fused with presynaptically localized proteins such as sytGFP or Brp-GFP can be expressed in the target neuron population (Wagh et al., 2006; Zhang et al., 2002). Likewise, the characterization of the postsynaptic arborizations can also be performed by the expression of reporter-fused postsynaptic proteins like Shank-GFP or dlg-GFP in the desired neurons (Harris et al., 2016; Zhang et al., 2007). The change in fluorescence levels in these type of reporters are often interpreted as synaptic structural modifications (Albertson and Doe, 2003; Gilestro et al., 2009; Hering and Sheng, 2003; Roy et al., 2007). In this study these tools are also employed as a means to investigate structural modifications at the subcellular level.

Most of these tools to characterize and analyze structural changes of the cells are based on a reporter in the entire cells or the neurites. However, when measuring structural synaptic plasticity in crowded neuronal populations such as dopaminergic neurons (DANs), as it is done in this study, one faces the

problem that fine axonal and dendritic arborizations cannot be disentangled. Thus, fine and small modifications can be masked. To overcome this obstacle, an elegant technique to visualize potential synaptic sites can be used. This technique is based on the reconstitution of splitGFP fragments (spGFP) and is typically referred to as GRASP (GFP Reconstitution Across Synaptic Partners) (Pech et al., 2013; Feinberg et al., 2008; Gordon and Scott, 2009). The two fragments of GFP (splitGFP) are expressed in complementary neuronal populations and localized extracellularly at the membranes. Thereby, GFP reconstitution occurs upon close proximity of two neurons, which might be indicative of synaptic connections. However, since this too, reports proximity only and does not necessarily proof the presence of synaptic sites, these reconstitution points are referred to as "potential synaptic sites".

1.2.5 Genetic tools to analyze functional neuronal activity and plasticity

As final genetic tool category, functional indicators provide a possibility to monitor the activity, i.e., membrane excitation, of the desired neuron population in *Drosophila*.

Real-time activity measurement;

The first technique used here is often referred to as Ca^{2+} imaging. It is based on the increase in fluorescence emission of a genetically encoded calcium indicator (GECI) upon Ca^{2+} rise in the cell upon membrane excitation. The most common Ca^{2+} indicator, also commonly used in *Drosophila* research, is called GCaMP (Hancock et al., 2019; Zariwala et al., 2012). GCaMP is a calmodulin-fused GFP reporter which undergoes a conformational change resulting from a rise in intracellular Ca^{2+} concentration following depolarization (Tian et al., 2009).

Imaging of the cellular activity can also be confined to synaptic sites and differentiated as pre- and postsynaptic activity by the restriction of GCaMP localization (Pech et al., 2015). This restriction can be achieved through the same logic as used for synaptically expressed reporter proteins. Two examples of pre- and postsynaptic Ca^{2+} indicators are Syp-GCamP3 and dHomer-GCaMP3, respectively (Pech et al., 2015). In this type of functional imaging, real time activity of Ca^{2+} indicators are visualized *in vivo* upon the presentation of a sensory stimulus to a tethered animal (Hancock et al., 2019).

Transcription-based activity measurement;

Alternatively, a transcription-based reporter expression, which depends on the activity of the cell, can also be used as a "cumulative activity" indicator. One of the intracellular Ca^{2+} reporter based on

transcription, and presumably resulting from neuronal activity, is called CaLexA (Masuyama et al., 2012). This technique is based on GFP transcription upon the transportation of a Ca^{2+}-responsive transcription factor into the nucleus (Masuyama et al., 2012). When the Ca^{2+} level increases in the cell, it drives the expression of GFP. Thus, the GFP level increases over time in a cumulative way. In this study this tool is used to measure slow physiological changes over time and neuronal activity *ex vivo*. These tools are employed in this study to correlate functional adaptations with experience-based structural neuronal changes.

1.3 Behavioral adaptations of *Drosophila* dependent on the internal state

This study is dedicated to investigate neuronal plasticity in the brain dependent on changes in the environmental conditions and, as a consequence, internal states. Experimentally, parametric changes in the food conditions are used as an instrument to determine changing environmental conditions (Toates, 1986; Lee et al., 2004; Pool and Scott, 2014; Wang et al., 2016). Any adaptation to changes in nutrient amount starts with a modulation of the internal state of the animals. Therefore, modulations in feeding- and foraging-related behaviors are explained in the following chapter.

1.3.1 Adjustments of feeding-related behavior in flies

Hunger as an internal state provides a strong drive for *Drosophila,* as it is the case for most animals, to initiate or change feeding-related behaviors such as foraging. Since foraging represents a complex set of behaviors that are costly in terms of energy, the hunger state ensures that animals seek for food only when needed (Toates, 1986). Thus, the foraging behaviors of the flies are tightly regulated by the internal state.

The first step of foraging behavior can start with sensory stimulation. The olfactory system and the sensitivity to external stimuli are bidirectionally tuned by hunger such that odor aversiveness is suppressed parallel to an increase in attractiveness of food related smells (Dethier and Chadwick, 1948; Ko et al., 2015; Pitman et al., 2009; Root et al., 2011). Additionally, the flies persist to follow the sensory cues over long distances when motivated by hunger (Álvarez-Salvado et al., 2018; Root et al., 2011; Sayin et al., 2019). An increase in odor attractiveness is promoted by the activity increase in certain olfactory receptor neurons (ORN), mediated by sNPF release, while dampening the ORN activities for

aversive odors is facilitated by the release of the neuropeptide tachykinin (Ko et al., 2015; Root et al., 2011).

Flies also show hyperactivity and increased locomotor behaviors upon starvation or calorie restriction in the dietary (Browne and Evans, 1960; Dietrich et al., 2015; Koon and Budnik, 2012; Lee et al., 2004; Yang et al., 2015). Increase in locomotion dependent on the hunger state of the flies supposedly promotes foraging behavior.

As a final step of foraging behavior, the flies can actively adjust eating behavior dependent on the internal states. It is no surprise that an increase in food consumption as well as the proboscis extension reflex (referred to as "PER" in this study) is correlated with an increased starvation period of the flies (Edgecomb et al., 1994). Additionally, flies can demonstrate nutrient-specific choices. For instance, the preference to protein-based foods is increased when flies are deprived of amino acids (Ribeiro and Dickson, 2010; Vargas et al., 2010). Similarly, female flies tend to eat more protein-rich food if mated, whereas unmated flies consume more carbohydrates (Lee et al., 2013).

In addition to foraging behavior, *Drosophila* can also adjust a variety of behaviors that are more directly related to food uptake in order to improve survival and fitness, or even the development and survival of future generations (Lihoreau et al., 2016; Yang et al., 2008). For instance, mated female flies prefer to feed on protein-rich food. However, they actively choose an oviposition site and prefer to lay egg on carbohydrate-rich food. Therefore, a female fly has to "calculate" a tradeoff between its own fitness and the development of the future generations (Lihoreau et al., 2016; Yang et al., 2008). Moreover, one very essential behavior regulated by the internal state, is sleep. Sleep and feeding behaviors are also mutually exclusive. The alertness of the flies is promoted and sleep is delayed upon the release of the hunger signaling neuropeptide NPF (Chung et al., 2017; McDonald and Keene, 2010). And a perhaps more abstract example is a report that the risk tolerance of flies is also increased upon starvation (Sih, 1980).

All of these behaviors exemplify that the internal state of flies is tightly regulated and that a great number of complex behaviors depend on these regulations. In this study, a potential adaptation of foraging- and the feeding-related behaviors based on the long-term experience of dietary conditions is analyzed. The rationale behind this approach is outlined in the following chapter.

1.4 Neuromodulation of an internal state and behavior in *Drosophila*

Internal states, modifying foraging behaviors are often achieved by the release of neuromodulators (Bargmann, 2012; Marder, 2012). This modulation determining the internal state generates alternative responses to the same stimuli (Ko et al., 2015). The majority of these neuromodulators are evolutionary conserved neuropeptides (Bargmann, 2012; Marder, 2012). A small part of hunger- and satiation-signaling neuromodulators is listed below. Besides, the role of these neuromodulators in feeding-related behaviors is also explained briefly.

The first and one of the most conserved internal state-signaling neuropeptides that regulates feeding is the insulin peptide. The fly equivalent of insulin is called *Drosophila* insulin like peptide (DILP), which promotes feeding and food seeking behavior (Jourjine et al., 2016; Ko et al., 2015; Root et al., 2011; Tsao et al., 2018). Adipokinetic Hormone (AKH) is another starvation-signaling hormone that is functionally analogous to mammalian glucagon. Starvation induces the release for this hormone, thus signaling hunger state. AKH and DILP work in a mutually inhibitory way (Buch et al., 2008; Inagaki et al., 2014; Jourjine et al., 2016). Additionally, the flies have two equivalents of neuropeptide Y (NPY) which also act as hunger signaling neuromodulators, i.e., NPF and sNPF. Beside the well-described promotion of hunger-driven food seeking behaviors, NPF-releasing neurons also enhance associative sugar-odor memories that are formed only in food-deprived flies (Brown et al., 1999; Krashes et al., 2007, 2009). Similarly, sNPF modulates various hunger-driven behavioral components such as the sensitivity to food odors as well as feeding itself (Inagaki et al., 2014; Root et al., 2011). As the final example for a hunger signaling neuropeptide, SIFamide (SIFa) peptide can be named. Neuronal activity of SIFa-releasing cells is elevated upon starvation (Martelli et al., 2017).

Further satiation-signaling neuropeptides are hugin and leukokinin (LK). Elevated *hugin* mRNA level has been observed in fed flies (Melcher and Pankratz, 2005; Schoofs et al., 2014). Likewise, the activation of LK-releasing neurons results in a decrease in food uptake (Al-Anzi et al., 2010; Zandawala et al., 2018). Finally, allatostatin A (AstA), a satiation-mediating neuropeptide, also regulates state-dependent foraging behavior (Hergarden et al., 2012).

Overall, the examples listed above show already a huge network of neurons communicating and regulating foraging and related behaviors in *Drosophila.* This network encompasses the entire brain of

the fly. In this study, experience-dependent structural changes in modulatory neurons that innervate the mushroom bodies (MB) of the central brain are analyzed. The main reason why the MB-related neurons are the central subject of analysis here is discussed in the following chapters in detail.

1.5 Role of mushroom body-extrinsic neurons in motivation-driven behaviors

The MB is a higher brain center in all insects, including D*rosophila* (Strausfeld et al., 1998). A huge number of studies has demonstrated roles of the MB in a wide range of experience-dependent, adaptive behaviors in *Drosophila,* such as olfactory learning and aspects of it, e.g., acquisition, stabilization and retrieval of associative memory (Dubnau et al., 2001; Krashes et al., 2007; McGuire et al., 2001; Schwaerzel et al., 2002; Waddell et al., 2000). Control of locomotor activity, sleep regulation, complex forms of visual learning, and courtship conditioning are also among the roles of the MB in experience-dependent behavioral adjustments (Joiner et al., 2006; Keleman et al., 2007; Liu et al., 1999; Martin et al., 1998; McBride et al., 1999; Pitman et al., 2006; Tang and Guo, 2001).

Beside well-documented roles of the MB in sensory integration, recent studies demonstrated that the MB and MB-extrinsic neurons are also involved in state-dependent food seeking behavior – even the regulation of fat storage as a result of the food intake (Al-Anzi and Zinn, 2018; Sayin et al., 2019; Tsao et al., 2018). Therefore, the MB and MB-related modulatory neurons are introduced.

1.5.1 The mushroom body as a sensory integration and behavior-instructing brain circuit

The MB is a higher order neuropil implicated in the processing and integration of information from several sensory modalities. For instance, the MB is required for olfactory and gustatory memory formation (Brembs and Wiener, 2006; Davis, 1993; Heisenberg et al., 1985; Liu et al., 1999). It is also involved in processing visual cues (Brembs and Wiener, 2006; Liu et al., 1999; Martelli et al., 2017). Sensory information, evaluating information and information about the animal's internal state converge onto the MB. This sensory information is processed in a way that the innate preference of the animal is shaped according to changing environment or internal state (Cohn et al., 2015; Kim et al., 2017; Krashes et al., 2009; Lewis et al., 2015; Owald et al., 2015; Tsao et al., 2018).

The adult *Drosophila* MB consists of ~2000-2500 intrinsic Kenyon cells (KCs) per hemisphere (Aso et al., 2009; Technau and Heisenberg, 1982). Three types of KCs form three different lobes (Crittenden et al., 1998; Technau, 1984; Technau and Heisenberg, 1982) called γ, α'/β', and α/β lobes (Figure 1.2, Figure 3.4B). These lobes are further divided into compartments that can be distinguished with the help of antibody stainings (Aso et al., 2014a). The compartments of each lobe are numbered according to the proximity of MB peduncle, i.e. α1, α2, α3, β1 and β2, etc.. Each compartment is functionally differentiated (Figure 3.4B; Aso et al., 2014b; Cognigni et al., 2018; Cohn et al., 2015). For instance, the proximal lobes integrate aversive, punishment-mediating modulatory inputs, whereas distal lobes process rewarding cues like sugar or water, dependent on the internal state (Waddell, 2016). Valence-based input is encoded by distinct classes of modulatory, dopaminergic neurons (DANs), each of which innervates the lobes in a particular compartment of the MB lobes. Thereby, this valence-based, i.e., punitive or rewarding information is integrated with the sensory representation at the level of KC axons (Cognigni et al., 2018; Cohn et al., 2015, Figure 1.2B).

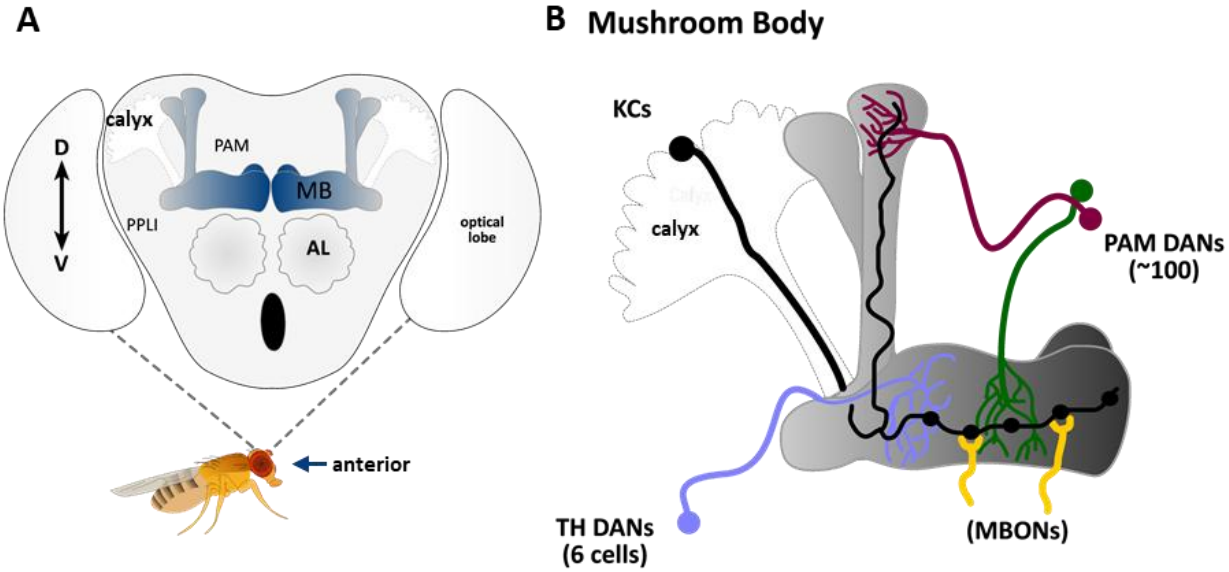

Figure 1.1 Schematic illustrations of a *Drosophila* brain and the MB. **A** Sketch of the *Drosophila* brain from an anterior view (Dorsal-Ventral, D-V, direction is also shown). The MB lobes are illustrated in blue. The lobes of the MB are more anterior located than the calyx. The primary projection area of olfactory receptor neurons are the antennal lobes (AL). The major populations of dopaminergic neurons (DANs) are located in the protocerebral posterior lateral (PPL) and protocerebral anterior medial (PAM) regions. **B** Sketch of a MB and MB-extrinsic neurons. The intrinsic MB neurons (Kenyon cells, KCs) receive sensory information in the calyx region. This information is integrated in the MB lobes with the valence of a stimulus or an internal state, signaled by the DANs. Two major DAN population, PAM and PPL-I DANs, are shown which innervate the lobes at distinct locations called axonal compartments. Not all types of DANs are depicted for simplicity. Finally, the information is integrated by mushroom body output neurons (MBONs) that instruct the execution of appropriate behavior.

Foraging behavior is often initiated by an olfactory sensory cue. Because of the MB's role in olfactory processing the MB-extrinsic neurons are also in the focus in the context of odor-guided foraging behaviors (Heisenberg et al., 1985; McGuire et al., 2001). Olfactory information from receptor neurons is picked up by olfactory projection neurons (PNs) in the antennal lobe (AL) (Gao et al., 2000; Vosshall, 2000). PNs convey the olfactory information further to two neuropils; the lateral horn (LH) and the MB calyx where the dendritic tree of intrinsic MB neurons (Kenyon cells, KCs) arborize (Laissue and Vosshall, 2008). Unlike the MB, the LH is believed to mediate innate responses to odors (Dolan et al., 2019). At the MB level, KCs integrate the olfactory information in terms of a "sparse code" (Campbell et al., 2013). This means that the KCs are more selective, and an overlap of odor representation is decreased a minimum at the MB level. The execution of the corresponding odor-driven behavior based on experience is achieved by the MB output neurons' (MBONs) activity. 21 different types of MBONs innervate 15 different compartments of the MB (Aso et al., 2014b; Tanaka et al., 2008). Each MBON is responsible for distinct behaviors, e.g., avoidance or approach behavior, based on integrated and modulated information at the level of KCs (Figure 1.2B, Aso et al., 2014b). This study focuses on experience-based, long term structural changes in DANs innervating the MB lobes.

1.5.2 Mushroom body-extrinsic dopaminergic neurons encode valence and adjust behavior

In the process of experience-dependent information integration, DANs provide a signal of valence (Burke et al., 2012; Huetteroth et al., 2015; Liu et al., 2012; Waddell, 2013). I reasoned that experience-dependent modulation of the corresponding behaviors should also be modulated in the long run by MB-related DANs. Therefore, structural changes of the DANs are investigated based on the long-term experience of external conditions as a mechanism to modulate the adaptive corresponding behaviors.

There are eight different DAN classes residing in distinct regions of the *Drosophila* brain (Mao and Davis, 2009). Two major DAN populations that provide reinforcement in the MB is PAM DANs and PPL1 DANs (Mao and Davis, 2009; Pech et al., 2013). The majority of the PAM DANs encode rewarding valence of a stimulus (Aso et al., 2010, 2012) whereas a small majority of them together with the PPL1 DANs encode aversive valence (Aso et al., 2010; Burke et al., 2012; Liu et al., 2012). These distinct sets of DANs encode either reward or punishment signals and project to complementary compartments of the MB (Burke et al., 2012; Cohn et al., 2015; Liu et al., 2012; Mao and Davis, 2009).

In associative learning, the temporal coincidence of the activity of a specific set of DANs with an odor stimulus yields in appetitive or aversive memory formation, based on the valence that is encoded by the respective DAN population. For instance, pairing an odor presentation with the γ1 or γ2-innervating DAN activation results in a aversive memory formation while a γ5 DAN activation with an odor presentation drives appetitive memory formation (Aso et al., 2012; Hige et al., 2015; Huetteroth et al., 2015).

Based on the activity of a specific subtype of DANs, the activity of corresponding MBON(s) that picks up the information from the identical compartment is modulated and the approach or the avoidance behavior is executed (Claridge-Chang et al., 2009; Owald et al., 2015). The reinforcement of the DANs can be mimicked by artificial activation of these DANs and similar memory formation or behavioral read-out can be induced (Aso et al., 2010; Burke et al., 2012; Claridge-Chang et al., 2009; Liu et al., 2012; Perisse et al., 2013; Schroll et al., 2006).

Whereas the roles of DANs and the entire MBs in associative olfactory learning are understood to a fair degree, additional roles of the MB are much less understood. One of the less-understood behavioral functions is the control of feeding and food uptake, and the modulation of this behavior as a result of experience. The involvement of the MB-extrinsic DANs in motivational control of foraging-related behaviors will be introduced in the following.

It has been known that 2 different subsets of DANs convey information onto MB about the sweetness and nutritional value of sugar (Burke and Waddell, 2011; Fujita and Tanimura, 2011; Huetteroth et al., 2015). Very recently, additional studies also demonstrated a direct involvement of the MB and related DANs in this foraging behavior and its adjustments based on the internal state (Chia and Scott, 2020; Sayin et al., 2019; Tsao et al., 2018). Not surprisingly, three of these recent studies show that DANs are involved in state-dependent food seeking behavior via communicating with hunger- or satiety signaling neuropeptides (Krashes et al., 2009; Sayin et al., 2019; Tsao et al., 2018). Activation or suppression of six different DAN populations appear to convey information about the internal metabolic state, thereby leading to an enhancement of foraging behavior (Tsao et al., 2018). Each of these DAN populations communicate with a different set of satiation- or hunger-signaling neuropeptides, such as insulin, AstA, sNPF, etc. Interestingly, these DANs appear to convey information also to the MB, where this signal is integrated with sensory cues, and which leads to food seeking behavior. According to recent studies, five out of 21 MBONs are involved in the circuitry underlying food seeking and corresponding behaviors

(Tsao et al., 2018). A direct involvement of these DANs are corroborated by manipulation of these DANs that alters foraging behavior accordingly (Sayin et al., 2019; Tsao et al., 2018).

Therefore, it is highly likely that the activity of these six types of DANs – or maybe some additional DAN populations – modulates foraging behavior. Here we hypothesize that a long-term exposure to particular food conditions with low or high caloric value might induce plasticity in these DANs in a way that the foraging behavior becomes adapted to the previous experience.

1.6 Examples of structural plasticity in the *Drosophila* brain

The research presented in this thesis aims to analyze structural plasticity underlying adaptive behavior in *Drosophila*. This idea is not entirely new and unique. In fact, there are several studies reporting that the *Drosophila* nervous system shows structural plasticity, e.g., during development in the larval stage or during the first days following eclosure (also called "critical period"; Doll et al., 2017; Hensch, 2004).

For instance, dendritic trees of larval motor neurons are modified by the level of input activity (Singh et al., 2010; Tripodi et al., 2008). In addition, the number of synaptic release sites at the neuromuscular junctions (NMJ) is also highly dependent on the neurons' activity levels in *Drosophila* larvae (Budnik et al., 1990; Sigrist et al., 2003). Another example of structurally modified neurons in the larval stages of *Drosophila* is the modulatory octopamine-releasing neurons (OANs). The structure of the OANs is modified in an autoregulated fashion leading to state-dependent increase in locomotor activity in starved larvae (Koon and Budnik, 2012; Koon et al., 2011).

In addition to the larval stage, an example of structural modifications during the critical period of *Drosophila* is fragile X mental retardation protein (FMRP)-dependent "refinement" in the MB. These refinements take place at presynaptic sites, leading to axonal refinement and even pruning (Doll et al., 2017; Tessier and Broadie, 2008). All these examples for structural plasticity take place during developmental stages of *Drosophila*.

As an experience-dependent integration center, the MB is also expected to have highly structural modifications during development. In insect studies, including *Drosophila,* it has been shown that the volume of the MB calyx is often modulated based on the experience of the animal. For instance, the volume of the calyx increases in honey bees by the activity of muscarinic cholinergic pathways (Ismail

et al., 2006). This postsynaptic increase assists a behavioral transition of the animal from the nursing stage to foraging (Groh et al., 2012; Krofczik et al., 2008). Similar to the bees, dendritic microglomerulus numbers and sizes undergo modifications in the *Drosophila* MB calyx as well. However, unlike the activity-induced changes, the size and number of postsynaptic glomeruli are enlarged when the input from the PNs to these synaptic sites is decreased or silenced (Kremer et al., 2010; Pech et al., 2015). Apart from these examples, reports of structural changes at the level of the MB are limited as yet. One of the few examples is that the MB calyx region becomes larger with aging, similar to the enlargement due to lack of input. When the enlargement of the MB calyx is suppressed by external spermidine supply, the aging effects such as decrease in the ability of memory formation can be reversed (Gupta et al., 2016).

These examples for plasticity in the MB all are restricted to the calyx region. In this study, structural plasticity in the MB lobes is investigated.

1.7 Scope of the study

The aim of this study is to investigate adaptational mechanisms in the adult *Drosophila* brain.
As one of the most important behavioral types, state-dependent foraging behavior is investigated. Then, the mechanisms behind these adaptive behaviors are investigated in terms of functional and structural changes in the nervous system. *Drosophila* is used as the model organism in this study due to the reasons explained in section 1.2. I focused on structural changes in MB-related neurons since the MB is highly involved in the experience and motivation-based modulation of t foraging behavior (Huetteroth et al., 2015; Sayin et al., 2019; Tsao et al., 2018).
Even though the structural re-arrangements in the adult fly nervous system seem to be limited, it is expected that the adult *Drosophila* nervous system is also subject to structural modifications underlying adaptive behaviors such as long-lasting memory formation or state-dependent behavioral adjustments (Bailey and Chen, 1988; Bailey et al., 2015). However, the mechanisms behind these long-lived behavioral adaptations are not fully comprehended. Therefore, this study aims to reveal mechanisms in terms of structural and functional modifications underpinning experience-depend long lasting behavioral adaptations based on internal, metabolic states.

2 Materials and Methods

2.1 Materials

2.1.1 Fly food

Fly food recipes are listed together with all ingredients in the three tables below. All the flies are maintained on standard food unless indicated otherwise.

Additionally, the hypocaloric dietary, hypercaloric dietary and isocaloric dietary foods are created as different food conditions. These types of food were used in the experiments where the effect of the caloric value is tested. Flies were transferred to these foods after 3d following eclosure, unless indicated otherwise. The food composition of these three dietaries is listed in the tables below.

Standard food recipe;

Ingredient (quantity in 20l)	**Company**
agar (205 g)	Gourvita GmbH
soy flour (200 g)	Pflanzensaftwerk GmbH & Co. KG
yeast (360 g)	Gourvita GmbH
cornmeal (1600 g)	ZIELER & CO. GmbH
sugar beet syrup (440 g)	Obermühle Rosdorf
malt (1600 g)	MeisterMarken - Ulmer Spatz
propionic acid (126 ml)	Carl Roth GmbH + Co. KG
nipagin (30 g)	Sigma-Aldrich Chemie GmbH
ethanol (140 ml)	VWR International GmbH

Hypocaloric food recipe;

Ingredient (concentration)	**Company**
corn meal (80g/l)	ZIELER & CO. GmbH
agar (5gr/l)	AppliChem GmbH
sucrose (20g/l)	Carl Roth GmbH + Co. KG
yeast (2.5g/l)	Commercial baking wet yeast

propionic acid (6.3ml/l)	Carl Roth GmbH + Co. KG

Isocaloric food recipe;

Ingredient (concentration)	**Company**
corn meal (80g/l)	ZIELER & CO. GmbH
agar (5gr/l)	AppliChem GmbH
sucrose (50g/l)	Carl Roth GmbH + Co. KG
yeast (20g/l)	Commercial backing wet yeast
propionic acid (6.3ml/l)	Carl Roth GmbH + Co. KG

Hypercaloric food recipe;

Ingredient (concentration)	**Company**
corn meal (80g/l)	ZIELER & CO. GmbH
agar (5gr/l)	AppliChem GmbH
sucrose (150g/l)	Carl Roth GmbH + Co. KG
yeast (20g/l)	Commercial backing wet yeast
pork fat (10g/l)	Commercial (Lard)
propionic acid (6.3ml/l)	Carl Roth GmbH + Co. KG

2.1.2 Fly strains

The fly strains used in this project are detailed in the table below. Fly sources (donor lab, company or the flies that were used in similar studies) are indicated in the "donor or reference" column. Flies that were combined in our lab are also indicated. Figures that contain data from experiments with particular flies are also indicated in the "Figure" column.

Genotype	**Chromosome carrying DNA insertion**	**Donor or reference**	**Figure**
UAS-*trans*TANGO	II, III	Bloomington (#*77482*)	Figure 3.9

MB247DsRED;UAS-MBGRASP (UAS-spGFP11, MB247-spGFP1-10)	II, III	(Pech et al., 2013a)	Figure 3.4, 5, 6, 14, 15
R58E02-Gal4	II	(Liu et al., 2012)	Figure 3.4
TH-Gal4	III	(Friggi-Grelin et al., 2003)	Figure 3.4
w^-; ; 20XUAS-GCaMP3	III	Bloomington (#32237)	Figure 3.5, 7
R58E02-Gal4; UAS-GCaMP3	II, III	Combined by B.C.	Figure 3.4
MB188B-Gal4	II, III	Bloomington (#68268)	Figure 3.4, 7, 8, 9, 10, 11, 12, 13, 14, 15, 16, 17, 18, 19
MB315C-Gal4	II, III	Bloomington (#68316)	Figure 3.9
MB441B-Gal4	II, III	Bloomington (68251)	Figure 3.5
MB195C-Gal4	II, III	Bloomington (68270)	Figure 3.5
MB110C-Gal4	II, III	Bloomington (68262)	Figure 3.6
MB83C-Gal4	II, III	(Aso et al., 2014a)	Figure 3.6
UAS-dHomerGCaMP3	II	(Pech et al., 2015b)	Figure 3.8, 11, 12, 13
UAS-sypGCaMP3	III	(Pech et al., 2015b)	Figure 3.8, 11, 12, 13
UAS-ChR-XXL	II	Gift from Nagel lab	Combined with UAS-MBGRASP
UAS-csChrimson-Venus	I	Bloomington (#55136)	Figure 3.10
UAS-Shi^{ts}	II,III	(Kitamoto, 2001)	Figure 3.10
UAS-gtACRI	II	Kittel lab	Figure 3.10
UAS-bPAC	II	(Stierl et al., 2011)	Figure 3.17
UAS-bPAC; UAS-MBGRASP	II, III	Combined by B.C.	Figure 3.16
UAS-ChR-XXL; UAS-MBGRASP	II, III	Combined by T.R	Figure 3.16

UAS-csCHrimson-RFP;;UAS-MBGRASP	I,III	Combined by B.C.	Figure 3.16
UAS-CaLexA	II,III	Gift from Ing Wang	Figure 3.14, 15
UAS.SIFarecRNAi, UAS-Dicer	I, II	Combined by T.R (Martelli et al., 2017)	Figure 3.18
UAS.SIFarecRNAi; UAS-MBGRASP	II,III	Combined by B.C.	Figure 3.18
UAS-DAR1shRNA	II	Gift from Tanimoto lab	Figure 3.17
UAS-Dicer (2x); UAS-DAR2RNAi	II, III	Gift from Wegener lab	Figure 3.17
UAS-DAR1shRNA; UAS-MBGRASP	II, III	Combined by B.C.	Figure 3.17
UAS-mCD8::GFP, UAS-n-syb::GFP	II	(Riemensperger et al., 2013)	Figure 3.8, 18, 19
UAS-DenMark; UAS-syteGFP	II, III	(Nicolaï et al., 2010; Zhang et al., 2002) combined by T.R.	Figure 3.8

2.1.3 Odorants/ Solvents

The following odors were used in learning experiments and functional imaging experiments. 3-Octanol and 4-Methylcyclohexanol were diluted in mineral oil to prevent evaporation, while apple vinegar was diluted in distilled water to make it more attractive for starved flies. The list of the odorants, the solvent and the supplying companies is indicated in the table below.

Name	**Company**
Mineral oil (M8410)	SIGMA-ALDRICH
4-Methylcyclohexanol	SIGMA-ALDRICH
3-Octanol	SIGMA-ALDRICH
Apple Vinegar	Alnatura Produktions- und Handels GmbH

2.1.4 Chemicals

The list of all the chemicals used in this study is shown in the table below, and in which solutions these chemicals were used is also indicated under the column “Solution used”.

Name	Company	Solution used
KCl	Carl Roth GmbH + Co. KG	Ringer’s solution
NaCl	AppliChem GmbH	Ringer’s solution, Digestion buffer, MES buffer, StockX
$MgCl_2$	Carl Roth GmbH + Co. KG	Ringer’s solution
$CaCl_2$	Carl Roth GmbH + Co. KG	Ringer’s solution
sucrose	Carl Roth GmbH + Co. KG	Ringer’s solution, Sucrose solutions
NaH_2PO_4	Carl Roth GmbH + Co. KG	PBS
Na_2HPO_4	Carl Roth GmbH + Co. KG	PBS
Triton X 100	Carl Roth GmbH + Co. KG	PBS-T
Albumin Fraktion V (bovine serum albumin – BSA)	Carl Roth GmbH + Co. KG	BSA
paraformaldehyde	Carl Roth GmbH + Co. KG	PFA
HCl	Carl Roth GmbH + Co. KG	pH adjustment
NaOH	Carl Roth GmbH + Co. KG	pH adjustment
AcX (Acrylol-X-SE)	Thermo Fisher Scientific GmbH	AcX solution
DMSO	SIGMA-ALDRICH	AcX solution
EDTA	SIGMA-ALDRICH	Digestion buffer
TrisCl	Carl Roth GmbH + Co. KG	Digestion buffer
Sodium acrylate	SIGMA-ALDRICH	StocX
Acrylamide	SIGMA-ALDRICH	StocX
N,N’ Methylane bisacrylamide	SIGMA-ALDRICH	StocX
TEMED	Carl Roth GmbH + Co. KG	TEMED
Amonium persulfate (APS)	SIGMA-ALDRICH	APS
4 Hydroxy Tempo (4TH)	SIGMA-ALDRICH	4HT
Proteinase K (800U7ml)	New England Biolabs GmbH	Digestion solution

MES	SIGMA-ALDRICH	MES buffer
All trans-retinal (ATR)	SIGMA-ALDRICH	Fly food for csChrimson flies

2.1.5 Solutions and buffers

The solutions that were prepared for the experiments using the chemicals detailed in the previous section are listed below. It is also shown in which experiments or procedures these solutions were used.

Name	**Ingredient**	**Comment**	**Experiments used**
Ringer's solution	5 mM KCl 130 mM NaCl 2 mM $MgCl_2$*$2H_2O$ 2 mM $CaCl_2$ 5 mM Hepes 36 mM sucrose dwater	pH 7.3 (adjusted with HCl or NaOH) stored at -20 °C after use at 4 °C	Fly brain dissection, Ca^{2+} imaging
PBS (phosphate buffered saline)	15 mM NaH_2PO_4 100 mM NaCl 85 mM Na_2HPO_4 dwater	pH 7.4 (adjusted with HCl or NaOH) stored at 4 °C	IHC
PBST (PBS + Triton X 100)	PBS 0.6 % Triton X 100	stored at 4 °C	IHC, reporter signal quantification
blocking solution	PBST 2 % bovine serum albumin	stored at 4 °C	IHC, reporter signal quantification
PFA (paraformaldehyde)	PBS 4 % paraformaldehyde 0.1 % NaOH	pH 7.4 (adjusted with HCl or NaOH) ingredients are mixed at 70 °C and pH adjusted at 20 °C stored at -20 °C	IHC, reporter signal quantification
ATR	1g of All-trans-retinal 14ml EtOH	Stored at -4°C, 10ul of ATR solution is	csChrimson expressing flies are

		mixed with 10ml of fly food before experiment	fed on ATR mixed food
1M sucrose	2M sucrose is dissolved in dWater and mixed with same volume of red food color	Stored at -4°C	CAFE assay
AcX/DMSO	10mg/ml AcX DMSO	Stored at -20°C as 10ul aliquots, in experiment diluted to 1:100 in MBS	Expansion microscopy
MBS (MES-Buffer Saline)	100mM MES 150mM NaCl dwater	pH 6 (adjusted with NaOH), stored at -4°C in darkness	Expansion microscopy
EDTA	0.5M EDTA dwater	pH 8 (adjusted with NaOH), stored at room temperature	Expansion microscopy
Tris-Cl	1M Tris dwater	pH 8 (adjusted with HCl), stored at room temperature	Expansion microscopy
Digestion buffer	0.5g/100ml Triton X 0.2ml/100ml EDTA (0.5M) 5ml/100ml Tris-Cl (1M) 4.67g/100ml NaCl dwater	5ml aliquots stored at -20°C	Expansion microscopy
Proteinase K (8U/ml)	8U/ml Proteinase K Digestion buffer	Proteinase K (800U/ml) is stored at -20°C, Digestion mixture is mixed with Proteinase K freshly before experiments	Expansion microscopy

StocX	8.6g/100ml Sodium acrylate 2.5g/100ml Acrylamide 0.15g/100ml N,N' M. bisacrlamide 11.7g/100ml NaCl PBS	1ml aliquots stored at -20°C in darkness	Expansion microscopy
4HT	0.5g/100ml 4 Hydroxy Tempo dwater	1ml aliquots stored at -20°C in darkness	Expansion microscopy
TEMED	1:10 dilution of TEMED dwater	1ml aliquots stored at -20°C in darkness	Expansion microscopy
APS	10g/100ml APS dwater	1ml aliquots stored at -20°C in darkness	Expansion microscopy

2.1.6 Consumables

All the tools that were used in experiments are listed together below with which companies they were obtained from.

Name	**Company**
pipette tips	Sarstedt AG & Co
cover glasses 18 mm x 18 mm	Thermo Fisher Scientific GmbH
cover glasses 24 mm x 60 mm	Th. Geyer GmbH & Co. KG
microscope slides	Carl Roth GmbH + Co. KG
Austerlitz INSECT PINS (0.2 mm)	Pin Service – Lucie Hrabovská
transparent tape rings	Avery Zweckform GmbH
VECTASHIELD (mounting medium)	Vector Laboratories, Inc.
transparent nail polish	L'Oréal International
forceps	Fine Science Tools GmbH
food vials	Sarstedt AG & Co

stab knife (5 mm blade)	Sharpoint
surgical disposable scalpel (11)	BRAUN – Aesculap AG
hypodermic-needle (1.1 x 50 mm)	Sterican – B. Braun Melsungen AG
scintillation vial (20 ml)	Sarstedt AG & Co
3-component dental glues	3M ESPE ptotemp II
Plastic cover slips	Plano GmbH
Whatman papers	MACHEREY-NAGEL GmbH & Co. KG
Learning machine	Custom-built
Training tubes	Custom-built
Capillary tubes (BALUBRAND 20ul)	SIGMA-ALDRICH
Red color food	Carl Roth GmbH + Co. KG
Parafilm	SIGMA-ALDRICH
DAM	Trikinetics Inc
96-well plate	Greiner Bio One International GmbH
Glass dishes for dissection	OMNILAB-LABORZENTRUM GmbH & C
UV glue	Nordenta Handelsgesellschaft mbH
UV gun	Dentaltix, Dentared Odontology Services, S.L.

2.1.7 Antibodies

Primary antibodies;

The antibodies used in this study are listed in the table below. Figures that contains antibody stainings in which these antibodies were used are also shown in the "Figure" column.

Antigen	**Raised in**	**Dilution**	**Source, Cat no.**	**Figure**
Dlg- discs large	mouse	1 : 200	DSHB, 528203	Figure 3.8
GFP- green fluorescent protein	chicken	1 : 1000	ABCAM, AB13970	Figure 3.5, 7, 8, 18, 19
Brp- burchpilot	mouse	1:100	DSHB, AB2314866	Figure 3.5, 7, 8, 9, 18, 19
mCherry	rabbit	1:200	ABCAM, AB183628	Figure 3.8
AstA	rabbit	1:1000	Wegener lab	Figure 3.18
SIFamide	rabbit	1:2000	Veenstra, Bordeaux	Figure 3.19
TH	mouse	1:50	Immunostar, 1240001	Figure 3.7

Secondary antibodies;

All secondary antibodies that were used in this study were raised in goat serum and the dilution was 1:300 in BSA solution for immunohistochemical stainings. For the expansion microscopy protocol, 1:200 dilutions of Alexa Fluor 488 and 568 fluorophore-containing secondary antibodies were used since these antibodies were not susceptible to the digestion procedure in the last step of expansion. The list of the antibodies and the figures demonstrated are shown in the table below.

Antigen	Fluorophore	Source, Cat no.	Figure demonstrated
mouse - IgG	Alexa Fluor 633	Invitrogen, A21050	Figure 3.5, 7, 18, 19
mouse - IgG	AlexA Flour 568	Life Technologies, A110004	Figure 3.8, 9
rabbit - IgG	Alexa Fluor 633	Invitrogen, A21070	Figure 3.7,
rabbit - IgG	AlexA Flour 568	Life Technologies, A11036	Figure 3.8, 9, 18, 19
chicken - IgG	AlexA flour 488	Life Technologies, A11039	Figure 3.5, 7, 8, 9, 18, 19

2.1.8 Microscopy Equipment

For two-photon calcium imaging, expansion microscopy imaging and immunohistochemistry imaging the following equipment was used.

2-Photon microscopy;

Name	Company
LSM 7MP	Carl Zeiss AG
mode-locked Ti-sapphire laser	Coherent Inc.
dichroic mirror (500-550/650-660 nm BP-filter)	Carl Zeiss AG
plan-Apochromat 20x (NA = 1) water immersion objective	Carl Zeiss AG

Confocal microscopy;

Name	Company
TSC SP8 confocal laser scanning microscope	Leica Microsystems GmbH
PL FLUOTAR 10x (NA = 0.3) air objective	Leica Microsystems GmbH
PL APO 20x (NA = 0.75) glycerol/water objective	Leica Microsystems GmbH
Argon-laser (488 nm)	Leica Microsystems GmbH

DPSS-laser (561 nm)	Leica Microsystems GmbH
HeNe-laser (633 nm)	Leica Microsystems GmbH

2.1.9 Software

For image acquisition, data analysis and visualization of the data the following software were used.

Name	Company	Address
Microsoft Office 2010 (Excel, Word, PowerPoint)	Microsoft Corporation	Data analysis and display
ImageJ	National Institutes of Health	Image analysis
OriginPro 8.5G	OriginLab Corporation	Statistics, data plotting
ZEN 2011 SP2	Carl Zeiss AG	2-photon imaging
Leica Application Suite X (LAS)	Leica Microsystems GmbH	Confocal imaging
MATLAB (R2012b)	MathWorks	DAM data analysis
Visual Basics of Applications (VBA) software	Custom-written	Trigger for odor delivery device

2.2 Methods

2.2.1 Maintenance of flies

All flies were maintained in an incubator with controlled temperature, humidity and light/dark cycle.. Flies were kept at 25°C and 60% humidity and exposed to 12h light per day, mimicking a day/night cycle. Conditions were the same for test flies used for experiments as well as for the maintained stock flies in the stock collection if not otherwise indicated in the experimental procedure.

2.2.2 Long-term dietary treatment

The experiments on investigating long-term dietary effects on behavior were performed with wildtype flies of the Canton-S (CS) strain. In the experiments in which the effect of the diet on neuronal connectivity and anatomy was investigated, the F1 generation of crossed flies was used. Experimental flies (either CS or crossed) were collected directly after eclosion (0d) and kept on standard fly food until

they were 3 days old (3d) before shifting them to “experimental food” so that brain development was completed and any dietary effects were not due to any developmental impairment.

Three different food conditions, hypo-, iso-, and hypercaloric, with different carbohydrate, protein and fat contents (composition of the special dietary food is described in 2.1.1) were used (Figure 2.1A). Isocaloric food was adjusted in a way that the caloric value and the nutritional value were similar to the standard food that is well-established in *Drosophila* research. Dietary exposure lasted for 7d, which was considered to be a long period in the lifetime of *Drosophila*. At the end of 7d, flies were either sacrificed for anatomical experiments or starved for behavioral tests (Figure 2.1B).

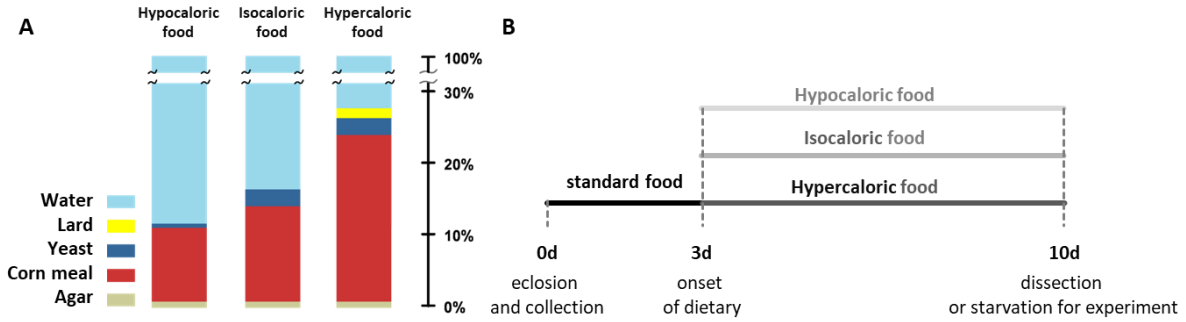

Figure 2.1 Experimental setup for long-term diet. **A** Nutrient composition percentage of hypo-, iso-, and hypercaloric food. Food composition is indicated as the primary source of a specific type of nutrition on the left-hand side. **B** Experimental timeline of diet dependent on the particular experiments. Flies were collected after eclosion and kept on standard fly food for 3d before a 7d-long dietary started.

2.2.3 Survival assay

For every experiment, 10 flies (5 males and 5 females) developed on standard food were collected immediately after eclosion and placed on different food conditions – hypo-, iso-, and hypercaloric condition. Flies were transferred to a new vial during the days for which data points shown in Figure 3.1A. The dead flies left in the vial were counted during these transfers. Then the viability was calculated as percentage of surviving flies for each time point. Each experiment was repeated 5-6 times for every condition. Male and female flies were pooled in one graph since the survival was not dependent on the flies' sex.

2.2.4 Proboscis extension reflex (PER) assay

10d old female CS flies that were exposed to different diets for a long-term period, as explained in the section of 2.2.2, were starved for 24 hours as non-starved flies do not exhibit PER (Wang et al., 2004).

Starvation was induced in the same way for every experiment simply by putting the flies in an empty vial. A wetted tissue paper was placed on the bottom of the vial to prevent dehydration and to ensure that any increase in food solution uptake was not due to the thirstiness but increased hunger-driven motivation. Then, starved flies were briefly anaesthetized on ice and tethered to a 1ml pipette tip using a three-component dental glue. Each fly was briefly touched with a 2M sucrose solution-soaked cotton swab on the labellum and immediately pulled back. This procedure was repeated five times per fly and proboscis extension incidents were scored as a percentage of proboscis extension responses (PER) for each fly and plotted as PER [%] (Figure 2.2A).

2.2.5 Capillary feeder (CAFE) assay

In order to measure the flies' food uptake within 24h, the capillary feeder (CAFE) assay was used, with minor changes when compared with the original report (Ja et al., 2007). For the experiments in which the role of certain neurons or signaling pathways in feeding were analyzed, 5-7d transgenic female flies that genetically expressed thermogenetic, optogenetic, or RNA interference tools were tested. For experiments in which long-term effects of diet or, as a comparison, optogenetic stimulation was analyzed, flies were either incubated with standard food for 3d following eclosion and placed for 7d on either different diets, or they were placed on isocaloric food in the "fly disco" apparatus for optogenetic stimulation. Flies were then tested for food uptake. Subsequent to either the 5-7d development or 10d for a given experimental paradigm, flies were starved for 24h in single small vials together with a piece of wet tissue paper as described above (Figure 2.2B). Flies that were not starved before the CAFE assay experiments typically failed to locate sucrose solution-filled capillaries within 24h.

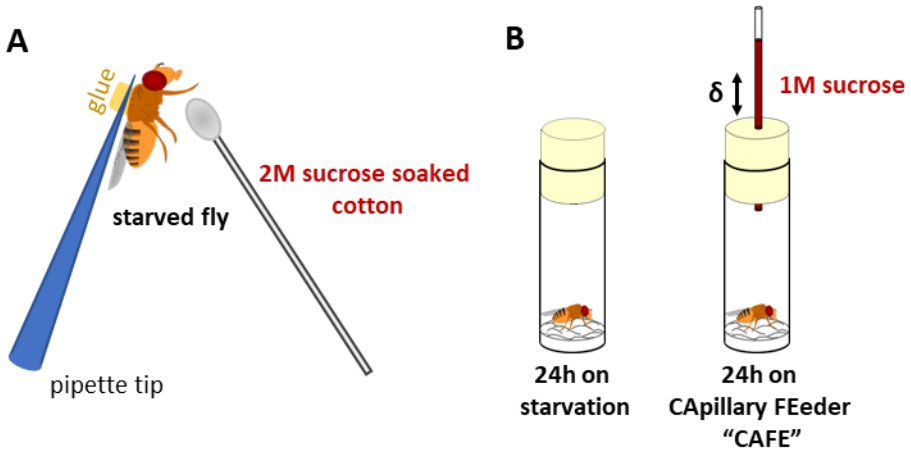

Figure 2. 2 Illustration of the PER assay and the CAFE assay. **A** Individual, 24h starved flies were tethered to a pipette tip and a sugar soaked cotton swap was presented to their proboscis briefly. The number of proboscis

extensions were counted. **B** Individual flies were starved in single vials for 24h with a wet tissue paper on the bottom of the vials. Subsequently, capillary tubes filled with 1M sucrose were placed by piercing through the sponge plug. The level of the sucrose solution was marked both at the beginning and after 24h to quantify sucrose consumption.

Following starvation, capillary tubes filled with sucrose solution (1M final concentration) mixed with red food color (1:1 ratio) were pierced through the vial plug such that the bottom tip of the capillary was not sticking out of the plug more than 1mm into the vial containing a single fly (Figure 2.2B). Vials were then placed back in the incubator and the change in sucrose level in the capillary was measured after 24h. The sucrose solution level was marked with a tiny permanent marker when the capillaries were placed and at the end of 24h period of CAFE assay. The difference between the two marking points was measured in mm. In order to eliminate the effect of evaporation, 4 "blank" vials (with no fly in the vial) were also measured the same way and the average evaporation level was subtracted from every measurement. Then, the millimetric measurements were converted into volume (15mm capillary length contains 1µl solution).

2.2.6 Learning and avoidance tests

Experiments that involved a two choice paradigm in the test phase (e.g. memory formation/learning experiments and avoidance test) were carried out in a custom-built T-maze machine that was adapted from the study of Tully and Quinn, 1985 (Figure 2.3A). This machine enabled one to train several groups of flies to associate an odor with a reward or punishment simultaneously. Subsequently (or without training), flies could be tested for odor preference with the same apparatus (Schwaerzel et al., 2002). Flies were transferred from training tubes to test tubes with the help of an "elevator mechanism" controlled by a lever (Figure 2.3.A). All training and test tubes in the apparatus were equipped with "odor cups" such that specific odors could be presented in specific tubes in a temporally controlled manner. The entire experiments, training phase of learning experiments and test phase of preference and learning experiments were conducted in a chamber in which optimum temperature and humidity (25°C and 60%, respectively) were maintained. The temperature of the chamber could also be increased up to 32°C (as required for thermogenetic experiments).

Training tubes, in which the appetitive and aversive stimuli (electric shock and sugar, respectively) were presented together with an odor, differed in design (Figure 2.2A'). Electric tubes were lined with copper grids that were connected to the poles of a voltage generator so that electric shocks could be delivered

simultaneous with an odor as a conditioned stimulus (CS+). On the other hand, appetitive, rewarding stimuli (sugar) were provided using training tubes which consisted of two layers. Between inner and outer layers of these training tubes, sugar-soaked Whatman paper or water-soaked Whatman paper was placed. The inner tube layer had an opening enabling the presentation of either sugar-soaked Whatman paper or water-soaked Whatman paper to be paired with different odors (CS+ and CS-, respectively) in the training phase (Figure 2.2A'). In the test phase, flies were given a choice between two tubes in which the CS+ and CS- odors were presented. In every two-choice odor assay, 1:36 diluted 4-methyl cyclohexamide (MCH) and 3-Octanol (3-Oct) were used as odorants.

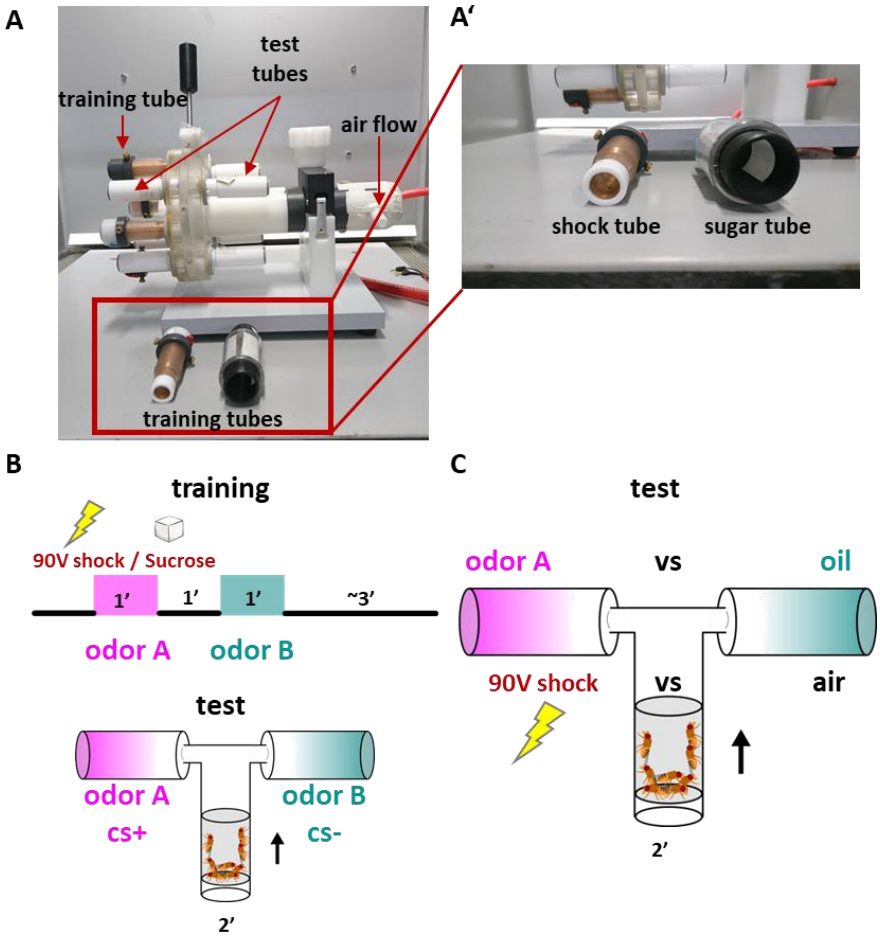

Figure 2.3 Preference and learning paradigm. **A** Picture of a custom built T-maze machine to test the learning ability or preference/avoidance of odor or electric shock. A lever helps to transfer the flies from the training tubes to the test tubes with an "elevator" in the middle. **B** Experimental paradigm for olfactory learning and memory. Each odor is presented for a minute with or without an unconditioned stimulus (thereby designated as conditioned stimulus+ or conditioned stimulus -, CS+ and CS-, respectively). After approximately three minutes, flies were transferred to the test tubes where they were presented with both odors as conditioned stimuli from opposite sides. The number of flies on each side was counted and a preference index was calculated. **C** Preference

test paradigm. Naïve odor or shock avoidance was directly tested against oil (in odor case) or only an air stream (shock avoidance case).

Appetitive associative learning and short-term memory formation;

In the appetitive learning paradigm, in which the flies' ability to associate an appetitive unconditioned stimulus (sucrose) with an odor was tested, 24h starved flies (if not indicated otherwise) were used. Flies were first stimulated with an odor (CS+) for a minute while exposed to sucrose-soaked Whatman paper. After a one-minute break, a second odor was presented (CS-) while the flies were exposed to water-soaked Whatman paper. Then, the flies were transferred to the test tubes where the two odors (CS+ and CS-) were presented in two different test tubes connected to the elevator from opposite sides and allowed to distribute for 2 minutes (Figure 2.2D).

Aversive associative learning;

In this paradigm, copper wired training tubes were used to train "non-starved" flies to associate a given odor with an unconditioned electric shock stimulus. The training and the test timing were exactly the same as appetitive training, except that the electric shock (90V) was presented 15 seconds after odor onset as 12 shock pulses (each pulse was 1.25 sec with 3.75 sec break) during the training (Figure 2.2D). Flies were then tested for preference between the electric shock-associated odor (CS+) and an "unpaired" odor (CS-). After 2 minutes of test period, the two test tubes were separated and the flies in each tube were counted. Preference indices were calculated based on the formula:

$$\text{preference index} = \frac{(\text{number of flies}_{\text{cs+}} - \text{number of flies}_{\text{cs-}})}{(\text{number of flies}_{cs+} + \text{number of flies}_{cs-})}$$

Learning indices were calculated as the average of the preference indices resulting from two reciprocal trainings, i.e., preference for the two odors were measured both as CS+ and CS-.

Avoidance test;

In experiments in which there was no training phase, the flies were immediately transferred to the test tubes and two stimuli were presented from two sides. Then, flies were allowed 2 minutes to choose a side (Figure 2.2E). In shock avoidance, one of the test tubes had the same structure as copper-wired aversive training tubes and in the counterpart test tube there was no stimulation but a negative air stream. Approximately 70 "non-starved" flies were transferred to the test tubes directly and tested for

2 minutes for their choice between 90V electric shock and air stream. In the odor avoidance test, one odor that was already aversive at a 1:36 dilution was delivered from one test tube. In the other test tube mineral oil was provided since both MCH and 3-Oct were dissolved in mineral oil to prevent evaporation. Then, the flies in each test tube were collected and counted for calculating the preference index. The preference index was calculated by the same formula above, except that CS+ and CS- were replaced by the stimulus (odor or shock) and blank (oil or air), respectively. For learning and preference experiments, the flies' ages were exactly the same as in the CAFE assay.

2.2.7 *Drosophila* Activity Monitoring (DAM)

10d old single male flies, after 7d exposure to different dietary conditions, were transferred to glass tubes (length = 6.5 mm, diameter = 5 mm) with one end filled with fly food (of the same composition as the food on which the animal was placed beforehand). In contrast to the CAFE assay, PER, and dissection experiments, only male flies were used as female flies egg laying behavior affects the measurements. The "food end" of the glass tubes were sealed with parafilm to prevent the food from drying while the other end was capped with an air-permeable cap, enabling flies to respirate. Sealed and capped tubes were placed in monitors (Trikinetics) in which a laser beam was projected across the middle of the tube and disruption of the laser beam ("beam crossing") was scored as a proxy for the flies' activity levels. The monitors were placed in a custom-built incubator in which light on- and offset, temperature, and humidity were controlled, and which was connected to a computer to record activity. Flies were incubated at a 12h light / 12h dark cycle during recording. Each monitor could hold up to 32 glass tubes, hence enabling 32 flies to be measured simultaneously. Flies were given two days to adapt to the new environment and light-dark cycle, meaning that the collected data in the first 2 days were discarded and the subsequent 3d data were analyzed. The experimental groups that were deprived from light completely were conducted separately instead of turning the lights off from the same group of flies.

Data analysis was performed using a custom-written MATLAB script "DACA" (*Drosophila* Circadian Analysis) that was written and kindly provided by Dr. Bart Guerten. In this analysis, the number of beam crossing events were counted and divided into different time bins. In this case, graphs were plotted in 15 minute bins if not otherwise stated on the y axis. The flies were considered as sleeping when there was no crossing of the midline for more than five minutes (Li et al., 2013). By this logic, activity was plotted as the number of beam crossings per 15 minute bin over the day, considering the light and

dark phase, how many sleeping episodes each fly displayed, how long the sleeping episodes were, how long flies slept in total, and finally, the time passed between light offset and activity decrease referred as “sleeping delay”.

2.2.8 IHC and sample preparation

Dissection;

Immunohistochemistry (IHC) experiments for the structural plasticity and protein expression analysis, was performed using 5-7d old flies raised on standard fly food. For quantification of the signal dependent on the animals’ long term (7d) experience, 10d old female flies (7d long-term experiment condition starting at 3d after eclosion, Figure 2.1B) were briefly anesthetized by CO_2 and placed on ice for at least 10 min before dissection. After proper anesthesia, flies were placed on a custom-made silicon-based dish and pinned with 0.2mm needles through the thorax. Brains were prepared in Ringer’s solution and fixed in 4% PFA (pH 7.4) at room temperature for half an hour on a shaker in black glass dishes. Fixation was terminated by washing the brains with PBS-T (0.6% Triton-X) three times for at least 20 min at room temperature.

IHC;

For protein expression or anatomical investigations, brains were stained against proteins of interest as follows. Subsequently to washing from fixation solution, brains were incubated in blocking solution (2% BSA containing PBS-T) overnight at 4°C on a shaker. Then brains were transferred into corresponding primary antibody (dilutions for each primary antibodies are listed in the materials section) diluted in blocking solution at room temperature for 5-7h on a shaker. Then, primary antibodies were washed the same way as fixative solution and replaced by corresponding secondary antibody dependent on the animal type that the primary antibody was raised in. All secondary antibodies were diluted 1:300 in blocking solution. The brains were incubated in the secondary antibody solution overnight at 4°C on the shaker in darkness. From this step on, samples were kept in darkness by covering the dish with aluminum foil until mounting. Finally, on the third day, secondary antibody was washed out and brains were mounted for imaging.

Mounting;

If brains were not subjected to immunostaining (as in the case of experiments involving signal quantification), they were directly mounted after washing off the fixative solution in a drop of

Vectashield placed on a transparent tape ring on rectangular coverslips (24mm x 60mm). Each brain was placed in a single tape ring with the anterior side facing upwards with the help of a 0.2mm needle held by forceps so that the position of the signal was both optimal to image brain regions of interest and consistent between samples. After positioning of the brain, each brain was covered by a 18mm x 18mm cover slip and sealed with nail polish. I paid attention that the samples were imaged on the same day subsequent to mounting. If not, brains were stored at 4°C in darkness until imaging, up to 2 days after mounting.

2.2.9 Confocal imaging

Experiments aiming at anatomical descriptions, synaptically localized reporter protein quantification, or protein expression analysis were carried out using an SP8 confocal LSM equipped with a 20X glycerol immersion objective if not otherwise stated. Samples that were mounted on the 24mm x 60mm cover slide were immobilized on a glass microscope slide with a drop of water so that the samples could be placed on the microscope stage.

To allow comparability, the imaging protocol was kept consistent between samples. Image pixel size was set to 1024x1024 and excitation laser power 25%. The samples were additionally magnified by the factor 2.14 using imaging software so that the entire mushroom body lobes were captured at the largest perspective. For excitation and emission adjustment, imaging of every type of experiment was done with the same settings. After imaging the files were saved with ".lif" extension. All imaged samples were then stored at 4°C in darkness.

2.2.10 GRASP signal and synaptically localized reporter protein quantification

In any kind of reporter protein quantification assay, e.g., GRASP quantification, pre- and postsynaptic reporter protein quantification, brains were not subjected to any staining and raw fluorescent was quantified immediately after fixation. After the long-term exposure paradigms (placement on different foods, long-term activation or inhibition), fly brains were removed, fixed and washed as described above. After the samples were mounted and imaged, quantification of the fluorescence signal was carried out using Image J software. Prior to signal measurement, a region outside of the brain was determined as background. Then, z projections of the maximum light intensity were generated by Image J for every axonal compartment of the mushroom body. The borders of the compartments were

determined using either the background staining as a reference or the expression of another reporter protein under the MB-specific driver MB247 (for example, in the case of MB-GRASP experiments, the reporter protein was MB247-DsRED) (Pech et al., 2013). Regions of interest (ROIs) for each compartment were determined and the mean light intensity values of the ROIs were measured as "raw" signals. Then, the relative light intensity was calculated by normalizing each value to the mean of the light intensities measured under isocaloric conditions. All these measurements and normalization were done within a compartment under different conditions. Therefore, the relative signal intensity means always equal to one for each compartments.

For long-term optogenetic stimulation experiments, two parameters were changed as control groups: The first parameter was the expression of the genetic tool and as control for this parameter, flies that were not expressing optogenetic tool were used. Additionally, the second parameter was the stimulus. Therefore, a group of flies placed under darkness as control for light stimulus parameter. The light intensity measurements were done exactly the same way as described above. Then the relative signal intensity was calculated by normalizing each value to the mean of its own genetic background measurements under complete darkness conditions. Since the flies expressing the genetic tool and the MBGRASP had different copy number of UAS binding site than the flies expressing only MBGRASP complex, I aimed to eliminate the artifact coming from the competition of UAS binding sites.

All experiments were replicated at least three times and normalization was done within every replication in order to eliminate false effects caused by the small parametrical changes that may differ from experiment to experiment such as the day time of the experiment, usage of confocal, etc. Finally, before determining the which statistical test to use, all data groups are subjected to a test for normal distribution, Kolmogorov-Smirnov. Since all data sets were normally distributed, I performed a one-way ANOVA followed by post hoc test Tukey in all signal quantitation as only one parameter – dietary - is different between groups. In the case of a two parameter change, i.e., light condition and genetic background, a two-way ANOVA was applied.

2.2.11 Expansion microscopy

This protocol was used to expand the samples in a way that the finer arborizations, that usually cannot be resolved by standard sample preparation and imaging techniques could be imaged and quantified. Physical expansion of the sample was achieved by several steps; perfusion of the sample by an acrylic-

based gel, gelation (or gelling) of the sample, digestion of the proteins in the brains that keeps cells intact, and finally the expansion of the gelated sample. I have utilized the protocol from Asano et al. (2018) with small modifications.

Preparation of gelating chamber;

In the study of Asano et al. (2018), gelation chambers were prepared during gelation. However, since they were not stable, in this study, a slightly different version of gelation chambers were prepared before the expansion microscopy experiments. Gelation chambers were prepared such that six pieces of sellotape were stretched on top of each other horizontally over a thick glass slide (Figure 2.4A) and 3 equally distributed slits (app. 2-3mm wide) were made with the help of a razor blade orthogonal to the tape layers (Figure 2.4B). Six layers of sellotape measured at approximately 500-600µm in height, perfectly fitting the fly brain, at approximately 500µm in depth, were used. Each slit contained a single brain and was covered by single plastic coverslip. Plastic covers were preferred as they were less sticky after the gel was polymerized and were easy to remove. Additionally, gelation chambers used in this study could be washed for continued use in further experiments.

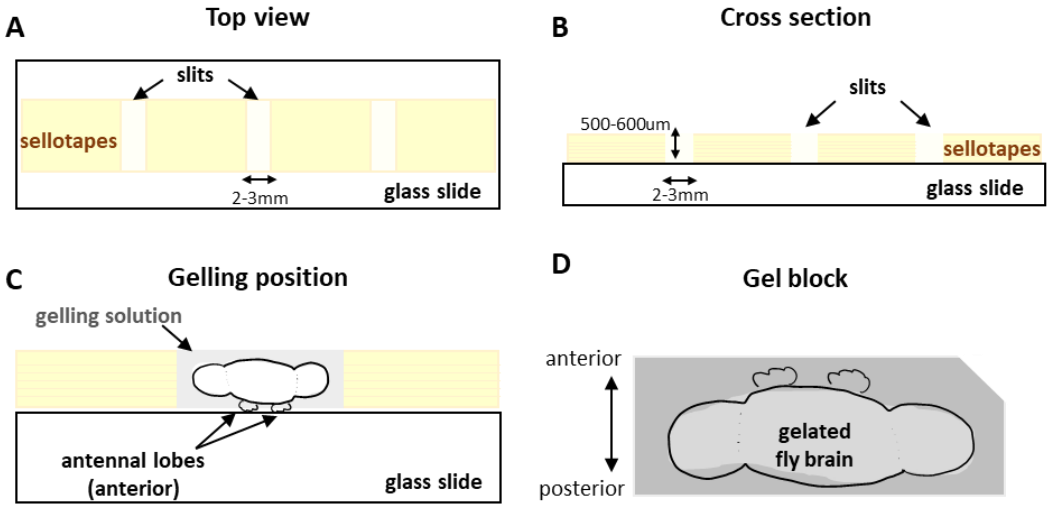

Figure 2.4 Illustration of the gelling chamber and gelation of the brain. **A** Top view of gelation chamber. Six pieces of sellotape were positioned on top of each other and three equally distributed slits are opened with a razor**. B** Side view of gelation chamber. Height of the slits are slightly higher than the fly brain. **C** Positioning of the fly brain inside the gelling solution. The anterior part of the brain was placed in a downward position, slightly touching the glass surface of the slide. **D** Illustration of the carved gel block containing a gelated brain. The gel block was trimmed from the corner to orient the anterior side.

Dissection and IHC;

Dissection and fixation of the female fly brain was performed exactly the same as it is described in 2.2.8. However, unlike the "regular" IHC protocol, the primary antibody was always used at twice the usual concentration, i.e. anti GFP (chicken) was diluted 1:500 in blocking solution instead of 1:1000, and the brains were incubated overnight at 4°C followed by room temperature incubation for 5 h on the shaker. The next day, the primary antibody was washed in the same way as the fixative and the solution was replaced by 1:200 diluted secondary antibody (instead of 1:300) overnight at 4°C in darkness on a shaker. From this step on, the samples were kept in darkness as much as possible. Finally, the secondary antibody was washed using PBS (instead of PBS-T) for the further expansion microscopy protocol.

Gelation of the sample;

In order to prepare the brains for perfusion with gelling solution, brains were incubated in AcX/DMSO solution in MBS for 24 h at room temperature in darkness (without shaking) in black glass dishes. Then, AcX/DMSO solution was washed with PBS three times for at least 20 min. Then, the samples were chilled on ice for a minute before being transferred into the gelling solution. The gelling solution was prepared the same way as described in Asano et al., 2018. Components of the gelling solution and the ratio of their volume in the solution are following; StocX, 4HT, TEMED, and APS with the ratio of 47:1.5:1:1 respectively. The gelling solution had to be freshly prepared and had to be used immediately after the last component is placed in the solution. The order of the components must be the same as stated above and the solution vortexed thoroughly after the last component is placed. Subsequent to washing ofo AcX/DMSO, the gelling solution was applied and the samples chilled further on ice for 60 minutes in darkness without shaking. Then, the brains were transferred into the gelating chamber that is described above. Prior to the transfer, approximately 20-50µl of gelation solution was pipetted into each slit in a way that the height of the solution was not above the tape walls. Then, the brains were transferred into the gelation chamber and positioned in a way that the anterior position was facing downwards and touching the bottom of the slit. Transferring and mounting of the brain into the gelation chamber had to be as quick as possible because since addition of the last component of gelling solution, APS, initiated the polymerization at room temperature. Finally, each sample was covered by plastic coverslips, making sure that each brain was covered entirely by gelling solution and that no air bubbles were created after the placing of the coverslips. The gelation chamber was placed in a 37°C incubator for 2 hours in darkness for polymerization. Subsequent to polymerization, coverslips were carefully peeled away and a small block of gel should be cut with the help of a razor blade (Figure 2.4C). At this stage the brains were visible in the gel and during cutting, a visible amount of gel surrounded

the gel. The gel block could also be trimmed in a way that the orientation of the brain was predictable (Figure 2.4C).

Digestion;

The digestion solution was also prepared freshly since it contains digestive enzymes. During gelation, digestive 800U proteinase K containing digestion buffer was prepared on ice. After cutting the gelated brain blocks, each block was transferred into 200µl of digestion solution in single wells of a 96 well-plate using a paint brush. Prior to transfer, a drop of digestion solution was put on the block to make transfer easier. The 96 well-plate was covered with aluminum foil to limit light exposure. After transferring each brain, the lid was closed and the plate was sealed tightly with parafilm to prevent evaporation. Samples were left at room temperature without shaking for 3d for digestion.

Expansion;

During the digestion period, the samples already started expanding by a factor of 1.5 to 2. Following 3 days of incubation for digestions, the digestive solution was replaced by water and samples were incubated in water for 40 min, refreshing the water halfway through.

Mounting for imaging;

All the samples were mounted and imaged immediately following expansion. Each gel block was placed on a glass slide and excessive amount of water was dried with tissue paper. Then, three component dental glue was mixed and used to surround the gel blocks using a toothpick. Since at this stage the brain was invisible, brains could be oriented such that the antennal lobe, hence also the MB lobes, were in an upward position by the help of trimmed shape of the gel block. A drop of water was placed on top of the gel block to prevent it from drying.

Imaging and colocalization analysis;

Following the stabilization of the gel blocks, the samples were imaged using a 10X air objective since the working distance allowed visualization of the expanded samples at such depth. The imaged sample files and imaging settings were saved as ".lif" and ".seg" files, respectively. Images of the samples were analyzed with Image J software. The images were smoothened using the mean filtering function with the factor 1 to refrain from a rough picture since the samples were expanded much above the optical spatial resolution. A threshold was applied to the images to eliminate background fluorescence.

Colocalization of the proteins of interest for quantification was then analyzed using the image calculator function. To do this, the two image channels of the same brain (each corresponding to a different proteins of interest) were separated as two separate images. The AND function of image calculator was then used between the two images in order to detect the co-localized pixels that showed a fluorescent signal in both channels.

2.2.12 Optogenetic stimulation

The optogenetic tools used in this study were ChR-XXL and csChrimson as light inducible depolarizing channel, bPAC as light inducible adenyl cyclase, and gtACRI as light inducible hyperpolarizing tool. Flies expressing ChR-XXL and bPAC were incubated on standard fly food (if otherwise stated)(Dawydow et al., 2014; Klapoetke et al., 2014; Mohammad et al., 2017; Stierl et al., 2011). However, external retinal supply is necessary for the proper function of csChrimson and gtACRI. Therefore, flies were placed on All-trans retinal (ATR)-containing food (1:1000 ratio of 250mM ATR and fly food) subsequent to eclosion in the experiments where csChrimson and gtACRI were utilized.

Light stimulation of optogenetic tools was done by placing the flies into a custom-built box-like construct, which is here referred to as the “fly disco”. The fly disco consisted of a box lined on the inside by LED light sheets (Figure 2.5A). This device allows one to deliver light pulses in desired intensity and frequency. During the experiments, the fly disco was placed in an incubator that could track and maintain the temperature and humidity at optimum conditions (25°C and 60%, respectively).

Flies were stimulated with 30 sec light pulses every minute with 10% light intensity (for both short- and long-term light stimulation; LED efficiency 160 lm/W, Luminous flux 1.885 lm). Intensity of the LED lights was determined for each genetic tool by expressing the corresponding tool in motor neurons responsible for muscle movement, and inducing the tool with different light intensities until paralysis was observed. Excessive amount of light intensity was refrained since strong light intensity produces heat and causes uncontrollable increase in temperature.

Two different fly discos were built for optogenetic tools: One with red (615-650nm) LEDs and one with white LEDs, to allow the use of different genetic tools that could be stimulated by white (blue) or red lights. ChR-XXL, bPAC, and gtACRI tools were stimulated by white light LEDs (10% intensity), while csChrimson was stimulated in the fly disco with red LEDs.

Short-term optogenetic stimulation;

To test the role of neurons of interest in specific behaviors, optogenetic tools were expressed in these neurons such that they could be activated or inhibited in a controlled manner. In such experiments 5-7d old flies that were raised on standard fly food were placed in the fly disco. Flies were exposed to 30sec light pulses with 30sec intervals during experiments which lasted for 24h.

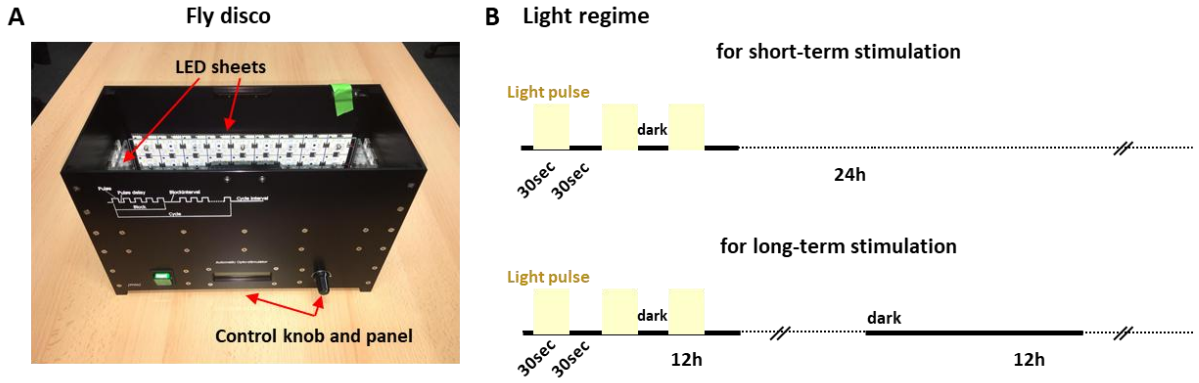

Figure 2.4 Optogenetic stimulator (fly disco) and light regime. **A** Picture of custom-built fly disco. Flies were stimulated by light pulses from LED sheets on the inner wall the machine and pulses were controlled by the control knob and panel. **B** Light regime for short-term (top) or long-term (bottom) optogenetic stimulation. 30sec pulses were delivered with 30sec intervals. For short-term activation this regime continues over 24h hours and for long-term stimulation this continues for multiple days.

Long-term optogenetic stimulation;

Long-term optogenetic stimulation experiments were conducted to investigate the effects of long-term activation or inhibition on the connectivity of neurons of interest The long-term activation protocol consisted of 30ses light pulses (10% intensity) with 30ses intervals given for 12h per day so that flies were not exhausted by constant brightness and so that the circadian rhythm was maintained (Figure 2.5B). Flies were raised on standard food and placed in the fly disco after 3d (as in the case of long-term diet exposure experiments). When moved into the fly disco, flies were also transferred from standard food to isocaloric food. However, in these experiments - since the effect of hypocaloric food was tried to be optogenetically mimicked - flies were placed on isocaloric food during long-term optogenetic stimulation. Anatomical experiments and behavioral experiments were performed to observe if the experimental outcome resembled exposure to hypocaloric food condition case even though flies were kept on isocaloric food.

2.2.13 Statistical analysis

All data sets were, first, subjected to a test for normal distribution using Kolmogorov-Smirnov test. Normally distributed data sets were subjected to either 1-way or 2-way ANOVA dependent on the number of parameters tested. ANOVA tests were followed by Tukey tests for multiple pairwise comparisons. For non-normally distributed data sets, either a Kruskal-Wallis test or a Statistics Permutation test followed by Benjamini and Hochberg correction were used.

2.2.14 2-photon Ca^{2+} imaging

Synaptically localized Ca^{2+} indicators (Pech et al., 2015) were expressed in neurons and calcium imaging was performed using 2-photon microscopy. 5-7d old female flies were used to test odor responsiveness and 10d of female flies' brain were imaged for functional adaptation to long-term dietary. Experimental time lines were as indicated in section 2.2.2. Flies without starvation were imaged throughout. Dissection of the brain and optical calcium imaging were done by Clare E. Hancock. Functional imaging experiments were conducted as described in Hancock et al., 2019.

Fly tethering and opening of the cuticle;

Prior to imaging, flies were briefly immobilized on ice and placed in a custom-built chamber which contained an approximately 2-3mm wide slit built on a glass slide, similar in construction to the gelling chamber used for expansion microscopy. Then, the fly was completely covered by a piece of sellotape and a small window was opened around the head with a razor blade. A small amount of UV-hardening dental glue was applied around the fly's head, leaving a small opening on top of the head, and using a UV light-emitting lamp. After flies were strongly fixed in place by dental glue, a drop of ice cold Ringer's solution was placed on top of the head and the cuticle was removed with a razor blade and fine forceps. Tracheae and lipid tissue were removed using forceps in a way that the dorsal of the brain was completely exposed. The chamber containing the prepared fly was then placed on the microscope stage for imaging.

Odor delivery and monitoring;

After placing the chamber on the stage, some more Ringer's solution was added on top of the fly brain and a water immersion 20X Zeiss objective was descended on the opened part of the head. The fluorescent signal emitted from the neurons was focused on through the binoculars. One of the MB

hemispheres was chosen at random and focused using Zeiss imaging software (Zen Black, 2011). A single z-position was monitored for 21.25sec at a time (as 85 frames, 4Hz). Odors were delivered using a custom-built olfactometer. Each odor was delivered for 2.5sec in a random order that varied between flies. Opening of olfactometer valves, and hence the odor delivery, was controlled by Visual Basics of Applications (VBA) software run in Zen. Odor onset was programmed as 6.25sec after imaging started (at frame 25). The odors used during functional imaging in this study were as follows: MCH (1:750 in mineral oil), 3-Oct (1:500 in mineral oil), Apple Vinegar (AV; 1:100 in water), and fly food (1g/ml of water). Captured frames were saved as image sequences in single files for each fly.

Image analysis

Functional imaging analysis was done using Image J. Single files for each fly were opened as image stacks and brain movement in the x and y directions was corrected using the open source ImajeJ plug-in "template matching". Images that contained strong movement in the z direction were omitted so that lower signal due to the movement out of the imaging plane was not considered as indicative of inhibition of the imaged neurons. Image stacks were smoothened by applying a median filter with factor 2. Further, a maximum z projection was also generated to more easily define the different MB compartments innervated by MB188B DANs. Separate regions of interest (ROIs) were assigned for the different compartments. After ROIs were defined and saved, the same ROIs were opened on the functional imaging stack and the mean fluorescence of the pixels within each ROIwas measured for each frame, through the time series (85 values in total for 85 frames). These values were called "F". For each fly, the mean F of the 8 frames that preceded odor onset (15^{th}-23^{th} frames) were calculated and defined as baseline (F_0) values. Then, the "ΔF" was calculated at each frame by subtracting F_0 from F. Finally, $\Delta F/F_0$ was calculated and plotted over time. Mean traces of each group of flies were plotted by calculating the mean $\Delta F/F_0$ against time (in seconds) and the standard error of the mean (SEM) is shown as shaded lines.

3 Results

The main goal of this study was to investigate structural plasticity in the adult *Drosophila* brain dependent on the experience of the internal state of the animal. Exposure to food with different caloric values was used as an experimental approach. Behavioral adaptations to these changes were investigated as well as structural and functional synaptic plasticity as a fundamental cause of these adaptations. I hypothesized that modulatory neurons innervating the mushroom body (MB) undergo structural modifications dependent on the long-term experience of internal state. These modifications were ultimately aimed to be analyzed as potentially underpinning adapted behavior.

3.1 Caloric value change in the dietary has no effect on the total lifespan of the flies

Prior to investigating any kind of dietary effects on behavior (or on physiological changes in the *Drosophila* brain), it was crucial to test possible impacts of the dietary on the animals' fitness. I made sure that the physiological effects of the dietary resulted from an adaptation to food experience but not from developmental or fitness dysfunctions. Therefore, the fitness of the flies was analyzed under different dietary conditions, i.e. -hypocaloric, isocaloric and hypercaloric dietaries. As a fitness parameter, I measured the total life span of the flies. It should be noted that all flies under any experimental conditions were raised on standard food until they were fully developed (Figure 2.1). Canton S (cs) flies were tested as wild-type flies in these experiments. Experimental details of calculating the survival rate of the flies under different food conditions are described in the method chapter.

Survival rates demonstrated that the longest living flies were 84 days old in every food condition (Figure 3.1A). Additionally, the ages of death of each fly were counted and compared under different food conditions (Figure 3.1B). The mean age of death was 43 days (± SEM 6, 4, respectively) under hypocaloric and hypercaloric food conditions. For the flies kept on isocaloric conditions, this value was 57 (± 5). Even though the mean value of survival under hypocaloric and hypercaloric conditions were lower than under isocaloric conditions, this decrease was not significant. Therefore, I concluded that the increase or decrease in the caloric value in my recipe does not lead to any change in the lifespan of the flies.

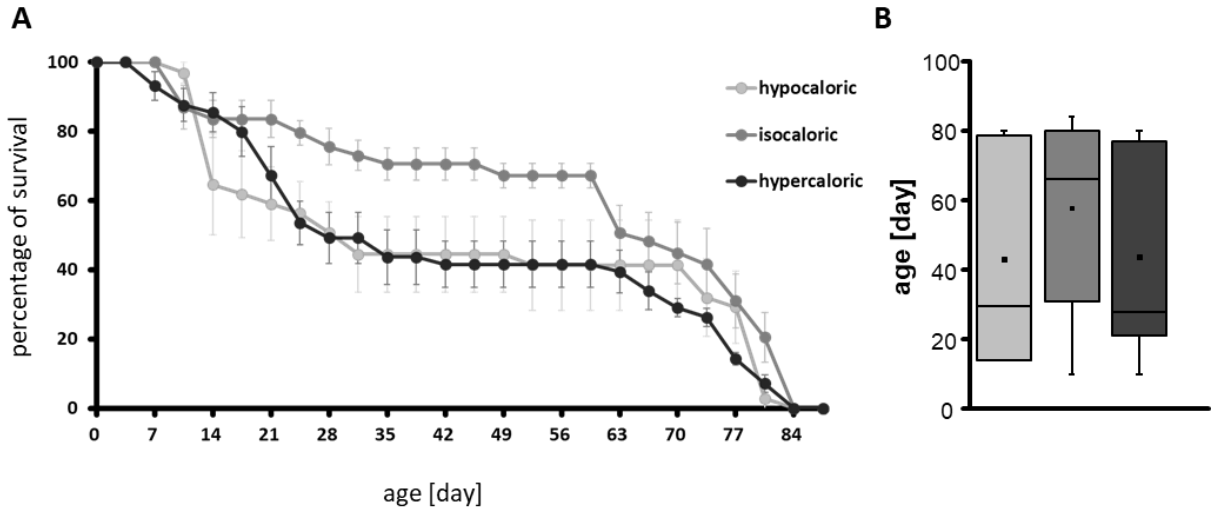

Figure 3.1 Survival rates of the flies on different nutritional conditions. **A** Survival rate on different food conditions. The oldest fly that died on every food type was 84 days old (dots are the mean of the survival percentage. Error bars indicate SEM). **B** Age of the flies on each food type. There was no statistical difference between different conditions (Kruskal Wallis test, p=0.1331,n=25-40).

3.2 Restriction of the calorie in the dietary causes adaptation in certain behaviors

After showing that the overall survival rate of the flies was statistically not significantly different, I asked which type of behaviors might be influenced by the diet. A collection of behavioral experiments related to the motor movement, motivation for food uptake, memory formation, odor and tactile sensation of the flies was performed under different food conditions. These behavioral adaptations were correlated with the physiological changes in the brain in the following chapters. Flies were subjected to the different caloric value dietaries for 7 days, and following behavioral assays were conducted to test the effect of the dietary (Figure 2.1);

First the proboscis extension reflex assay (PER), food uptake with capillary feeder assay (CAFE assay), and appetitive memory formation were analyzed. Fruit flies exhibit these behaviors only if they are motivated. Therefore, the animals subjected to these behavioral experiments were starved prior to the test. The effects of the caloric value on certain sensory systems were also tested in terms of odor avoidance or electric shock avoidance. Additionally, learning and memory formation was also tested under different dietary conditions with an aversive associative olfactory learning paradigm. Flies were not starved in these experiments. Finally, the locomotor activity and sleep were examined. These

examinations were performed by observing and measuring the activity of the flies for 3 days while the same type of food was maintained during the experiment.

3.2.1 Food uptake is enhanced upon previous experience of low calorie value of food

In this section, the behaviors that depend on the internal state and the motivation for food uptake were examined after the exposure of the flies to different dietaries for seven days. As the first example of these behavioral types, PER percentages showed that the flies fed on isocaloric food extend their proboscis 20% of the times upon sugar stimulation. This score was significantly more (> 50%) in flies fed on the less caloric value and significantly less in flies fed on the high-calorie diet (Figure 3.2A). These results confirmed that when the caloric value was restricted in the dietary, flies tend to extend their proboscis more to an appetitive gustatory stimulus. Since *Drosophila* extends the proboscis only in dependence of the motivation for food uptake, the increase in the PER score under the calorie restriction condition indicates an increased motivation to do so (Wang et al., 2004).

As a second behavioral test, food consumption of the flies was also measured in µl per day. The measurements of the consumed sucrose volume showed that the flies consumed around 0.4 µl sucrose solution per day when previously exposed to the isocaloric diet. However, when the flies were exposed to less calories, food consumption increased significantly compared to the flies under isocaloric and hypercaloric conditions (Figure 3.2B). All flies were starved for 24h and given the same sugar solution during experiment. Therefore, the increase in the food uptake is concluded to reflect an adaptation dependent on the calorie restriction.

As the final motivation-dependent test, appetitive memory formation under different food conditions and different starvation periods were measured. The appetitive learning ability of *Drosophila* is highly dependent on the internal state (Tempel et al., 1983). In my case, satiated flies also failed to associate a conditioning stimulus (odor) with an unconditioned appetitive stimulus (sugar) (Figure 3.2C). Additionally, the learning scores of all the fly groups starved for 24 hours were around 0.5 and not different from each other under any conditions either (Figure 3.2C). However, when the starvation duration was 6h, the flies that were exposed to calorie restriction in dietary demonstrated a significantly higher learning index (>0.5) compared with the flies fed with isocaloric or hypercaloric diets (Figure 3.2C). This memory formation under the 6 hours starvation period is an indication of an enhanced motivation based on the internal state of the flies that experienced a long-term calorie

restriction.

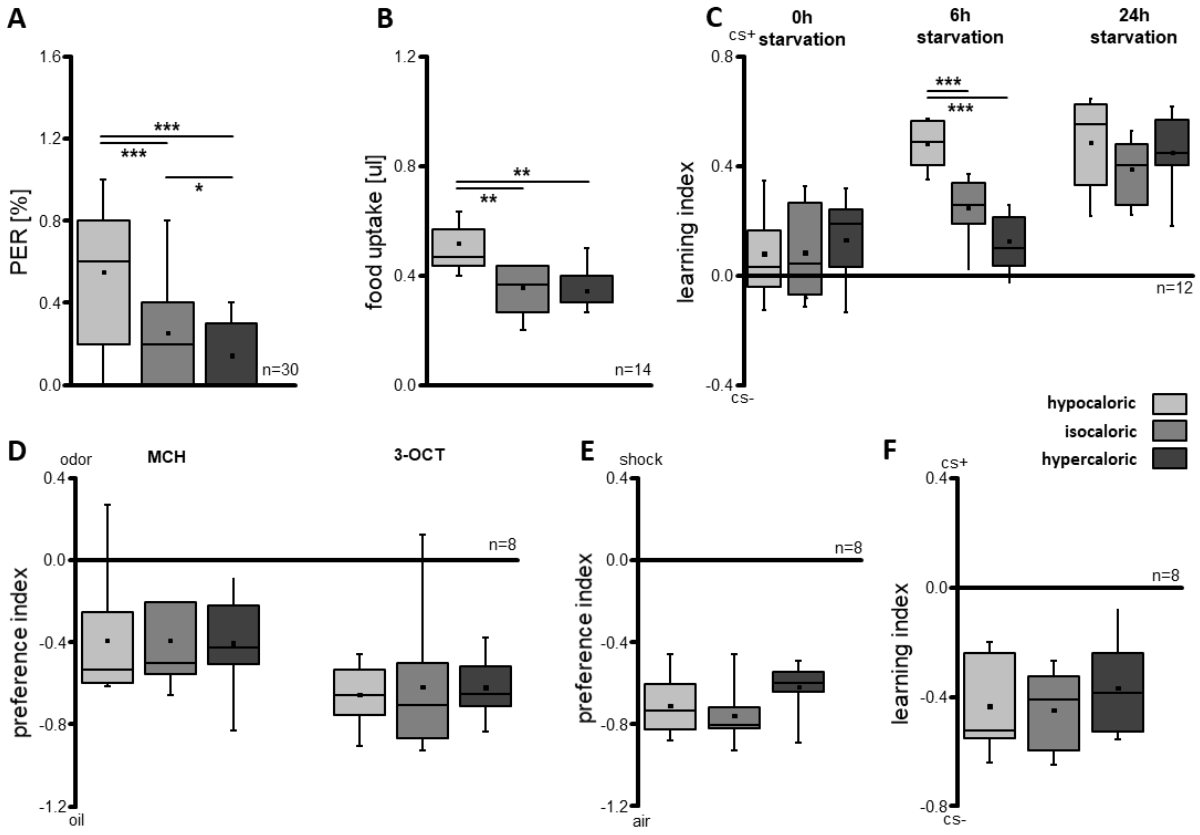

Figure 3.2 Behavioral adaptations dependent on the long-term different dietary. **A** PER score (%) upon sugar stimulus dependent on the diet. PER increased significantly along with the decrease in the caloric value. **B** Food uptake (µl) measured by CAFE assay. Restriction of the calorie in the dietary caused an increase in the sugar solution consumption. **C** Appetitive memory formation scored as learning index. The flies showed an enhanced score under short starvation condition when the caloric value of food was restricted. **D** Odor preference and **E** the electric shock avoidance scored as preference index. These scores were not altered dependent on the dietary as well as the **F** aversive olfactory memory formation (One-way ANOVA followed by Tukey tests,* p<0.05, ** p<0.01, *** p<0.001; PER, learning and avoidance experiments were performed by Haiko Poppinga).

3.2.2 Aversive learning and aversive responses to repulsive stimuli are not affected by the previous experience of high or low caloric values of the food

In the previous section, the foraging and feeding-related behaviors of the flies were shown to be dependent on the caloric value of the food. This is not surprising as more hungry animals eat more, approach food more vigorously by proboscis extension, and show a higher motivation to appetitively learn. In this section, the dependence of an aversive olfactory sensation, shock avoidance, and aversive olfactory memory formation were tested. These behaviors are not dependent on the internal state of

the flies. Hence, any effect of the caloric value restriction on these behaviors would conclude that the adaptation is not restricted to the feeding-related behaviors.

Two-choice assays showed that the flies showed avoidance against repulsive odors (1:36 dilution of 3-Oct and MCH; Figure 3.2D) as well as an electric shock stimulus (90V; Figure 3.2E) were not affected by different dietaries. The aversion score towards two odors utilized in this study were also not different from each other. As the same concentrated odors were used in all learning experiments, the enhancement in the appetitive learning upon the calorie restriction is concluded as increase in motivation rather than the adaptation in the olfactory sensation.

Additionally, the flies exposed to different dietaries were tested for aversive associative memory formation. Exposure to different dietary conditions did not affect the aversive stimulus learning ability either (Figure 3.2F). The flies tested for aversive memory were also starved for 6h so that the change in the memory formation could be compared to the previously observed appetitive memory formation enhancement.

As a result, I conclude that the motivation for food uptake increases when the calorie value of the food is restricted. Moreover, these effects of the dietary are restricted to feeding-related behaviors including appetitive learning.

3.2.3 The flies' locomotor activity and sleep is not altered by the dietary

It is known that flies exhibit hyperactivity and arousal as well as the sleep delay when starved (McDonald and Keene, 2010). Thus, I tested the activity and sleep behavior of the flies exposed to different dietaries for two reasons: The first reason was to see if these behaviors are also affected as a result of different food conditions. The second reason was to understand if the flies, if restricted in calories, show more arousal or hyperactivity like starved flies. Here it should be noted that the corresponding fly food was supplied during the experiment.

To analyze the last type of behavioral adaptation, 10d old male flies that were exposed to different dietaries for 7 days were tested for their activity by counting the number of crossings of the midline laser beam in the activity monitor (see section 2.2.7). Flies were considered as "sleeping" if no beam

crossing was observed in five minutes. Following these counts, the average actogram of the flies and the standard error (SE, shaded area) are plotted against the light/dark period of the day (Figure 3.3).

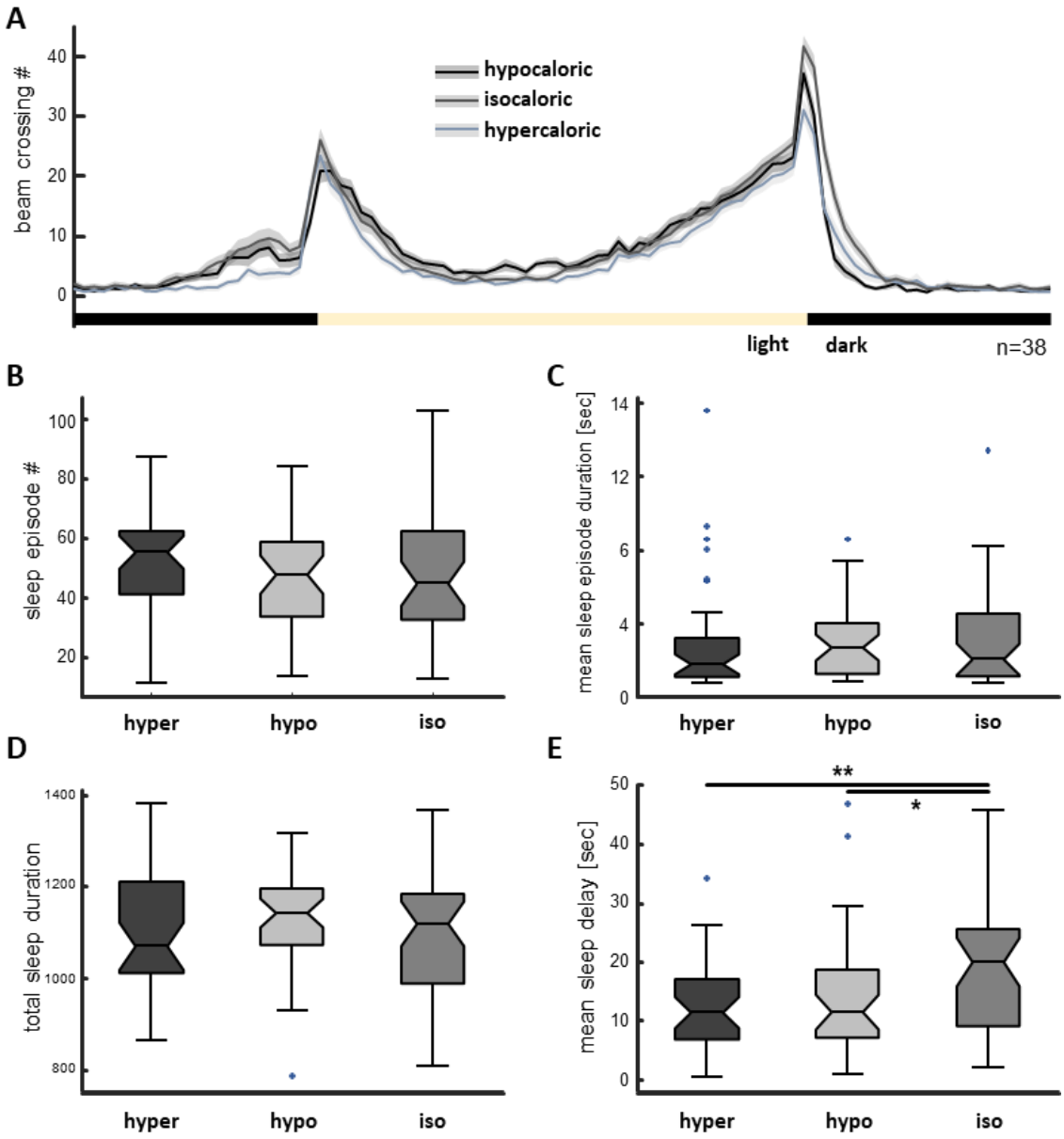

Figure 3.3 Long-term diet effect on the activity and sleep regulation. **A** Actogram of the flies as beam crossing number per 15 minutes plotted against light/dark cycle. The activity pattern was not influenced by the long-term diet. There was a slight late activity amplitude increase under isocaloric food condition (line is the mean trace, shaded areas are SE). **B** Number of the sleep episodes, **C** averages of the sleep durations, and **D** total sleep durations of the flies (in sec) under different dietary conditions. The sleeping behavior in terms of the average duration and the number of sleep episodes, hence the total sleep duration was not affected by the long-term exposure to different dietaries. **E** Latency of the sleep in seconds under different dietary conditions. The flies

subjected to high or low-calorie dietaries showed early sleeping (Statistics: Permutation test followed by Benjamini and Hochberg correction, **p=0.00175, *p=0.0131; in collaboration with Dr. Bart Guerten).

The actogram plot demonstrates that the circadian rhythm of the flies followed the same pattern under any dietary conditions. In all cases an activity bout was observed with the onset of the daylight (first bout) and shortly before the sleep induction following the daylight offset (second bout). The only difference was that the amplitude of the second activity bout was the highest when the flies experienced an isocaloric dietary (Figure 3.3A). This means that any decrease or increase in the caloric value of the dietary results in early evening activity decrease.

Moreover, the analysis of the sleep episodes demonstrated no difference under any dietary conditions. Flies had the same number of sleeping episodes as well as the average sleep episode duration independent of their dietaries (Figure 3.3 B and C). The total sleep duration also remained unaltered correlated with the number and the duration of the sleep episode number (Figure 3.3D). However, when the sleep initiation was measured, I observed that any kind of change in the caloric value of diet results in an early sleep compared to the flies fed with isocaloric diet (Figure 3.3E). These results were also correlated with the decrease in the second activity bout.

Here, I draw the conclusion that locomotor activity and circadian rhythm of the flies are not influenced by the exposure to high or low caloric values in the food, except for the initiation of the sleep. Additionally, no arousal or sleep delay was observed under calorie restriction conditions. This means that the flies restricted in terms of nutrition are not constantly starved when fed with hypocaloric food.

In summary, the behavioral tests conducted with the flies with a prolonged pre-experience of food conditions with high or low caloric values demonstrated that feeding-related behaviors of the flies such as PER (Figure 3.2A), food uptake (Figure 3.2B), and the appetitive olfactory learning (Figure 3.2C), reflected the motivation for food uptake. On the contrary, other sensory abilities, like aversive odor avoidance (Figure 3.2D) or shock avoidance (Figure 3.2E), were not altered; neither was aversive olfactory learning and memory formation (Figure 3.2F). Finally, the circadian rhythm and activity of the flies also remained unaffected, except for a slight sleep delay (Figure 3.3). Thus, these adaptations to the change in the nutritional conditions were restricted to feeding-related behaviors.

3.3 Calorie restriction alters the connectivity in the fly brain

The main motivation of this study is to demonstrate that certain connections in the adult fly brain remain plastic. So far, I demonstrated that modifications in feeding-related behaviors of *Drosophila* can reflect a long term calorie restriction.

In this chapter, structural neuronal circuit modifications underlying behavioral adaptations will be described. I focused on structural and functional plasticity of the MB-related DANs dependent on the food conditions (see section 1.5).

To examine the connectivity of the MB-related neurons, I utilized the method of splitGFP (spGFP) reconstitution that occurs as a result of close proximity between neurons (Feinberg et al., 2008; Pech et al., 2013). In this study, this reconstitution was referred to as "GRASP" signal (or fluorescence) and used as a measure of potential connectivity, as in other studies (Feinberg et al., 2008; Gordon and Scott, 2009; Pech et al., 2015). As a first step, GRASP fluorescence between the Kenyon cells and MB-extrinsic DANs was measured in flies exposed to different dietaries.

3.3.2 SplitGFP reconstitution between distinct dopaminergic neurons and Kenyon cells is altered upon prolonged calorie restriction

To investigate a potential change in connectivity between the MB KCs and different populations of DANs, transgenic flies expressing one part of the splitGFP under the MB-specific promoter Mb247 (Schulz et al., 1996) and carrying a transgene of the second part of splitGFP under UAS control were crossed with the flies expressing specific DAN-Gal4 drivers. The working principle of the reconstitution of spGFP is illustrated in Figure 3.4A. Altogether, the resulting flies that were analyzed contained the following transgenes: 1.) One domain of the splitGFP under control of KC-specific promoter, 2.) the complimentary domain that is driven by the UAS (MB247-spGFP11 and UAS-spGFP1-10 respectively; Pech et al., 2013). 3.) In addition, DsRed was expressed also under control of the MB-specific promoter mb247 (Riemensperger et al., 2005) as a landmark. These flies were exposed to hypocaloric, isocaloric and hypercaloric dietaries for 7 days, and the GRASP fluorescence was quantified.

I aimed at investigating the majority of DAN populations that innervate the three lobes of the MB (α/β, α'/β', and γ; Figure 3.4B; Strausfeld et al., 1998).Three different fly strains expressing Gal4 drivers for different DAN populations were crossed with the UAS-MBGRASP flies, i.e., R58E02-Gal4, TH-Gal4, and MB188B-Gal4 (Figure 3.4B; Friggi-Grelin et al., 2003; Liu et al., 2012). R58E02-Gal4 labels the majority of the PAM cluster DANs that innervate the vertical lobes of the MB. The compartments of the MB that are predominantly innervated by these DANs are α1, β1 and β 2, β'2, γ4 and γ 5 (Mao and Davis, 2009; Rohwedder et al., 2016; Figure 3.4B and Figure 3.4D).

The TH-Gal4 driven DANs originate from the PPL1 cluster and are involved in aversive learning. These neurons innervate the horizontal MB compartments like α3, α'3, α'1, α'2, β2, and β'2, (Friggi-Grelin et al., 2003; Pech et al., 2013; Figure 3.4B and D).

The third population of DANs that was analyzed in this study is driven by a split Gal4 (spGal4) driver; the MB188B-Gal4 (Aso et al., 2014). These DANs derive also from the PAM cluster and innervate mainly the β'1 and γ3 compartments and partially the γ4 compartment (Figure 3.4B and Figure 3.4C). These three different DAN populations are referred to as R58E02-DANs, TH-DANs, and MB188B-DANs in this study.

In the connectivity analysis, the fluorescence intensity of splitGFP reconstitution was quantified separately for each compartment and normalized to the mean fluorescence under isocaloric food conditions. Thus, the mean of the fluorescence intensity of each isocaloric fly group is equal to 1 for each compartment.

GFP reconstitution between R58E02-DANs and KCs (and similarly TH-DANs and KCs) were described in study of Pech et al., 2013. My confocal imaging stacks of the splitGFP reconstitution fluorescence of different drivers demonstrated an additional partial and dimmer signal in some compartments which were not described in this study as the main innervated compartments (Figure 3.C and D). These signals must be due to the proximity of two spGFP expressing partners. Thus, the fluorescence signal was also more variant. Any fluorescence change in such compartments would require a further investigation with a more specific driver line. However, all compartments that were innervated mainly or partially, were analyzed and included in the graphs (Figure 3.4C and Figure 3.4D).

I observed a wide range of variance in the GRASP signal in the MB compartments which has dim fluorescence signals resulting from R58E02-DANs and TH-DANs (Figure 3.4D). Despite this varience, there was no statistically significant change in the overall fluorescence intensity among the different feeding conditions. There were also no compartment-specific changes under any conditions (Figure 3.4D). These results suggest that the connectivity between these DANs and KCs were not affected by the food conditions.

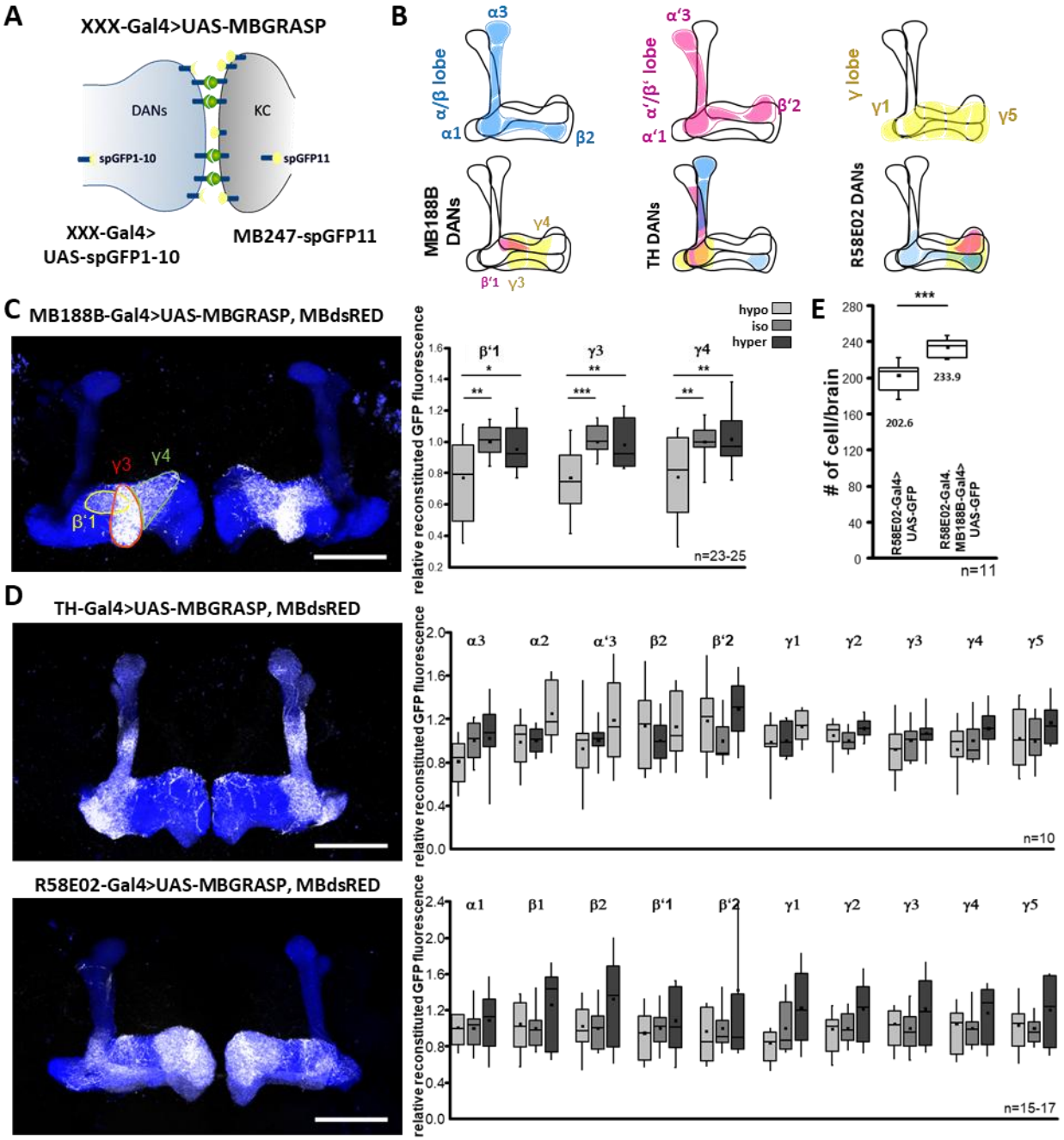

Figure 3.4 Change in splitGFP reconstitution fluorescence between KCs and DANs dependent on the long-term diet. **A** Illustration of the working principle of spGFP reconstitution (also called "GRASP") technique. The spGFP

was reconstituted by the proximity of the two potential synaptic sites between the KCs and DANs. Different DAN populations were driven by a specific Gal4 line. **B** Illustrations of the MB lobes (α/β, α'/β' and γ lobes) on the upper row. Innervation patterns of populations of DANs used (bottom row). The three populations of DANs examined here innervated the MB differentially in a complementary manner (partial or superficial innervations are not included). **C** Confocal stack of the splitGFP reconstitution between the MB188B DANs and the KCs on the left side. MB 247-DsRED labels the MB (splitGFP reconstitution in grey, MB247-DsRED in blue). The relative fluorescence dependent on the dietary is shown on the right-hand side. Different compartments innervated by the MB188B DANs are shown in yellow, red and green lines (β'1, γ3, and γ4, respectively). The splitGFP reconstitution fluorescence decreased dependent on the calorie restriction in dietary (One-way ANOVA followed by Tukey-test, ** $p<0.01$, *** $p<0.001$). **D** Confocal stack of splitGFP reconstitution between TH-DANs or R58E02 DANs (on the left column) and the relative fluorescence (on the right column; splitGFP reconstitution in grey, MB247-DsRED in blue). Relative fluorescence values in R58E02-DANs and TH-DANs did not show any significant change under different food conditions (One-way ANOVA followed by Tukey-test, $p>0.05$). **E** Number of t DAN somata expressing GFP per brain. 202 (SD ± 18) cells were labeled by the R58E02 driver and 233 (± 12) by the MB188B and R58E02 drivers together (Students' t-test, *** $p<0.001$; all scale bars 50µm).

On the contrary, the splitGFP fluorescence of the MB188B-DANs showed a significant decrease (~30%) in all compartments under hypocaloric dietary condition. This decrease was significant to the isocaloric and hypercaloric correspondence (Figure 3.4C). Since the decrease occurred in the same fashion in all compartments, I assumed that the decrease in connectivity occurs homogenously. Hence, in the future plots, the overall average signal was calculated and summarized as one plot instead of a compartmentalized fashion.

As a conclusion, MB188B. DANs have lower physical proximity to the MB KCs dependent on the long-term experience of the calorie restriction whereas the proximity between other DANs and KCs remain unaffected in the *Drosophila* brain.

3.3.3 Dopaminergic neurons of the MB188-Gal4 driver line are not entirely part of those dopaminergic neurons labelled by the R58E02-Gal4 driver line

The MB188B-DANs cover MB compartments that are not covered by the R58E02- and TH-DANs. The R58E02-Gal4 driver was considered to label almost all PAM DANs (Liu et al., 2012). However, the γ3 and 4 compartments of the MB were not covered by this driver line (Figure 3.4B and D). It is also known that the PAM-DAN number is greater than the number of the DANs labeled by the R58E02-Gal4 (Aso et al., 2014a; Mao and Davis, 2009; Tanaka et al., 2008). To determine the fraction of MB188B neurons that belong to the R58E02-driven PAM cluster DANs, the number of the R58E02-DANs and the number of the R58E02-DANs together with MB188B-DANs were counted by expressing GCaMP3 as a reporter

protein in these cells. This revealed that there were 202 (± 18.7) R58E02 DANs per brain. When both cell populations were counted, there were 233 (± 12.1) cells labeled per brain (Figure 3.4E). These results indicated that the most common PAM DAN driver R58E02-Gal4 fails to cover all the PAM DANs entirely and there are at least 30 more cells per brain that are not labeled by it.

Additionally, the difference between two cell populations is supposedly the number of the cell labeled exclusively by the MB188B driver. This difference was calculated as 31 cells per brain. However, in the activity quantification assay (in section 3.7), I observed more than 40 cells per brain driven by the MB188B-Gal4. Thus I concluded that at least 10 cell per brain in the *Drosophila* PAM DANs are labeled by both the R58E02-Gal4 and MB188B-Gal4 drivers (Figure 3.4E).

3.3.4 The connectivity of dopaminergic neurons innervating the γ3 compartment of the mushroom body and Kenyon cells remains unaffected

Based on the connectivity analysis using splitGFP reconstitution and the cell number analysis on R58E02-DANs, I concluded that the R58E02-Gal4 driver fails to label all DANs that innervate the γ3, γ4 and β'1 compartments. Some of the DANs from the PAM cell cluster innervate only the γ3 compartment (Aso et al., 2014a). These very specific DANs can be labeled using other Gal4 driver lines, i.e., MB441B-Gal4 and MB195C-Gal4. These two driver lines label ~14 and two cells per hemisphere, respectively (Aso et al., 2014a).

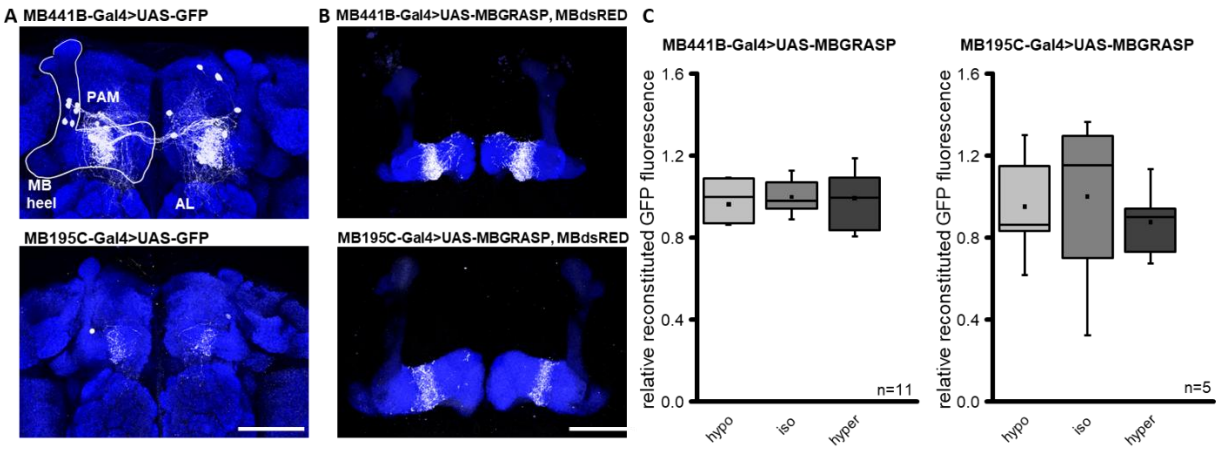

Figure 3.5 Connectivity between the γ3 DANs and KCs dependent on the long-term exposure to different caloric food values. **A** Confocal stacks of the GFP expressing MB441B and MB195C-DANs. The GFP was expressed in ~14 and two somata respectively residing on the PAM region (grey is GFP signal, blue is Brp background staining, MB is indicated by white borders, PAM and AL is located). **B** Confocal stacks of the GRASP signal between the KCs and

MB441B and MB195C DANs. These DANs innervated the γ3 compartment (GRASP in gray, DsRED in blue; scale bar 50µm) **C** Quantification of the relative GRASP fluorescence. There was no change observed under different dietary conditions (One-way ANOVA, p>0.5).

I questioned whether the MB188B-DANs are a homogenous cell population and if these two DAN populations show a similar change in connectivity with KCs in dependence to a prior experience of low caloric food as it is the case for MB188B-DANs. Therefore, the connectivity of these DANs to the MB was also analyzed under different dietary conditions. First, I confirmed the cell numbers and the connectivity of the MB441B-DANs and MB195C-DANs. The fly brains expressing GFP under the control of these drivers were stained against a presynaptic marker protein Burchpilot (Brp) as a background to identify the neuropils (Figure 3.5A). Additionally, the connectivity in the MB γ3 compartment was also confirmed by the expression of the MBGRASP complex in these cells (Figure 3.5B).

When the splitGFP fluorescence intensity between these DANs and the KCs was quantified under different food conditions, no significant change was observed between the various conditions (Figure 3.5C). Based on these results, I concluded that the connectivity of these γ3-innervating DANs and KCs do not undergo any structural modifications. Additionally, the connectivity decrease occurred homogenously in the MB188B DANs upon calorie restriction (Figure 3.4C). Thus, it is likely that these DANs are not a part of the MB188B DANs.

3.3.5 The connectivity of mushroom body output neurons innervating the γ3 compartment remain unaffected

In order to obtain a better understanding of the decrease in the connectivity between MB188-Gal4 DANs and KCs, all components of the MB-related cicuitry in the same functional compartment were subjected to a similar connectivity analysis under different dietary conditions. Another component in the MB circuitry are the MBONs (Tanaka et al., 2008). Additionally, based on the earlier results, I asked if the re-wiring of the MB188B DANs and KCs was also reflected in a re-wiring of the respective downstream neurons. Therefore, in the following section the connectivity analysis of the corresponding MBONs are shown under different dietary conditions.

There are two MBON drivers called MB110C-Gal4 and MB83C-Gal4 that label a pair of neurons on each hemisphere (Aso et al., 2014a). These MBONs are likely to be downstream of the MB188B DANs since these MBONs innervate the β’1 and γ3 compartments on the MB (Aso et al., 2014a; Figure 3.6A). When

the splitGFP fluorescence intensity between these MBONs and KCs was quantified, no difference was observed under different dietary conditions (Figure 3.6B). Therefore, I concluded that the connectivity of the MBONs and KCs was not affected either by the experience of different dietaries.

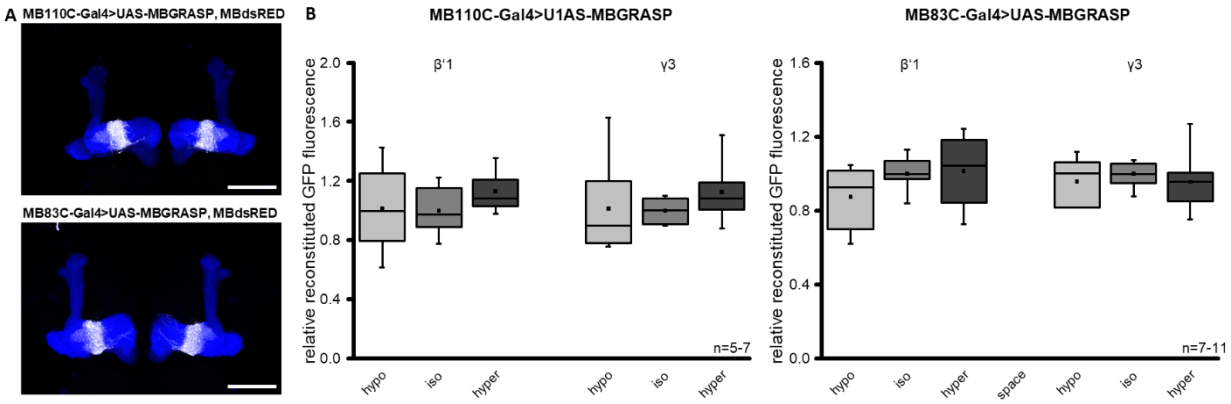

Figure 3.6 Connectivity between the γ3 and β'1 innervating MBONs and the KCs dependent on the long-term diet. **A** Confocal stacks of the GRASP signal of the MB83C MBONs and MB110C MBONs. The GRASP signal confirmed the innervation to the γ3 and β'1 compartments of the MB (GRASP in grey, DsRED in blue; scale bar 50µm). **B** Quantification of the relative GRASP signal of both MBONs under different dietary conditions. There was no change observed in the connectivity dependent on the dietary (One-way ANOVA, $p>0.5$).

As the final component of the MB-related circuitry, the KCs were also examined. A study conducted by David Vasmer in his doctoral study showed that the KCs do not differ in terms of cell structure under any dietary conditions (Vasmer, 2017). The same dietary conditions were presented to the flies in this study as well.

Therefore, I concluded that the connectivity decrease in the MB-related neurons under hypocaloric condition was specific for MB188B DANs.

3.4 Structural properties of the dopaminergic neurons labelled by the driver line MB188-Gal4.

In the previous chapter, a first indication of potential structural changes was shown. To obtain a more comprehensive understanding of these putative connectivity changes, I tried to characterize the structures of the MB188B-DANs in detail. The dissection and synaptic compartmentalization of the

MB188B DANs neurites was crucial to decipher how and where the structural changes might exactly occur.

Therefore, in this chapter, dendritic and axonal arborizations along with the pre- and postsynapses themselves were investigated. Finally, neurons postsynaptic to these DANs were also investigated.

3.4.1 Dopaminergic neurons of the MB188B-Gal4 strain are a subpopulation of the dopaminergic neurons of the PAM cluster

I showed already in the cell number analysis that the MB188B-DANs are part of the PAM cluster. It has been also shown that these neurons reside in the PAM region of the brain (Aso et al., 2014a). My anatomical pictures of these DANs also demonstrate that the cell bodies of the MB188B-DANs reside within the PAM region (Figure 3.7A). However, I argued above that there are at least 10 cells per brain that were exclusively labeled by the MB188B driver and not by the commonly used driver R58E10-Gal4 (Figure 3.4E). Therefore, I addressed the possibility that this driver line may label an additional group of cells that may not be dopaminergic. Thus, a further verification was needed to prove that the MB118B neurons are all dopamine-expressing PAM neurons prior to conducting any anatomical investigations.

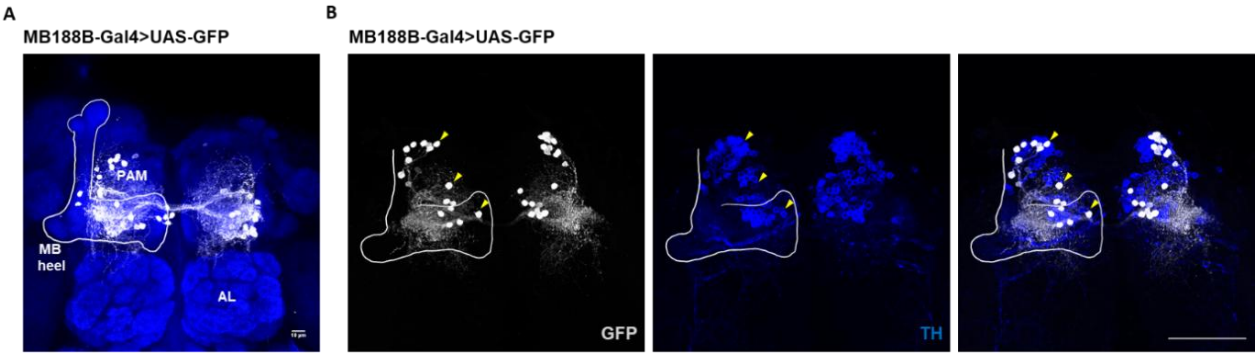

Figure 3.7 Characterization of MB188B-Gal4 DANs. **A** Confocal stack of the GFP expression under the control of the MB188B-Gal4 driver. The MB188B DANs were confirmed to have the cell bodies on the PAM region (white line is the borders of the MB, GFP in gray, Brp background in blue; scalebar 10µm). **B** Confocal stack of the GFP expression in the MB188B cells and the anti- tyrosine hydroxylase (TH) staining. Each cell body labeled by the GFP was positive for the TH antigen. (yellow arrowheads; white line is the border of the MB; GFP in gray, Brp background in blue; scalebar 50µm).

Tyrosine hydroxylase (TH) is the rate-limiting enzyme in the DA biosynthesis and accepted commonly used marker for dopamine-releasing neurons (Budnik and White, 1987). Therefore, GFP-expressing

MB188B-DANs were stained using an antibody against TH. I confirmed that the somata of these neurons were localized to the PAM region (Figure 3.7A). Additionally, all MB188-DANs expressing GFP were TH positive (Figure 3.7B). Thus, all the MB188B cells are dopaminergic PAM cluster neurons.

3.4.2 Dopaminergic neurons of the MB188-Gal4 strain have reciprocal synapses with Kenyon cells

For a further structural analysis, the anatomy of the MB188B-DANs was dissected into dendritic branches and axon terminals by expressing a dendritic marker DenMark (Nicolaï et al., 2010) and the presynaptic marker sytGFP for the axon terminals (Zhang et al., 2002). At a first glance, the dendritic tree and axon terminals seemed like two distinct neurites that are either branching outside of the MB or innervating in the MB, respectively (Figure 3.8A). These results gave me a first impression that the majority of MB188BDANs receive input from the surrounding of the MB. Also, they mainly provide output onto the KCs, which supports the general idea that DANs are mainly presynaptic to the KCs (Claridge-Chang et al., 2009; Mao and Davis, 2009; Riemensperger et al., 2005).

However, in addition to this general anatomical organization, the confocal microscopy images of DenMark and sytGFP localizations revealed that some sytGFP signals occured also outside of the KCs (Figure 3.8A, yellow arrowhead). Moreover, there was also DenMark staining directly on the MB lobes, especially on the β'1 region (Figure 3.8A). This can be explained by the well-described reciprocal synapses between DANs and KCs (Cervantes-Sandoval et al., 2017; Eichler et al., 2017; Inagaki et al., 2014).

In order to confirm this possibility, and also to eliminate potential cross-reactivity of antibodies, a further analysis of pre- and postsynaptic neurites was performed. Pre- and postsynaptically localized functional sensors, UAS-sypGCaMP3 and UAS-dHomerGCaMP3 respectively, were expressed simply as markers under control of the MB188B-Gal4 driver line. Then, the fly brains were stained against the GFP and a background marker Bruchpilot. As a result, an overall pre- and postsynaptically localized GFP expression was observed. (Figure 3.8B).

These results provided a further indication that there was no clear functional input-output distinction between the dendritic branches of the MB188B-DANs and the axonal terminals. Having pre- and postsynaptic compartments nearby can also be indicative of reciprocal synapses (Cervantes-Sandoval et al., 2017; Eichler et al., 2017).

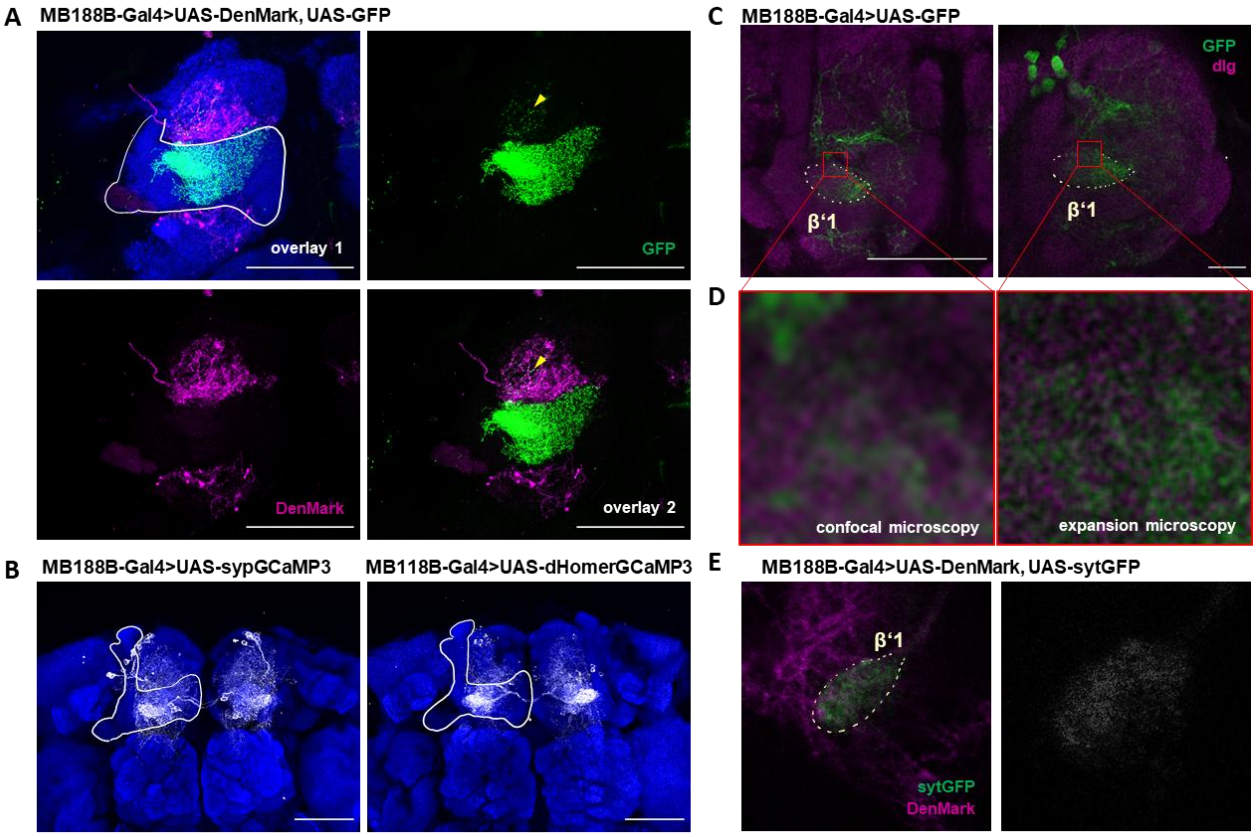

Figure 3.8 Anatomical dissection of dendrites and axons of MB188B-DANs. **A** Confocal microscopy stack (z-projection) of the dendritic tree marker DenMark and the presynaptically localized sytGFP in MB188B-DANs. The presynaptic compartments of the MB188B-DANs innervated mainly the MB (indicated by the white line), while the dendritic arborization mainly surrounded the MB. Some co-localizations between two signals were also observed (indicated with the yellow arrowhead; background Brp in blue, GFP in green, DenMark in magenta; scale bar 50µm). **B** Confocal microscopy stack (z-projection) of GFP staining against pre- and postsynaptically localized Ca^{2+} indicators (sypGCaMP3 and dHomerGCaMP3, respectively; Brp in blue, GFP in grey, MB is indicated by the white line; scale bar 50µm). Expression pattern of the pre- and postsynaptically localized indicators were not distinct from each other. **C** Single confocal plane of the GFP expression in the MB188B DANs imaged by the standard imaging protocol (on the left column) and by the expansion microscopy protocol (on the right column; anti-GFP in green, anti-Dlg in magenta; scale bar 50µm). **D** The red areas indicated in C were magnified. Fine arborizations of the MB188B-DANs (in green) and the postsynaptic background staining (in magenta) could be resolved. **E** Single plane of an expansion microscopy image of the DenMark and sytGFP expressions in the MB188B DANs. The MB β'1 compartment innervation of the MB188B DANs was indicated (dashed yellow line). The dendritic tree was labeled in magenta whereas the presynaptic puncta were in green in the left panel. Double positive pixels for both markers (supposedly reciprocal synaptic sites) were shown in grey in the right panel.

To test the possibility of the reciprocal synapses more directly, a recently developed imaging technique called "expansion microscopy" was used on the fly brains that expressed DenMark and sytGFP in MB188B-DANs. This technique is based on the physical expansion of the sample by perfusion with an

acrylic based gel (Asano et al., 2018; Chen et al., 2015). This technique was employed to visualize finer arborizations that cannot be resolved under the regular sample preparation and imaging techniques.

By taking the advantage of the expansion microscopy technique I could expand the samples by approximately four times (Figure 3.8C). The finer structures that were not possible to detect using confocal laser scan microscopy became visible in the expanded sample (Figure 3.8D). Additionally, a co-localization analysis of the dendritic arborizations (magenta) and the presynaptic sites (green) was also possible (Figure 3.8E). Colocalized pixels are shown in grey in Figure 3.8E.

In conclusion, this structural analysis revealed that the MB188B neurons are part of the PAM DANs and most likely have reciprocal synapses with KCs that can possibly undergo modification upon the experience of nutrition restriction.

3.4.3 Dopaminergic neurons of the MB188B-Gal4 line are also postsynaptic to themselves

Based on the results showing that the MB188B DANs have reciprocal synapses on the MB (Figure 3.8), it is logical to think that these synaptic sites might provide reciprocal feedback. The mechanism behind this feedback might be an autoregulation or a regulation from the MB itself. The first possibility suggests that the MB188B DANs are both pre- and postsynaptic to themselves. Therefore, I have tested the possibility of the MB188B DANs being postsynaptic to themselves. I took the advantage of a recent system that labels all the postsynaptic downstream partners of a cell population of interest called *trans*TANGO (Talay et al., 2017). The *trans*TANGO system is based on a pan-neuronally expressed cleavable postsynaptic receptor and downstream mtdTomato expression upon the cleavage of this receptor. Thereby, the mtdTomato would be expressed only in the cell population postsynaptically connected to the interested cell population. Furthermore, the cell populations of interest are labeled by the expression of GFP. To determine the neurons that are postsynaptic to of the MB188B-DNAs, the MB188B-Gal4 driver was combined with the UAS-*trans*TANGO. Thus, the MB188B DANs were detected by GFP expression whereas all the postsynaptic partners were labeled by mtdTomato.

A number of neurons labeled by mtdTomato, located in a variety of the brain regions, were observed as postsynaptic to the MB188B DANs. For example, some neurons were localized in a most dorsal part that could be potentially neuromodulators such as SIFa (Martelli et al., 2017; arrowhead; Figure 3.9A).

Moreover, a quite wide range of postsynapses is distributed across the entire CNS (Figure 3.9A), including the MB.

Since this study is focused on structural plasticity in MB-extrinsic DANs, the MB and surrounding cells expressing mtdTomato were subjected to further characterization (Figure 3.9B and C). A population of the PAM neurons seemed to express mtdTomato (Figure 3.9B). However, what was more interesting here is that some double-labeled cell bodies were also observed (Figure 3.9B; yellow arrowhead). These results indicated that a part of the MB188B PAM DANs was postsynaptic to itself. This post-synaptic MB188B DANs could be an evidence for an autoregulatory mechanism. Therefore, it can be speculated the structural connectivity decrease could be achieved by a feedback mechanism dependent on the MB188B DANs own activity upon calorie restriction. Here, the additional feedback coming from the MB cannot be ruled out.

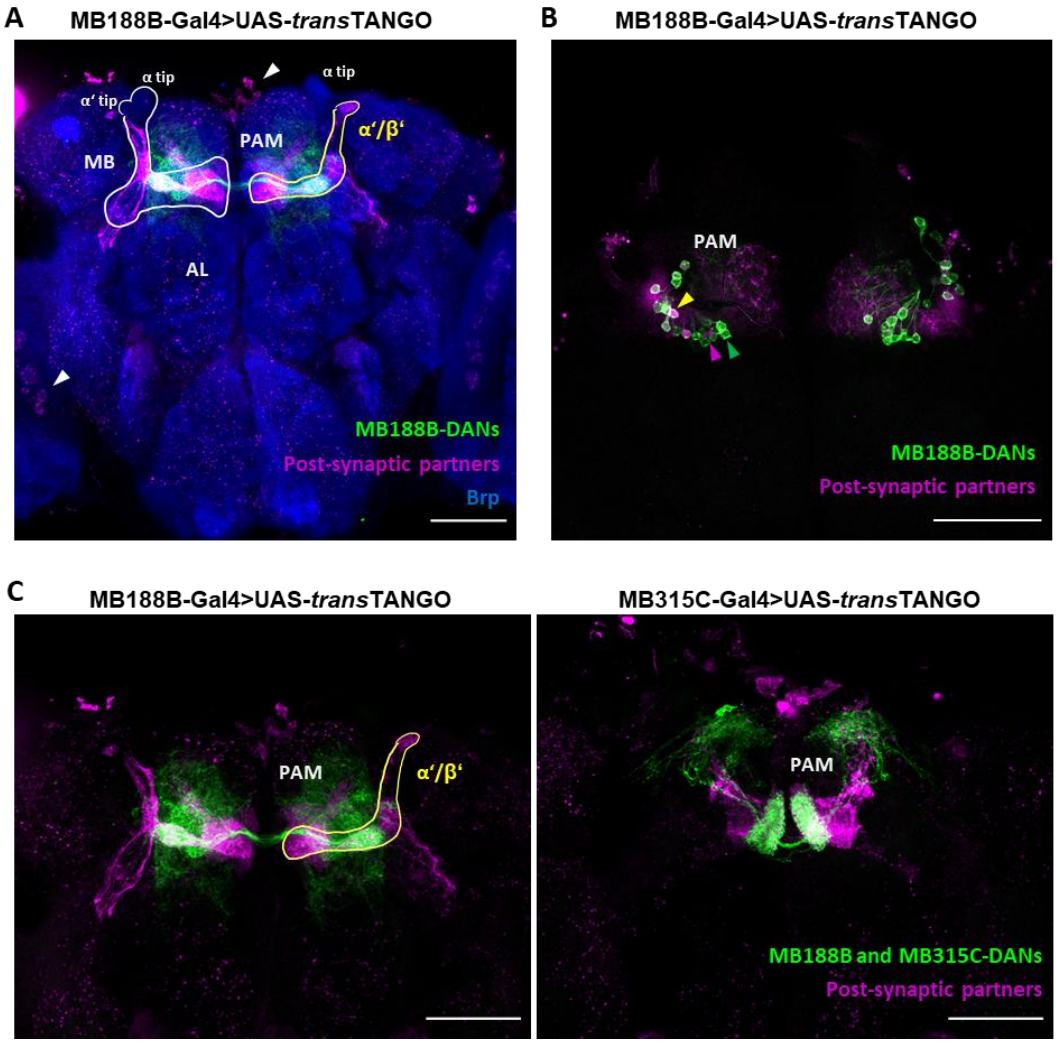

Figure 3.9 Analysis of **"**postsynaptic partners" of the MB188B-DANs. **A** Confocal stack of the MB188B-DANs (in green) and the postsynaptic neurons (in magenta) labeled by the *trans*TANGO system in the central part of the brain. Only the α'/β' type of the KCs (indicated in yellow line; whole MB is indicated in white line) appeared to be postsynaptic to the MB188B DANs along with other cell types (indicated by white arrowheads as examples). **B** Confocal stack of the anterior part focused on the PAM region. There were only magenta positive PAM DAN cell bodies (indicated by magenta arrowhead). Additionally, the double-labeled cell bodies of the MB188B DANs (indicated by yellow arrowhead) were also. Not all of the MB188B DANs were double positive (indicated by green arrowhead). **C** Confocal stack of the MB188B DANs and the γ5 innervating MB315C PAM DANs (in green), the postsynaptic neurons (in magenta) labeled by the *trans*TANGO system, respectively. The γ-type KCs were not labeled in both cases (the MB is marked by the white line, the α'/β' lobe is marked by the yellow line, GFP in green, mtdTomato in magenta, Brp in blue; scale bar 50μm).

In addition to the double-labeled cells, I observed a quite strong mtdTomato expression in the α'/β' lobe of the MB, whereas there was almost no expression in the γ lobe (Figure 3.9A and C). There are two possible explanations for this situation. Either, the MB188B-DANs do not have any presynaptic connections or communication between the γ type of KCs. Or, alternatively, the pan-neuronal driver of the postsynaptic marker complex fails to label the γ type of KCs. To eliminate the possibility of such an experimental artifact, I monitored the postsynaptic partners of another DAN population of the PAM cluster (MB315C DANs). The connectivity of these DANs to the γ5 compartment of the MB is very well-known (Aso et al., 2014a). Therefore, the UAS-*trans*TANGO flies were crossed with the MB315C-Gal4 driver in parallel to the MB188B Gal4 driver. Similar to the MB188B DANs case, no mtdTomato expression was observed in the MB315C DANs as well as the MB188B DANs (Figure 3.9C). Thus, the lack of mtdTomato expression is most likely an experimental artifact due to failed expression under pan-neuronal promoter. As a result, I concluded that a subpopulation of the MB188B-DANs is postsynaptic to MB188B DANs as well as the MB and a variety of other neurons in the CNS.

3.5 Functional properties of the dopaminergic neurons labelled by MB188-Gal4

Behavioral experiments under different food conditions demonstrated that feeding-related behaviors adapted when the caloric value of the dietary was restricted. Additionally, this adaptation occurred along with the potential connectivity decrease of the MB188B DANs.

As the MB-related neurons are involved in internal state-dependent foraging behaviors (Sayin et al., 2019; Tsao et al., 2018), I reasoned that the observed structural changes might give rise to the motivational adaptation in accordance with the calorie restriction. To address this possibility, the

function of MB188B-DANs in feeding-related behaviors was investigated. Similar feeding-related behaviors such as appetitive associative learning and food consumption were tested upon the manipulation of the MB188B DANs function. Here, I took the advantage of the thermogenetic and optogenetic tools to manipulate these DANs as described in 1.2.3.

3.5.1 Dopaminergic neurons labelled by the MB188-Gal4 line are involved in food uptake

Before I addressed the hypothesis that the modification of the MB188B DANs is causative for the feeding-related behavioral adaptation, the role of the MB188B DANs in food uptake was investigated. Thus, the food consumption of the flies was measured upon the manipulation of MB188B DANs.

The MB188B-Gal4 driver was combined in the same flies with the excitatory and inhibitory optogenetic tools UAS-csChrimson (red-shifted Channel Rhodopsin) or UAS-gtACRI (Anion Channel Rhodopsin), respectively (Govorunova et al., 2015; Klapoetke et al., 2014). The light regime and the experimental settings are described in the methods section 2.2.12. In addition to the optogenetic inhibitory tool, the heat-sensitive dynamin mutant Shi^{ts} was also used to block the output of the MB188B DANs during feeding (van der Bliek and Meyerowrtz, 1991; Grigliatti et al., 1973; Kitamoto, 2001). Finally, only Gal4 expressing, and only corresponding tool containing flies were tested parallel as genetic control. The second control was the absence of the heat or light stimulus. Since two parameters were changed and compared, a 2-way ANOVA was used as statistical test.

5-7d old flies raised on standard food with corresponding genotypes were used in the experiments. Food uptake of these flies was measured by CAFE assay while the MB188B DANs were manipulated with the corresponding genetic tools.

The gtACRI was activated by a strong, white light while the csChrimson was activated by red LEDs (615-650nm) in a custom-built light chamber termed “fly disco” as described in the method chapter. As control group, the flies were kept in darkness in the optogenetic experiments – experimental conditions are plotted as “light” and “dark” conditions. Additionally, the working temperature of the Shi^{ts} was referred to as “restrictive temperature” (32°C) whereas the control temperature was referred to as “permissive temperature” (25°C) in my graphs. For the restrictive conditions, the temperature was increased to 32°C 10 minutes prior to every experiment where Shi^{ts} was utilized. The acting period of the Shi^{ts} was determined as 10 minutes by measuring the time until flies, that expressed Shi^{ts} in motor

neuros controlling the muscle contraction, were immobilized at 32°C. During the starvation period of the CAFE assay, flies were kept in darkness for optogenetic experiments and under permissive temperature for thermogenetic experiments.

The results demonstrate that the food uptake of the flies was enhanced by ~30% when the MB188B DANs were inhibited by gtACRI (Figure 3.10A). The genetic control flies and all the dark control group flies consumed around 0.5µl sucrose solution. However, the flies expressing the gtACRI in the MB188B DANs consumed more than 0.8µl of sucrose solution during CAFE assay when the gtACRI was optogenetically stimulated ($p<0.001$). There was no significant difference observed between the genetic control of the experiments. The increase in feeding upon inhibition of the MB188B-DANs was reproduced using thermogenetic tools as well. The synaptic output of the MB188B DANs was blocked by the dynamin mutant Shi^{ts} and the food uptake were measured using the CAFE assay. The food consumption of the flies expressing the Shi^{ts} in the MB188B DANs was enhanced as well compared to genetic control groups under both the restrictive and permissive temperature (75% and 30% respectively; Figure 3.10B). These two feeding enhancement were not significantly different from each other.

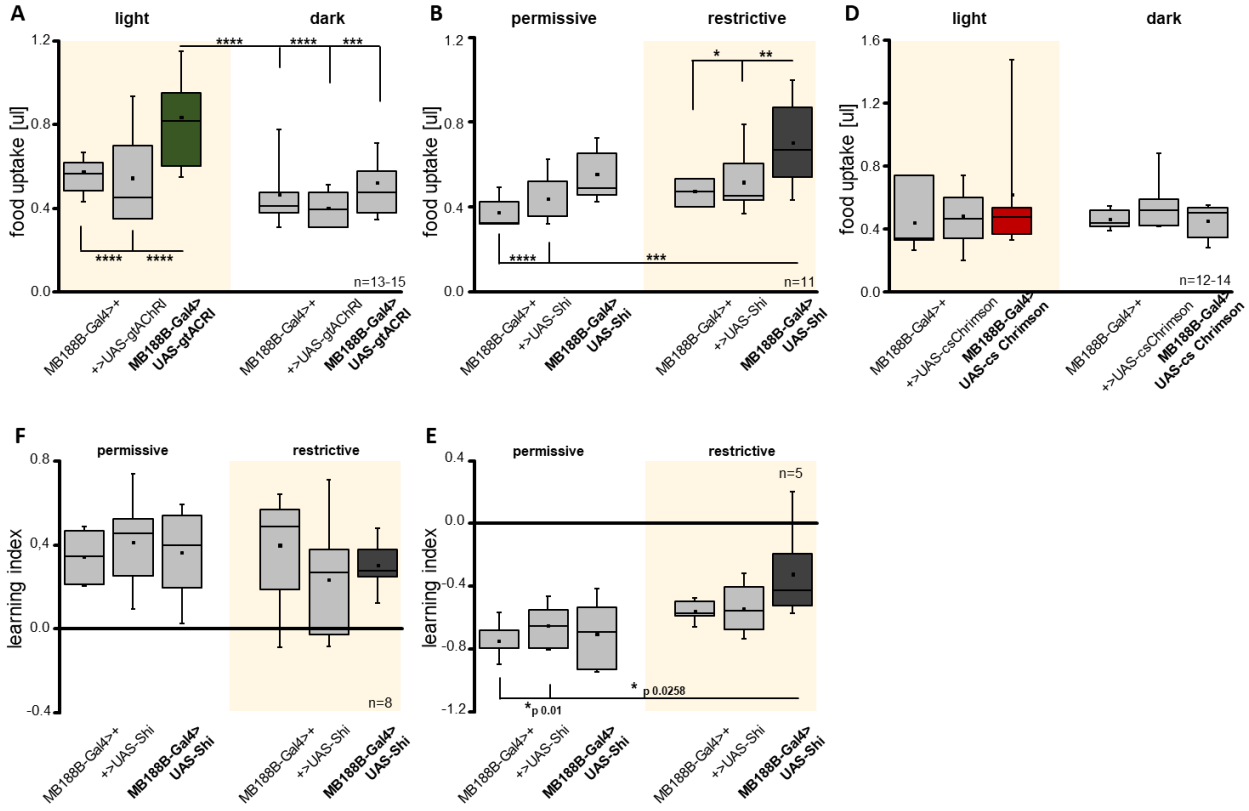

Figure 3.10 Role of the MB188B-DANs in feeding and learning behaviors. **A** Food uptake (in µl) of the flies expressing the inhibitory optogenetic tool gtACRI in the MB188B DANs. Inhibition of the MB188B DANs during feeding resulted in an increased food uptake (Statistic two-way ANOVA followed by Tukey tests, ****p<0.0001,***p=0.0004). **B** Food uptake of the flies expressing the thermogenetic tool Shi^{ts} that blocks the synaptic output in the MB188B DANs. Enhancement of the food uptake upon the blocking of the MB188B DANs were reproduced by the Shi^{ts} expression (Statistic two-way ANOVA followed by Tukey tests, ****p<0.0001,***p=0.0006,**p=0.0047,*p=0.0419). **C** Food uptake of the flies expressing the excitatory optogenetic tools csChrimson in the MB188B DANs. Activation of the MB188B DANs during feeding did not affect the food uptake (Statistic two-way ANOVA followed by Tukey). **D** Appetitive and **F** aversive olfactory related associative memory formation of the flies that are expressing the Shi^{ts} in the MB188B DANs. Blocking the synaptic output of the MB188B DANs during the acquisition and retrieval of the memory did not affect the memory formation ability (the experimental groups are colored for simplicity; statistics two-way ANOVA followed by Tukey tests,*p values are indicated on the plots).

Since the inhibition of synaptic transmission from the MB188B DANs created the same effect as hyperpolarizing them using the optogenetic tool gtACRI, this increase in food uptake at the restrictive temperature was expected. The permissive temperature was considered as insufficient for the Shi^{ts} mutant expression. Yet, I observed a similar increase in the food uptake at 25°C. This increase might be resulted from the leaky expression of the mutant Shi^{ts} under permissive temperature. If the mutant dynamin was expressed even in to a small degree, this might result in decreased synaptic output leading the feeding enhancement.

On the other hand, the depolarization of the MB188B DANs during the feeding assay by the optogenetic tool csChrimson upon red light stimulation did not affect the food uptake (Figure 3.10C).

All in all, these results show that the MB188B-DANs are involved in the circuitry behind the food uptake behavior, but only in a unidirectional way. The inhibition of these DANs resulted in an increase in the food uptake. Therefore, it is possible that the structural plasticity of these DANs might affect feeding behavior in an adaptive manner.

3.5.2 Dopaminergic neurons of the MB188-Gal4 line do not play any role in learning and memory formation

In the previous part, my data suggested an involvement of the MB188B-DANs in feeding. Another behavior that was shown to be enhanced upon calorie restriction was the appetitive learning ability under the short period of starvation (Figure 3.4C). Therefore, a potential role of the MB188B DANs was also examined in the context of appetitive memory formation.

Similar to the previous part, the MB188B-Gal4 driver line was crossed with the UAS-Shi^{ts} expressing flies (experiment group). Then, the memory formation and the retrieval of these flies together with the genetic control flies were tested under permissive and restrictive temperatures. The flies were tested in both appetitive and the aversive associative learning paradigms.

The appetitive associative learning scores of the flies in every group are around 0.3-0.4. No statistically significant difference was observed between the genetic control conditions and temperature control conditions (Figure 3.10D). Similarly, no significant difference in the aversive learning score was observed in the experimental group flies under the restrictive temperature compared to its corresponding genetic control groups (Figure 3.10E). The slight decrease in the learning score in the test group (indicated by dark color) was only significant to the learning scores of the genetic control groups under the permissive temperature. The significance in the decrease could be the temperature and genetic effect combined instead of the learning deficiency. Additionally, it should be noted that the sample size of this experiment was lower than usual sample size.

In this chapter, I analyzed the function of the MB188B DANs in learning and feeding behaviors. I concluded that the MB188B DANs were not involved in learning but in food uptake behavior. The involvement of the MB188B-DANs in the food uptake circuitry supports my hypothesis that the structural changes of the MB188B-DANs can be an explanation for food uptake adaptation under the hypocaloric dietary condition. Unlike the hypocaloric dietary effect on the appetitive learning, the manipulation of the MB188B DANs *per se* does not lead to any impairment or enhancement in the appetitive memory. However, the hypothesis depicted above can still be applied as the learning score enhancement under hypocaloric dietary could also be a result of an increased food uptake motivation (i.e., “hunger”) rather than an increase in memory formation ability.

3.6 Structural and functional adaptation of dopaminergic neurons covered by MB188B-Gal4 occurs at the postsynaptic sites

As stated earlier, I hypothesized that structural modifications in the MB188B-DANs are a cause of behavioral adaptations occurring as a result of the calorie restriction conditions. So far, the structural modifications that were examined in this study by using the tool splitGFP reconstitution (or, sometimes

termed “GRASP”). In previous chapters, a decrease in connectivity was shown between the MB188B-DANs and KCs using this tool. However, I argued that the reconstitution can also occur by the proximity between two neurons along with the synaptic connections. Another uncertainty about the tool GRASP was that, since spGFP is fused with a membrane-bound protein, its localization is not specific to the pre- or postsynaptic compartments. Therefore, the synaptic sites of the connectivity change in the DANs upon the calorie restriction could not be spotted by utilizing this tool.

Additionally, it is also important to know if the connectivity decrease changes the response of the MB188B DANs to certain odors, especially the odor-related odors considering the possibility of these DANs role in metabolic state encoding. If so, these functional adaptations can be also differentiated in terms of synaptic sites.

Therefore, in the following section chapter, I analyzed the occurrence site of the structural adaptations in further detail. I also asked the question whether structural adaptations of the MB188B-DANs give rise to any further response adaptations upon long-term calorie restriction in the dietary.

3.6.1 Postsynaptic sites of the MB188B DANs are re-arranged upon calorie restriction

To address the question where the structural re-arrangement happens, dependent on long-term dietary, I took the advantage of the pre- and postsynaptically expressed functional indicators, sypGCaMP3 and dHomerGCaMP3, respectively. The fluorescence of these synaptically expressed functional indicators in the MB188B DANs was measured under different caloric dietaries.

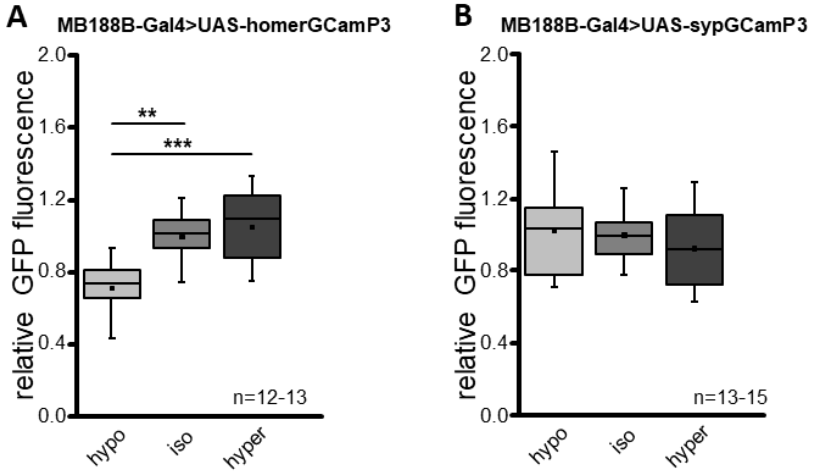

Figure 3.11 Synaptic structural changes of the MB188B-DANs dependent on the long-term diet. **A** Relative GFP fluorescence quantification of the postsynaptically localized dHomerGCaMP3 in the MB188B DANs and **B**

presynaptically localized sypGCaMP3 under different food conditions. Postsynaptically localized reporter fluorescence decreased under less caloric diet. Presynaptically localized reporter fluorescence remained the same under different food conditions (Statistics one-way ANOVA followed by Tukey test, ***p<0.001, **p<0.01).

The flies carrying the MB188B-Gal4 driver were crossed with the UAS-sypGCaMP3 and UAS-dHomerGCaMP3 containing flies. Then, similar to the GRASP experiments, flies were subjected to different dietaries for 7d. Eventually, the fly brains were dissected and the GFP fluorescence of syp- and dHomerGCaMP3 was measured. The GFP fluorescence was normalized to the mean of its corresponding isocaloric group. These quantifications were done without performing any further antibody staining as in the case of the GRASP experiments.

As a result, relative postsynaptically localized GFP fluorescence showed a decrease corresponding to the GRASP decrease upon nutrition restriction (Figure 3.11A). However, no difference in the presynaptically expressed GFP fluorescence was observed (Figure 3.11B). Thus, I concluded that the decrease in the connectivity takes place at postsynaptic sites, but not at presynaptic sites.

3.6.2 The dopaminergic neurons covered by MB188B-Gal4 respond to fly food odor

Additional to the structural analysis of the synaptic sites, adaptation of the response to an odor stimulation in these synaptic sites was also analyzed. However, prior to analyzing any functional stimulus-response adaptation, the responsiveness of the MB188B DANs odor stimulation had to be tested. Therefore, the dynamics of the presynaptic and postsynaptic responses of the MB188B DANs upon the presentation of certain odors were measured by two-photon Ca^{2+} imaging. Since the role of the MB188B DANs in the motivational adaptation was investigated in this study, apple vinegar (AV) and fly food dissolved in water were presented as food-related odors. In addition MCH and 3-Oct odors were chosen as non-food related odors since these odors were utilized in the learning and odor avoidance experiments.

5-7d old flies expressing pre- and postsynaptic sensors (sypGCaMP3 and dHomerGCaMP3, respectively) in the MB188B DANs were presented the 4 odors; MCH (1:750 dil.), 3-Oct (1:500 dil.), AV (1:100 dil.) and fly food (1g/ml), while the response of these synaptic sites were measured using 2-photon microscopy.

Fly food odor responses of pre- and postsynapses are shown as representative traces and images in Figure 3.12A and B. In these images, the stack of the eight frames (2sec) before the odor delivery is shown as pre-response. The stack of eight frames following the odor onset were demonstrated as odor response for both MB188B-Gal4>UAS-sypGCaMP3 and the MB188B-Gal4>UAS-dHomerGCaMP3. Additionally, the difference between pre-response and the response was also shown for both cases (Figure 3.12A and B). The GCaMP3 fluorescence was much clearer in the β'1 compartment of the MB whereas a weak expression was visible in the γ3 region. In contrast, I failed to observe any reliable background fluorescence or any odor-evoked response upon the odor presentations in the γ4 region (Figure 3.12A and B). A stronger signal in the sypGCaMP3 was observed compared to the dHomerGCaMP3. These signal levels were correlated with the previous anatomical results showing that the main innervations of the MB188B DANs on the MB are presynaptic (Figure 3.8).

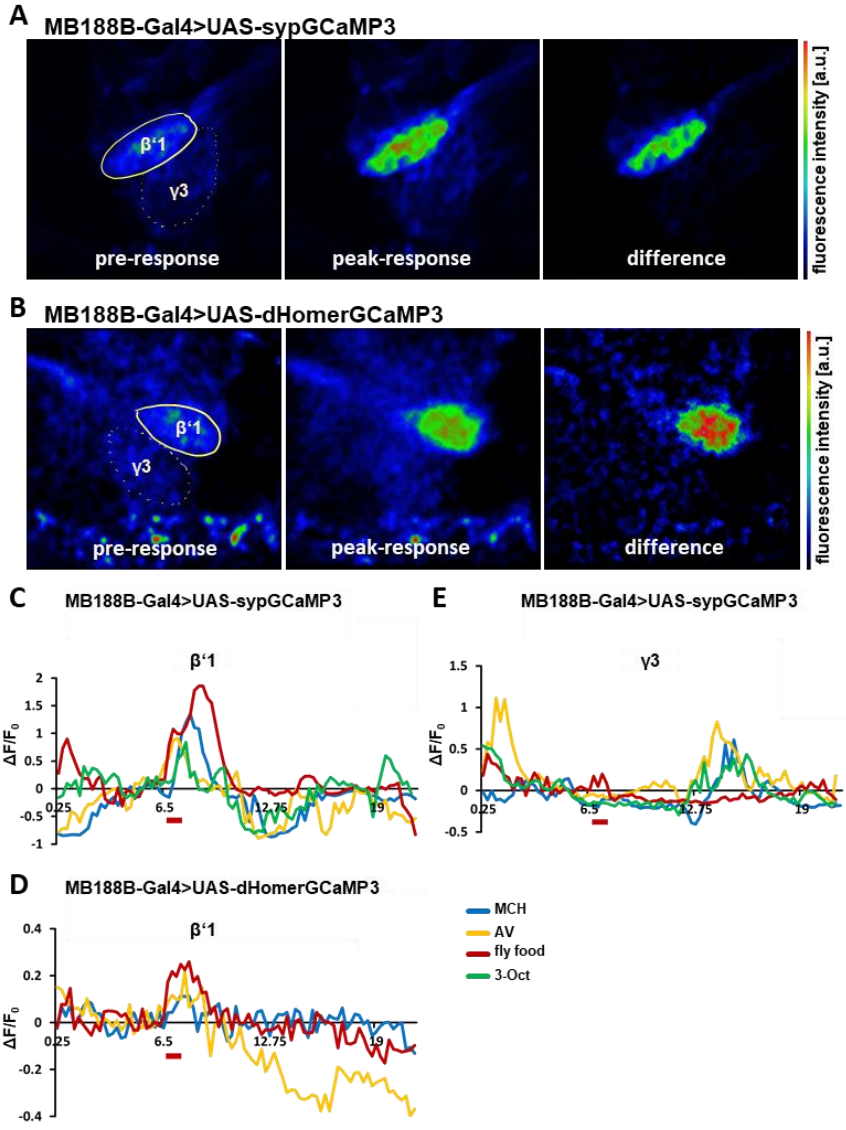

Figure 3.12 Odor evoked-responses of the MB188B DANs. **A-B** Representative examples of the presynaptic and postsynaptic food odor responses, respectively. Ca^{2+} signals of the pre- and postsynaptic indicators (syp- and dHomerGCaMP3 respectively) prior to the odor presentation (left column), response to the fly food odor (middle column), and the difference between the pre-response and odor response (right column). The β'1 and γ3 regions were distinguishable and indicated by a straight and dashed line, respectively. **C-D** Odor response traces of the sypGCaMP3 and dHomerGCaMP3 respectively upon different odor presentations in the β'1 compartments plotted as ΔF/F0 against the time axis (in sec). The red bar under the time axis shows the odor delivery onset and the duration (2.5sec). The stronger response was observed against the fly food odors. **E** Odor response traces of the sypGCaMP3 upon different odor presentations in the γ3 compartment. A late signal was evoked upon the offset of the β'1 signal (courtesy of Clare E. Hancock).

The calcium dynamics of a single fly expressing either the MB188B-sypGCaMP3 or MB188B-dHomerGCaMP3 are shown in Figure 3.12C and D. Each of these two flies was presented 4 odors as described. The response of the β'1 and γ3 compartments were analyzed separately. These traces demonstrated a strong response to the fly food odor presentation while the response to AV and 3-Oct were relatively weak. Interestingly, the MB188B DANs also showed a strong response to MCH (Figure 3.12C and D). In this particular single fly case, I observed an off response in the γ3 compartment following the offset of the β'1 response except for food smell (Figure 3.12E). However, this response dynamic between different compartments was not observed in every response traces. Finally, in the case of the 3-Oct response measurement of the dHomerGCaMP3, the signal was lost due to technical reasons. Therefore, the 3-Oct response was not included in Figure 3.12D.

3.6.3 Postsynaptic responses of the MB188B DANs to the food odors depend on the dietary

Subsequent to testing the responsiveness of the MB188B DANs, the adaptation in the pre- and postsynaptic response change dependent on the long-term calorie restriction was measured. These functional adaptations could then also be correlated with the structural plasticity of these DANs.

10d old female flies expressing the pre- and postsynaptic Ca^{2+} indicators in the MB188B DANs, were stimulated with fly food odor under 2-photon microscopy following the exposure to different dietaries. Then the responses in corresponding synaptic sites were monitored. Fly food odor was chosen here as the response against this odor was greatest. Additionally, I speculated that the food smell response should be adjusted if the structural plasticity in these DANs is the underlying reasons for the feeding-related behavioral adaptations.

As a result, the average response traces of the postsynaptically localized dHomerGCaMP3 showed a slight increase in the β'1 compartment under calorie restriction conditions (Figure 3.13A). Similarly, there was also a slight increase in the γ3 region response (Figure 3.13B). The increase in the γ3 region was rather a late response that could be aroused by the activity of the β'1 and could be an indication of a self-feedback mechanism. On the other hand, I did not observe any difference between the response of the presynaptically localized sypGCaMP3 in any compartments under different food conditions (Figure 3.13C and D).

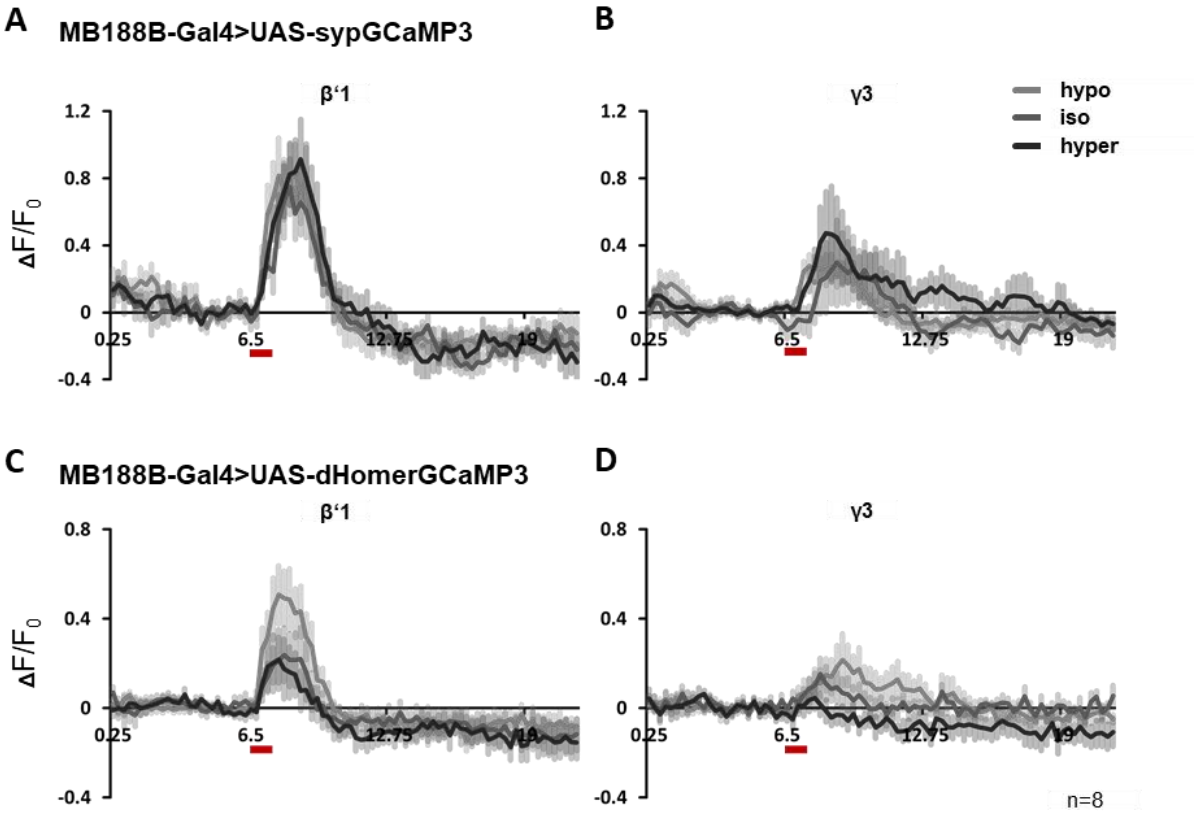

Figure 3.13 Food odor-evoked response change in the MB188B DANs dependent on the dietary. **A-B** Food odor response traces (ΔF/F0) of the MB188B DANs expressing the presynaptically localized sypGCaMP3 Ca^{2+} indicator plotted against the time (in sec). Responses of the β'1 and γ3 innervations of the MB188B DANs were plotted respectively. No difference in the presynaptic response was observed under different dietary conditions. **C-D** Food odor response traces (ΔF/F0) of the MB188B DANs expressing the postsynaptically localized dHomerGCaMP3 Ca^{2+} indicator. There was a slight increase in the postsynaptic response of the MB188B DANs in each compartment to the fly food odor (line is the mean; shaded area SE; the red bar indicates the odor presentation; odor onset 6.25sec for 2.5sec; courtesy of Clare E. Hancock, n=8).

In this chapter of the study, I showed that the MB188B DANs were responsive to food-related odors indicating the role of the MB188B DANs in feeding-related behaviors again. Moreover, I showed that the MB188B DANs underwent not only the structural changes but the postsynaptic response also

changes slightly. This slight increase needed to be examined further. It could also be a result of the structural plasticity.

3.7 Functional and structural adaptation is a compensatory, long-term process

Up to this point, structural and functional adaptations dependent on the calorie restriction were shown. Additionally, the role of the MB188B DANs in feeding was shown. Structural changes in these DANs were aimed to be associated with the feeding-related behavioral adaptations upon the calorie restriction. From this point on, I will discuss possible mechanisms behind these structural changes. To begin with, the dynamics of the structural and functional adaptations were crucial to understanding during the exposure of the long-term diet.

Considering the life span of an adult *Drosophila,* I set long-term experimental paradigms as 7d. As a result of this long-term exposure, I was able to detect the adaptations in fly behaviors as well as the structure in a group of MB-related modulatory neurons. However, it was also possible that these adaptations were rather an immediate effect of nutrition restriction or even of starvation. Thus, in this chapter I will address three questions: What are the dynamics of the functional and structural adaptations under different food conditions? At which time point the structural and functional adaptations take place? And finally, does the effect of calorie restriction result from starvation?

As the functional imaging of the neurons was not informative about the dynamics of the cell activity over time, accumulated cellular activity was measured by taking the advantage of a tool called “CaLexA” (Masuyama et al., 2012). GFP expression quantification in the cell body compared under different conditions was taken as increased activity of the cells over time. Additionally, GRASP fluorescence was used as connectivity measurement.

To examine the dynamics of the connectivity change, the MB188B-Gal4 driver line was crossed with the UAS-MBGRASP expressing flies. 3d old female flies were placed on different dietaries as described before. Then, the reconstituted GFP level was measured at different timepoints following the onset of the dietary, 1d, 3d, 5d, 7d, 14d, and 28d after onset. Similar to the connectivity change, the activity analysis was done in the same way with the flies expressing CaLexA in the MB188B DANs.

3.7.1 Functional and structural changes do not depend on starvation

Prior to the analysis of the activity and structural changes over time, I wanted to eliminate the possibility that structural and functional plasticity under hypocaloric food condition resulted from the constant starvation of the animal due to the lack of nutrition. Therefore, I measured the connectivity and the activity of the MB188B-DANs under different starvation periods, 24h and 48h.

5-7d old flies expressing the MBGRASP constructs and the CaLexA in the MB188B DANs were starved for 0h, 24h and 48h in parallel. Then, the GFP signal was quantified as described above. As a result, no significant difference in the CaLexA signal (Figure 3.14A) and the GRASP signal (Figure 3.14B) was observed between the starved and non-starved flies.

It is also possible that the small changes in the activity upon hunger may not be detectable by the CaLexA tool. As for the connectivity change, I concluded that structural re-wiring is a long term process and the starvation is not the reason behind this phenomenon.

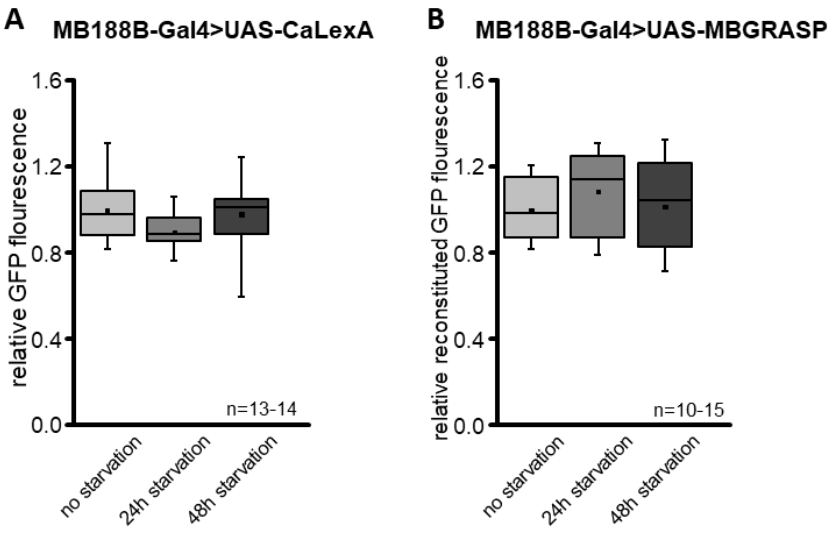

Figure 3.14 Functional and structural modifications upon the starvation. **A** Relative CaLeXA signal quantification in the starved and non-starved flies. The functional changes due to starvation were not detected by the measurement of the GFP signal of the CaLexA. **B** Relative GRASP signal quantification. Starvation had no effect on the connectivity between the MB188B DANs and KCs (Statistics one-way ANOVA followed by Tukey test, $p>0.5$).

3.7.2 Change in activity of MB188B-DANs occurs earlier than structural changes

In this section, I aimed to test the activity and connectivity changes of the MB188B DANs over time following the onset of the diet. To do so, I compared the relative GRASP signal and CaLexA signal

expressed in the MB188B DANs at different time point of the dietary with the corresponding isocaloric conditions.

However, before I compared the relative GRASP and CaLexA change, I wanted to understand the dynamics of the connectivity and the activity of these DANs independent of any change in the experience of the flies. Therefore, I compared the GFP signal levels measured under only isocaloric food condition over different periods.

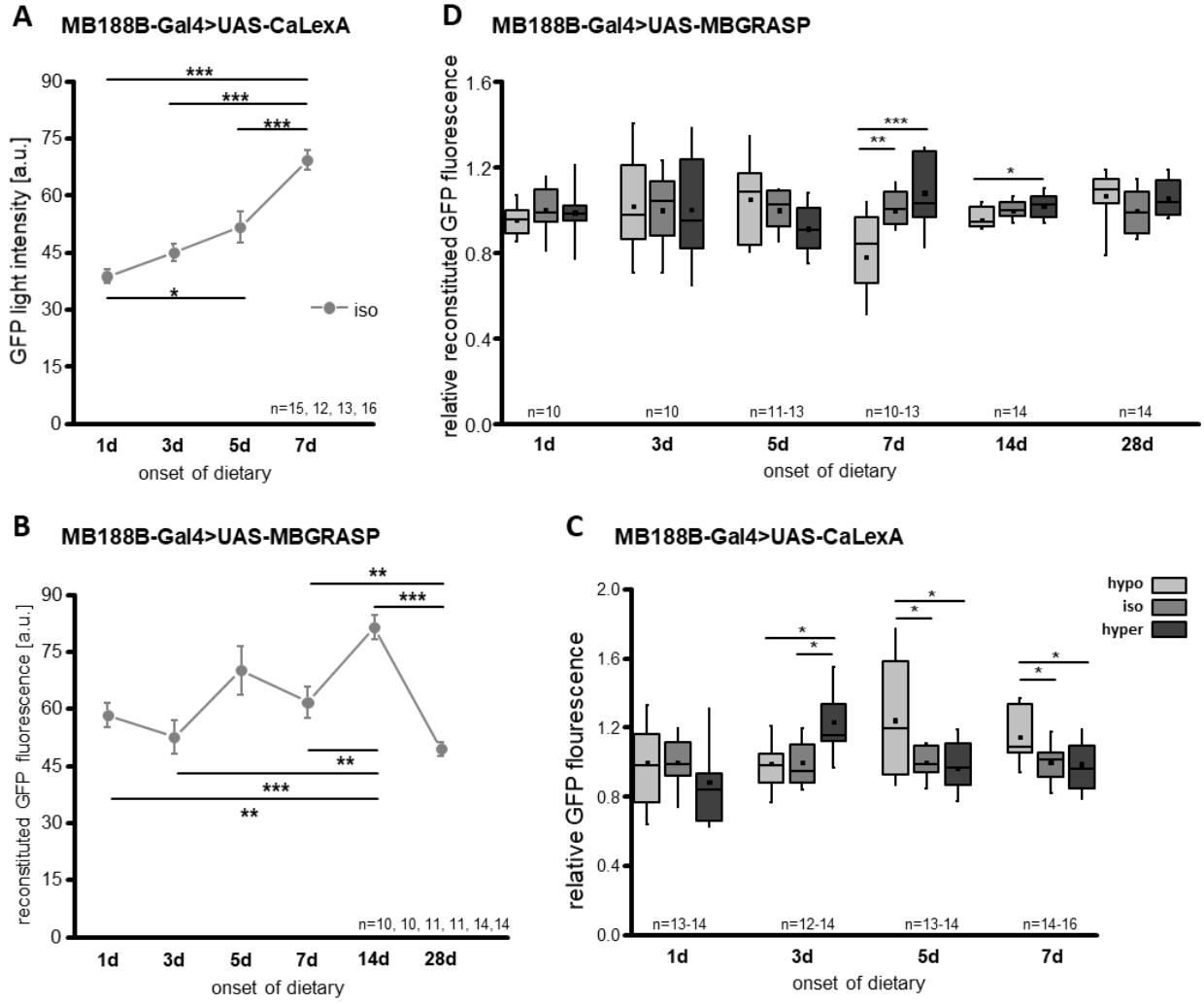

Figure 3.15 Dynamics of the functional and structural changes over time under different dietary conditions. **A-B** Quantifications of the GFP signal over time under isocaloric food conditions (Dots are the mean values, error bars are SE; statistics one-way ANOVA followed by Tukey test, ***p<0.001, **p<0.01, *p<0.5). **A** GFP signal increased with the fly age indicating the accumulation of the GFP over time. **B** The GRASP signal also increased with the fly age and started decaying due to the aging after 14d following the dietary onset. **C** Quantification of the relative CaLeXA signal under different food conditions at different time points following the dietary onset. The activity of the MB188B DANs was significantly higher in the flies exposed to the calorie restriction after 5d following the dietary onset. This increase remained significant in the later time point (7d). **D** Quantification of the

relative GRASP signal under the different dietary conditions at different time points after the dietary onset. The decrease in the connectivity started after 7d due to the caloric restriction. The decrease in the connectivity maintained for a while but not after 28d (Statistics one-way ANOVA followed by Tukey test, ***p<0.001, **p<0.01, *p<0.5).

A steady increase in the CaLexA signal was observed over time as expected since the GFP was transcribed and accumulated over time (Figure 3.15A). Two arguments could be given to explain the increase in the CaLexA signal: First, the GFP turnover could be much slower than its transcription/translation. Second, the GFP that was transcribed upon the cellular activity may not be degraded at all. In any case, steady accumulation of the GFP over time ensures that the GFP signal is a reliable activity measurement.

Similar to the CaLexA signal, the reconstituted GFP signal showed an increase in the early stage of flies and reached a saturation at 5d after the dietary onset (Figure 3.15B). The reconstituted GFP signal remained stable over a certain period of time followed by a sharp decrease after 28d from the dietary onset (Figure 3.15B). Dynamics of the MB188B DANs activity was expected to be different than the connectivity since the CaLexA is an accumulative activity indicator. On the other hand, the connectivity of the neurons can increase or decrease depending on the age of the flies, or structural re-arrangement of the neurons for any reason. This slight increase in the GRASP signal can be explained by the ongoing development of the brain (or of the MB-related neurons). Since the GRASP signal reaches a peak after 5d following the onset of diet, the initial measurements after 7d dietary were considered as in the reliable range to measure the long-term effect of the dietary. Finally, the GRASP decrease observed in the later onset of the dietary (28d) was speculated as connectivity lost as a result of aging. Thus, the connectivity change measurements may not be reliable during these ages because the GRASP signal decays due to the advanced age of the flies.

After comparing the CaLexA and GRASP fluorescence dynamics in the fly brain independent of diet, next, I analyzed how the signal of the CaLexA and GRASP changed over time dependent on the exposure to different dietaries relative to the isocaloric correspondence.

The CaLexA measurement showed that the relative activity of the MB188B DANs was increased after 5 days following the onset of the diet under hypocaloric food condition (Figure 3.15C). This increase remained significant after 7 days of dietary exposure. In addition, an increase under hypercaloric

condition was also observed in 3days after the dietary onset, but this increase was not continuous over time in the long run (Figure 3.15C).

On the other hand, the GRASP measurement between different dietary conditions showed a late adaptation relative to the functional adaptation. No significant difference was observed under any dietary condition until 7 days following the dietary onset. However, the connectivity was decreased after 7 days (Figure 14.D). Even though the relative decrease relative to isocaloric condition was maintained after 14 days, it was rather less drastic. Finally, there was no difference observed 28 days following the onset of the diet. This small GRASP signal difference between dietary conditions at 14 days and the complete abolishment of this difference at 28 days was expected due to the advanced age of the flies. Therefore, the abolishment of the structural plasticity in the long term was concluded as independent of the external conditions.

Moreover, the increase in the CaLexA signal under the hypercaloric condition is observed former to the decrease in the GRASP signal under the same condition. This temporal difference in the occurrence of the functional and structural adaptations could be an indication of activity-induced structural plasticiy (Figure 3.15C and D).

As a result, I concluded that the changes in the activity and the structure of the MB188B DANs did not result from the constant food deprivation of the flies. On the contrary, the changes occur in a prolonged manner as an adaptation to the long-term nutrition restriction. Additionally, the functional adaptations of the MB188B DANs take place prior to the structural adaptations, which can be the main reason behind the structural adaptation.

3.8 Structural synaptic plasticity can be induced optogenetically

As stated earlier, the dynamics of the structural and the functional changes in the MB188B DANs demonstrated that the activity of the MB188B DANs increased prior to the decrease in the connectivity (Figure 3.15). This situation gave rise to the possibility of activity-dependent structural change mechanisms. Thus, I questioned if an early activity increase could be a reason behind the structural changes.

I addressed this question by artificially depolarizing the MB188B DANs over a long period by the csChrimson and the ChR-XXL tools. Then, the GRASP fluorescence was examined. A decrease in the connectivity was expected if the connectivity decrease was long-term depolarization-dependent under hypocaloric conditions. Additionally, I artificially increased the cAMP level by the light-gated adenylate cyclase bPAC (Stierl et al, 2010) as a second mechanism and examined any potential GRASP change. This tool was used considering the possibility of metabotropic signal transduction as a downstream of (auto)regulation mechanism based on the MB188B DANs activity increase. In these experiments in which the effect of the hypocaloric food were mimicked, I kept the flies on the isocaloric food during the long-term light stimulation. The light stimulation started when the flies were 3 days old as in the case of the onset of dietary. Prior to the onset of the light stimulation, the flies were allowed to fully develop on the standard fly food as usual.

3.8.1 Long-term optogenetic activation of the dopaminergic neurons covered by MB188B driver does not lead to any structural change in the MB188B DANs

To answer the question if the long-term activity increase results in the connectivity decrease, I crossed the flies expressing an optogenetic activation tool, either the UAS-csChrimson or UAS-ChR-XXL and UAS-MBGRASP with the flies containing the MB188B-Gal4 driver. Experiments were performed as described above (and also see 2.2.12). I also tested genetic control flies in which only the MBGRASP complex was expressed in the 188B DANs but not the optogenetic tool. Additionally, I subjected half of each genetic group to darkness as control of unstimulated MB188B DANS.

The relative GFP fluorescence under the light stimulation condition was calculated by normalizing the data to the mean GRASP intensity of the corresponding background under dark conditions. I aimed to eliminate the effect of the Gal4 protein dilution due to the different copy numbers of the UAS construct. Thus, the mean of the “dark groups” for both crosses is equal to 1 in the relative reconstituted GFP fluorescence plots (Figure 3.16).

As a result, increasing the activity of the MB188B DANs by depolarizing the cells for a long period with csChrimson did not create any difference in the GRASP signal between any group (Figure 3.16A). Similarly, activating the MB188B DANs for a long period by the ChR-XXL did not lead to any change in the GRASP signal between genotypes either (Figure 3.16B). However, I observed a bleaching effect in the GRASP signal due to the strong and long-lasting light stimulation independent of optogenetic tool

expression (Figure 3.16B). Therefore, I concluded that the long-term depolarization of the MB188B DANs by the cation channels based on channelrhodopsins do not mimic the decrease in the connectivity.

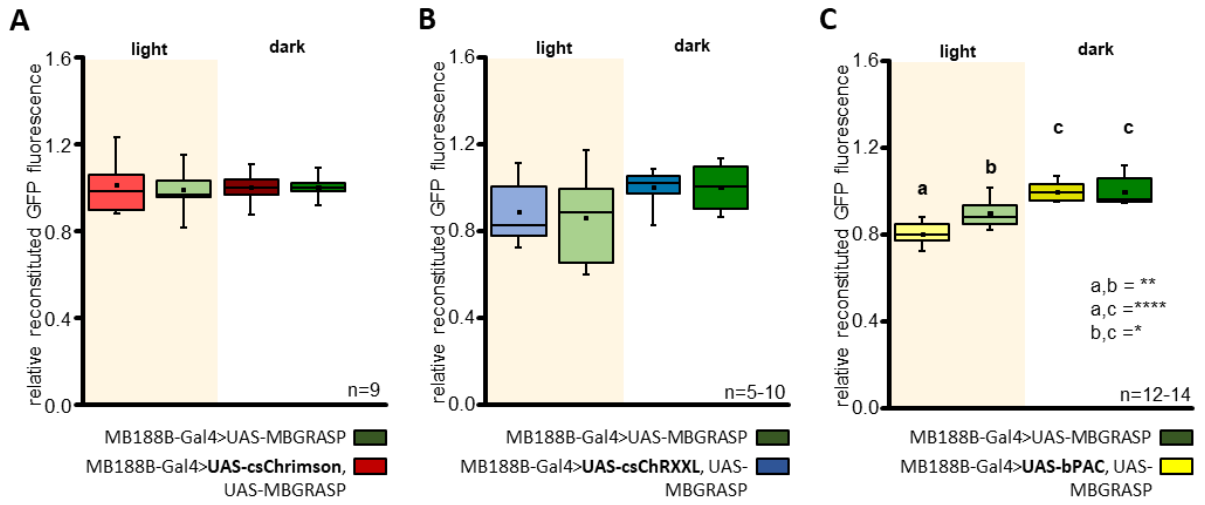

Figure 3.16 Induction of the structural changes in the MB188B DANs. **A** Quantification of the relative GRASP signal in the MB188B DANs upon the long-term activation via the csChrimson. No GRASP difference was observed between the optogenetically activated MB188B DANs and non-activated DANs. **B** Quantification of the relative GRASP signal in the MB188B DANs upon the long-term activation via the ChR-XXL. No difference was observed between the relative GRASP signals of the ChR-XXL expressing and non-expressing DANs. However, the light induction had bleaching effect on the GRASP signal (Statistics two-way ANOWA, p=0.0471 between the light treated groups and dark groups). **C** Quantification of the relative GRASP signal in the MB188B DANs upon the long-term induction of the cAMP production via the bPAC. The long-term cAMP induction created a decrease in the relative GRASP signal. The bleaching effect of the white LEDs were also observed in this experiment (Statistics two-way ANOVA followed by Tukey test, ****p<0.0001, **p=0.0072, *p=0.0127).

3.8.2 Long term induction of the cAMP increase can mimic the effect of the hypocaloric dietary on the MB188B DANs structure

In the previous part, I concluded that it is not the long-term artificial depolarization of the MB188B DANs promoting the structural induction. Next, I increased the cAMP level of the MB188B DANs for a long period to test the resulting effect on the structural changes.

Thus, I expressed the UAS-bPAC under the MB188B-Gal4 driver along with the UAS-MBGRASP. Experimental design and data analysis were performed in the same way as in the case of the csChrimson (or the ChR-XXL). White LED lights were used to simulate bPAC.

Here, I also observed that light stimulation *per se* causes the GRASP signal to bleach independent of the fly genotype as in the case of the ChR-XXL (Figure 3.16B). However, the change in the GRASP signal due to the structural modification was still detectable since the relative GRASP fluorescence was calculated. The GRASP signal quantification showed that when the cAMP level was increased by the light stimulation in the MB188B DANs, the connectivity decreased compared to the flies that did not express the tool bPAC (Figure 3.16C).

As a result, I concluded that the effect of the hypocaloric dietary on the connectivity, which was a decrease in the GRASP signal, could be mimicked by the long-term artificial induction of the cAMP production even under isocaloric dietary. In contrast, long-term depolarization of MB188B DANs failed to create the same effect.

3.9 Artificial induction of the structural changes alter food uptake

The ultimate aim of this study was to investigate the behavioral adaptations and the underlying structural changes dependent on the long-term experience of different caloric value dietary in *Drosophila*. I figured that the MB188B DANs decrease their connectivity on the KCs under low calorie food condition. More strikingly, this decrease can be induced artificially by the elevation of the cAMP level in the cells.

What is most interesting at this point is, whether the behavioral adaptations can also be induced by the artificial induction of this structural decrease. Therefore, in this section, I artificially induced the structural changes as described previously. Then, I tested the food uptake behaviors of the flies along with the appetitive learning enhancement under the short time starvation period. In this way, the connectivity decrease in the MB188B DANs could be directly linked to the adaptations in the feeding-related behaviors.

3.9.1 Long-term elevation of the cAMP results in an increased food uptake when it is followed by an acute induction

Previously, I showed strong evidence that the MB188B DANs were involved in the neuronal circuitry responsible for the motivation for food uptake. Additionally, I proved that these DANs were also

subjected to the structural modifications upon calorie restriction. However, a direct evidence of the structural modifications resulting in the feeding increase was required.

Thus, I took the opportunity to induce the structural changes in these DANs to test if the behavioral output of the flies was similar to the flies fed with hypocaloric dietary. In response to this question, I crossed the MB188B-Gal4 flies with the UAS-bPAC. Genetic control flies expressing only one copy of either driver or the genetic tool were also tested in parallel.

Then, I subjected the flies to the long term light induction as well as complete darkness. Afterwards, the flies were starved and tested in the CAFE assay for food uptake in the complete darkness. As a result, no increase in the food uptake was observed that might develop from the long term induction of the structural changes in the MB188B DANs (Figure 3.17A). The food consumption of all the flies was around 0.4-0.µl independent of the early long-term light exposure.

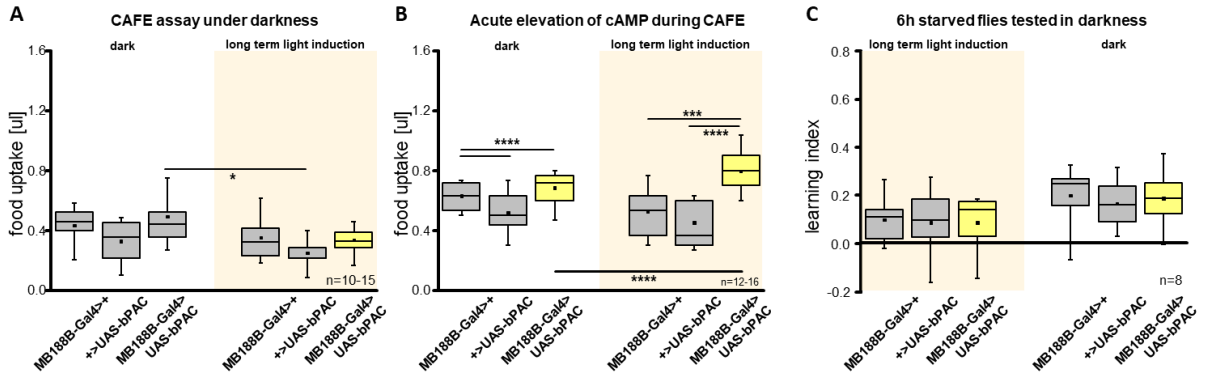

Figure 3.17 Effect of the structural plasticity induction in the MB188B DANs on the feeding-related behaviors. **A** Food uptake upon creating the structural changes measured in darkness. The early long-term stimulated flies did not exhibit any difference in the food uptake (Statistics two-way ANOVA followed by Tukey test, *p=0.0136) **B** Food uptake upon creating the structural changes measured under the light stimulation to maintain the cAMP level. The acute elevation of the cAMP combined with the long-term elevation resulted in the enhancement in the food uptake (Statistics two-way ANOVA followed by Tukey test, ****p<0.0001, ***p=0.0002). **C** Appetitive learning scores of the flies subjected to the long term light induction. The long-term light induction did not lead to an appetitive memory formation enhancement under six hours starvation condition (Statistics two-way ANOVA followed by Tukey test).

Additionally, I conducted the same experiment while the flies were acutely stimulated by light during the CAFE assay in addition to the long-term activation. Here, as the control group, the flies that were not subjected to the long-term induction were tested again. I observed a general increase in food uptake when the cAMP level kept increased independent of the early long-term induction. Interestingly

enough, when the acute elevation in the cAMP was combined with the long term structural effect of the cAMP elevation, the food uptake was enhanced by ~30% (Figure 3.17B). This enhancement was significant to its corresponding genetic controls as well as the only acutely induced flies (Figure 3.17B). Thus, I concluded that the food uptake of the flies was increased as in the hypocaloric dietary condition case, when the induction of the structural modification was combined with the elevation of the cAMP during the food uptake test.

3.9.2 Induction of the structural changes does not affect the learning performance of the flies

Following the enhancement of food intake, I questioned whether the same enhancement could be observed in the appetitive olfactory learning performance of the flies. If the structural change induction in the MB188B DANs could increase the motivation of the flies, the appetitive learning ability under a shorter starvation period (6h), would be also enhanced similarly as under the hypocaloric condition.

Thus, the connectivity decrease was induced as in the previous experiments. Then, the appetitive associative learning ability of the flies was tested after the 6h starvation period. It should be noted that the learning experiments were performed without any further light stimulation. The flies that were subjected to artificial induction of the structural changes failed to show a stronger learning performance compared to those flies that did not express the optogenetic tool or exposed to the early light stimulation (Figure 13.7C). The learning scores of all flies were around 0.2-0.3. This score was expectedly less compared to the 24h starved flies' learning performance.

I concluded that the induction of the structural plasticity did not enhance the appetitive learning scores (Figure 3.17C). Here, it should be emphasized again that the experiments were conducted without further light induction. This means that the cAMP level was not acutely increased during the experimenting as in the food uptake. Thus, it is still possible that the induction of the plasticity might enhance the appetitive memory formation if the cAMP level was kept high during the experiment.

All in all, either the structural changes were not involved in the learning and memory formation or increase in the motivation could not be achieved due to the lack of the acute cAMP increase. On the other hand, I finalized that the structural modifications in the MB188B DANs affect the motivation for food uptake if the downstream cAMP level remained elevated.

3.10 MB188B DANs-mediated food uptake is affected by neuropeptides

By now, it was shown repeatedly that the MB188B DANs were involved in the circuitry orchestrating the feeding behavior. Additionally, I speculated that the modulation of the structure of these DANs leads to the following modulations of the feeding behaviors. Starting from this chapter, I focused on the circuitries modulating the motivational state. I questioned the involvement of these circuitries in the MB188B DANs-mediated food uptake behaviors. Additionally, the role of these circuitries was also investigated in the context of the structural adaptations in the MB188B DANs.

Food uptake in insects is regulated by hunger- and satiety-signaling neuropeptides, similar as in the mammals. *Drosophila* has also a huge number of neuropeptides that signal for the satiation and hunger in the fly brain inhibiting or inducing the food uptake, respectively (see section 1.4). I showed that the lack of activity, as well as the decrease in the connectivity, in the MB188B DANs enhanced food uptake. Therefore, it is highly likely that the activity of the MB188B DANs is regulated by neuropeptides and the structural modifications are a result of this long-term regulation. In this chapter, I aimed to figure out if the MB188B DANs interact with any neuropeptide to promote the food uptake and if these interactions lead to structural modifications.

3.10.1 The MB188B DANs are involved in the food uptake decrease upon the AstA satiety neuropeptide release

As I showed that the MB188B DANs were involved in food uptake, I reasoned that it is highly plausible that the MB188B DANs obtain information about the internal state from neuropeptides. One well-known satiety-signaling neuropeptide AstA is shown to inhibit the feeding behavior of the flies. It is also known to inhibit the γ3 innervating PAM DANs (Hergarden et al., 2012; Yamagata et al., 2016). These two arguments make the AstA a strong candidate to be the state-dependent signaling neuropeptide on the MB188B DANs.

To examine the communication between the MB188B DANs and the AstA, I first questioned whether the arborizations of the MB188B DANs were in proximity or contact with the AstA neuropeptide. Therefore, I stained the AstA neuropeptide in the brains expressing GFP in MB188B DANs. Confocal

microscopy images focused on the PAM and MB area revealed that the AstA peptide was co-localized with the MB188B-DANs mainly outside of the MB (Figure 3.18A). I showed earlier that the dendritic tree of the MB188B DANs were also arborizing mainly outside of the MB (Figure 3.8).

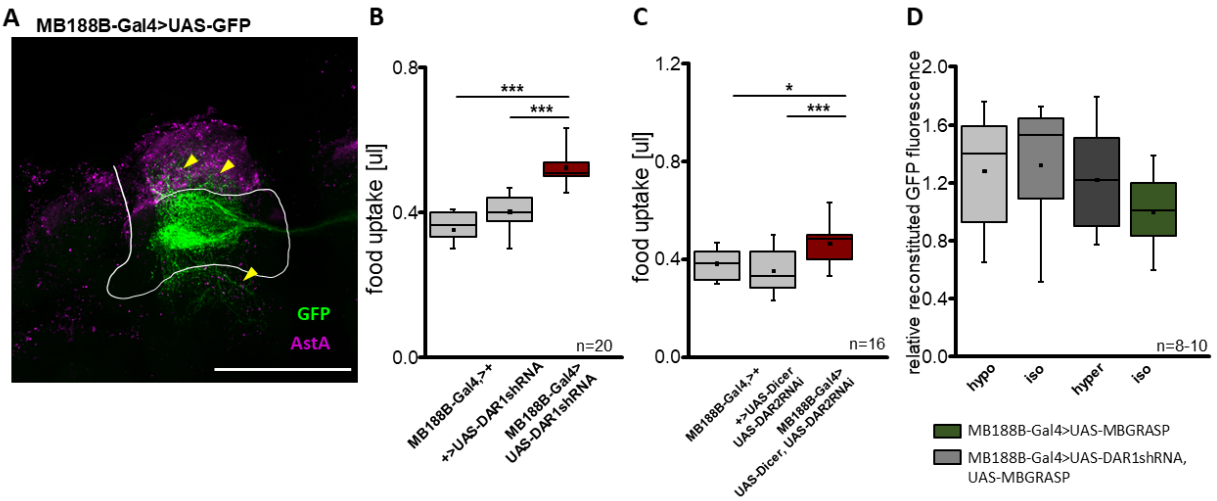

Figure 3.18 Role of the AstA satiety neuropeptide in the M188B DANs-mediated feeding and the structural adaptation. **A** Confocal stack of the AstA immunostaining on the fly brain expressing GFP in the MB188B DANs. The AstA peptide co-localized with the GFP mostly outside of the MB (indicated by the yellow arrowheads; GFP in green, AstA in magenta, MB indicated in white borders; scalebar is 50µm). **B-C** Food uptake upon AstA downstream signaling downregulation by RNAi interference of the AstA receptors, DAR1 and DAR2. Food uptake of the flies was enhanced upon AstA receptor downregulation in the MB188B DANs (Dicer is expressed to enhance the effect of the RNAi; Statistic one-way ANOVA followed by Tukey test, ***p<0.001, **p<0.01, *p<0.5) **D** Relative GRASP quantifications between the MB188B DANs and KCs under different caloric value dietaries when the AstA receptor was downregulated in these DANs. No connectivity modification was observed when the AstA receptor signaling was disrupted under different dietaries (Statistic one-way ANOVA followed by Tukey test).

Next, I tested the neuronal communication of the AstA with the MB188B DANs. I took the advantage of a RNA interference tool to downregulate the downstream signaling of the AstA in the MB188B DANs. There are two receptors of AstA in *Drosophila;* DAR1 and DAR2 (Larsen et al., 2001). I expressed the RNAi interference tools against these two receptors, UAS-DAR1shRNA and UAS-DAR2RNAi, respectively in the MB188B DANs. Then, the food uptake of the flies was tested in the CAFE assay. The flies that had one copy of either the driver or the receptor RNAi were treated as control groups.

Since the inhibition of the AstA is known to promote the feeding behavior, this downregulation was expected to lead to the feeding enhancement if the MB188B DANs are involved in AstA-mediated feeding circuitry. As expected, an increase in food consumption was observed when downstream of

AstA is downregulated in the MB188B DANs (Figure 3.18B and C). By this enhancement, I came to the conclusion that the MB188B DANs are a part of the AstA-mediated feeding circuitry.

3.10.2 Downregulation of the AstA neuropeptide signaling in the MB188B DANs disrupts the dietary-dependent structural modification

The MB188B DANs were shown earlier to undergo structural re-arrangements upon calorie restriction. Additionally, I showed that the AstA neuropeptide conveys the information about the internal state. Considering the fact that the AstA is a satiety signaling neuropeptide, AstA was expected to decrease under the hypocaloric condition, thus promoting the food uptake. This phenomenon was mimicked in the previous section by down-regulation of the downstream signaling in the MB188B DANs. Therefore, I reasoned that the long-term decrease in the AstA signaling dependent on the low-calorie dietary exposure could be the cause of the induction of structural plasticity.

To test this possibility, I expressed the RNA interference tool, DAR1shRNA, under the MB188B-Gal4 driver together with the MBGRASP. The flies were exposed to the different caloric value dietaries to test if the structural re-arrangement was maintained. The relative GFP reconstitution was calculated by normalizing the values to the GRASP signals in the flies that do not express interference tool and are fed with isocaloric dietary.

GRASP measurements showed that the long-term calorie restriction did not lead to any connectivity decrease in the DANs anymore when the AstA signaling was disrupted in these DANs (Figure 3.18D). Therefore, I concluded that the disruption of the AstA signaling in the MB188B DANs also resulted in the disruption of the structural re-arrangements.

In accordance with our AstA signaling investigation, I drew the conclusion that the MB188B DANs acquired information about the internal state of the flies via the AstA signaling. The long-term reduction in the AstA signaling, hence the increase in the activity of the MB188B DANs, resulted in the structural modifications. I showed previously that the long-term elevated cAMP also yielded in a structural decrease in MB188B DANs. Thus, it is also possible that elevated cAMP originated from the activity increase due to lack of AstA neuropeptide.

3.10.2 SI Downregulation of the SIFamide neuropeptide signaling does not disrupt the dietary-dependent structural modification

In parallel with a satiety signaling neuropeptide, the role of a hunger neuropeptide in the MB188B DANs-mediated food uptake was also tested. I took the SIFamide as the hunger signaling neuropeptide since the feeding of the flies is promoted upon SIFa release (Martelli et al., 2017). Thus, I conducted the same type of experiments as in the case of the AstA signaling investigation to test the role of SIFa in this circuitry.

Initially, I characterized the proximity of the SIFa neuropeptide by immunostaining against the SIFa antigen in the fly brains where the MB188B DANs were expressing the GFP. A wide-range of co-localization between the GFP reporter and the SIFa staining was observed especially on the MB (Figure 3.19A, yellow arrowhead). Previously, I demonstrated that the arborizations of the MB188B DANs on the KCs was primarily presynaptic. Thus, the vicinity between the DANs and the SIFa on the MB is highly likely and that the SIFa is postsynaptic to the MB188B DANs rather than providing the information to these DANs.

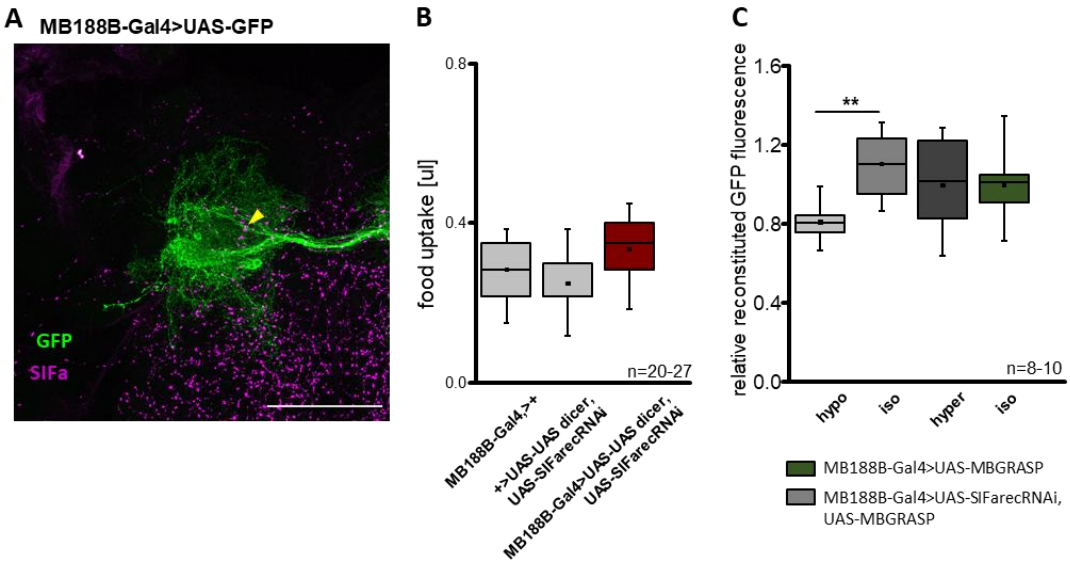

Figure 3. Role of the SIFa hunger neuropeptide in the M188B DANs-mediated feeding and the structural adaptation. **A** Confocal microscopy imageof the SIFa immunostaining on the fly brain expressing GFP in the MB188B DANs. The SIFa peptide co-localized with the GFP also on the MB (indicated by the yellow arrowhead; GFP in green, SIFa in magenta; scalebar is 50μm). **B-C** Food uptake upon SIFa downstream signaling downregulation by RNAi interference of the AstA receptors, SIFarec. Food uptake of the flies was not affected upon SIFa receptor downregulation in the MB188B DANs (Dicer is expressed to enhance the effect of the RNAi; Statistic one-way ANOVA followed by Tukey test, p>0.5) **D** Relative GRASP quantifications between the MB188B

DANs and KCs under different caloric value dietaries when the SIFa receptor was downregulated in these DANs. Decrease in connectivity was not affected by disruption of SIFa downstream signaling (Statistic one-way ANOVA followed by Tukey test, **p<0.01).

Next, I downregulated the SIFamide receptor (SIFarec) by expressing the SIFarec-RNAi, an RNA interference tool, in the MB188B DANs. With this way, the possible downstream signaling of SIFa peptide in these DANs would be disrupted. Then, the food uptake of the flies was measured by CAFE assay. The downregulation of the SIFarec did not lead to any change in the food uptake of the flies (Figure 3.19B).

Finally, the effect of SIFa signaling on the structural modifications dependent on the dietary was also measured in the same way as AstA signaling. Similar to the feeding behavior, the downregulation of the SIFarec in MB188B DANs did not have any effect on the structural plasticity as well. The disruption of the SIFa signaling pathway in the MB188B DANs could not prevent the decrease in the connectivity of the MB188B DANs upon calorie restriction (Figure 3.19C).

As the connectivity of the MB188B DANs on the MB remained decreased compared to the isocaloric food conditions, and the food uptake remained unaltered upon the SIFa signaling disruption, I concluded that the SIFa signaling is not informative on the functional and structural modifications of the MB188B DANs. However, an input to the MB188B DANs about the internal state of the flies through SIFa signaling cannot be ruled out.

All in all I showed that calorie restriction in flies is a suitable tool to investigate the mechanisms of the physiological and behavioral adaptations in *Drosophila.* The flies exhibited adapted behaviors upon long-term calorie restriction exposure such that food-seeking behaviors were enhanced. In addition to these adaptations, I showed that a population of modulatory neurons in the adult *Drosophila* brain remained plastic and underwent structural refinements upon calorie restriction. These neurons are called MB188B DANs in this study. The MB188B DANs decreased their connectivity on the MB upon calorie restriction in the diet.

I argued that these structural refinements underlie the behavioral adaptations by showing several pieces of evidences: First, the MB188B DANs were shown to be involved in the feeding-related

behaviors. Second, the communication of these DANs was proven with AstA satiety neuropeptide. This communication provides an increased food uptake with a decreased AstA signaling.

Additionally, the structural refinement of the MB188B DANs could be induced by the elevated cAMP level. This elevation was possibly a downstream regulation mechanism of the decreased AstA satiety signaling. When this induction was combined with the maintained cAMP rise in the MB188B, food uptake of the flies was enhanced mimicking the long term exposure to the hypocaloric diet. These findings provided further evidence that the structural modifications of the MB188B DANs are involved in the adaptation of food uptake upon the long term calorie restriction.

4 Discussion

4.1 Significance of this study

Adaptation is of utmost importance for any organism to survive in an ever-changing environment. There are different types of adaptations occurring at the individual level (Ebenman, 1992; Werner, 1992) or even through the generations via genetic modifications (Alberch et al., 1979; Donoghue and Dong; for *Drosophila* studies: Burke et al., 2010; OROZCO-terWENGEL et al., 2012). This study focused on adaptations that took place at the level of individuals dependent on the environmental factors and, as a result, intrinsic states.

Adaptation can occur in a short-term period, like generating familiarity to an odor or punishment expectancy (e.g. Hattori et al., 2017; Riemensperger et al., 2005). These types of adaptation are often rather short-lived. On the other hand, the animals can also exhibit long-lasting adaptations (e.g. Luckinbill et al., 1984; Partridge and Farquhar, 1981; Partridge et al., 1987).This study presented here focused on relatively long-lasting adaptations. Ultimately, I aimed at pinpointing changes in the nervous system underlying these adaptations dependent on the environmental conditions. It was investigated how neuronal networks are re-structured in the *Drosophila* brain such that it gives rise to behavioral adjustments.

4.2 Experimental approaches

4.2.1 *Drosophila* and behavioral adaptation

Drosophila melanogaster was chosen as the model organism in this study for a number of reasons, that is explained in section 1.2 extensively. Additional to these traits, a variety of phenotypic plasticity can be observed under environmental manipulations at the individual level (e.g. Luckinbill et al., 1984; Partridge and Farquhar, 1981; Partridge et al., 1987; Dethier, 1976). This makes *Drosophila* a suitable model organism to investigate the effect of long-term condition changes. This study, as well, provides further contribution in these phenotypic plasticity examples. In this study, I also showed that flies are adjust food uptake dependent on the caloric value of experienced dietary. I further demonstrated that these adjustments remain stable. For instance, flies consumes more food than the flies under

hypocaloric and isocaloric conditions even when they are exposed to same caloric value of sugar solution (Figure 3.2B).

4.2.2 Caloric value of food as an instrument to investigate adaptation

To investigate the effect of the environmental conditions on plasticity of the brain and the reflection in behaviors, I utilized the nutritional value as a parameter. What *Drosophila* feeds on has a large influence on its behavior, as in the case in almost all organisms. For instance, the abundance (or absence) of a nutrition in the diet alters the food uptake such that the flies actively decide how much and which type of the nutrition to consume (Lihoreau et al., 2016; Yang et al., 2008). Considering the great impact of feeding on organisms, different dietary conditions, hypo-, iso- and hypercaloric conditions, were chosen as different environmental condition in the experiments of this study.

Flies were subjected to hypo-, iso- and hypercaloric conditions for an extended period of time (7d). In addition, neuronal modifications often occur during "critical periods", which is typically the first days after eclosure (Hensch, 2004; e.g. Doll et al., 2017). The onset of the dietary was after this period (Figure 2.1). In this way I wanted to make sure that the effect of the dietary results in adaptations to the changing environmental conditions but not a developmental modification due to malnutrition. Finally, the underlying structural modifications in related circuitries were investigated.

In the food recipes used, the caloric value of the food was tuned to create three types of dietaries without changing the content of the fly food – except the fat addition to the hypercaloric dietary. There were several proofs that these recipes did not affect the behaviors that might be caused by the lack of nutrition; For instance, it is known that the nutritional restrictions can have impact on the lifespan (Chippindale et al., 2004; Min and Tatar, 2006). However, the lifespan of the animals did not grossly change under any conditions in my experiments (Figure 3.1). In addition, flies show arousal and hyperactivity when starved (Lee and Park, 2004; McDonald and Keene, 2010; Yang et al., 2015; Yu et al., 2016). In my case, there was no increase in activity under calorie restriction conditions either (Figure 3.3). Therefore, I concluded that the recipes used in this study do not lead to any impairment or lethality in the flies. Thus, these recipes are suitable to use as the changing parameter of environmental conditions.

4.2.3 Role of MB in integration of nutritional value

Motivation for food uptake is studied extensively among animals (Hull, 1951; Kennedy, 1987; Thorpe, 1956; Tolman, 1949). Similarly, extensive researches are conducted to disentangle the neuronal networking underlying state-dependent food uptake in *Drosophila* (Lin et al., 2019). In section 1.4, a detailed list of neuromodulators is given as example. State-modulating neuropeptides span the entire nervous system of *Drosophila* including the MB (Martelli et al., 2017; Ni et al., 2019; Shao et al., 2017).

The MB is already known as an integration region for different sensory modalities (Brembs and Wiener, 2006; Davis, 1993; Heisenberg et al., 1985; Liu et al., 1999; Brembs and Wiener, 2006; Liu et al., 1999; Martelli et al., 2017). Since the last decades, the MB is in the focus for the state-dependent behavior studies. For instance, the first study showed that MB is required for hunger-driven appetitive memory formation by communicating with dNPF-mediated dopamine signaling (Krashes et al., 2009).

Following the study of Krashes et al., 2009, additional studies showed an involvement of the MB in hunger driven food seeking behaviors (Sayin et al., 2019; Tsao et al., 2018). These studies also revealed an involvement of the MB in a compartmentalized manner. For instance, the α3, β2β′2a, β′2a, α′2α2, and γ2α′1 compartments of the MB innervated by six different modulatory populations integrate distinct information about the internal state. Then, the corresponding behavior is executed by the MBONs innervating the same regions via inhibition or disinhibition (Tsao et al., 2018).

This study can also take place among the others showing the involvement of the MB in the modulation of state-dependent behaviors. Additionally, the compartments innervated by MB188B DANs were shown for the first time incorporating the integration of hunger signaling in feeding behavior.

4.2.4 Hunger state encoded by DANs

In the previous section the involvement of the MB in motivation based adaptations was discussed. In this section I will discuss the role of MB related DANs in these behaviors. I will also implement the findings in this study in already existing circuitries underpinning the motivation-based food uptake behavior adaptation.

It is known that the association of an appetitive (or aversive) stimulus with an odor happens at the MB level (Kim et al., 2007; Owald et al., 2015; Qin et al., 2012; Schroll et al., 2006). The valence of a stimulus is thought to be encoded as rewarding or punishing, which is mainly mediated by DANs.

Similarly, the involvement of the MB in state-dependent food uptake is modulated by the DANs (Krashes et al., 2009; Sayin et al., 2019; Tsao et al., 2018). In these studies, DANs have been shown to encode hunger and satiety beside reward and punishment.

For instance, the inhibition of a pair of DANs (MB-MP DANs) has been shown to be enough for the retrieval of hunger-dependent appetitive memory in satiated flies (Krashes et al., 2009). These DANs also were reported to communicate a hunger signal dNPF to encode hunger.

In addition, the activity of the DAN population investigated in this study, MB188B DANs appears also to be informative about the hunger state. Lack of the MB188B DANs activity apparently provides information about the hunger state. This information also occurs in a compartmentalized fashion and via neuropeptide communications, as is the case in the other DAN-modulated states Furthermore, activity increase (or the lack of activity) has also been shown to be informative about the energy level or sucrose presence in different DANs (Krashes et al., 2009; Musso et al., 2015; Tsao et al., 2018; Yamagata et al., 2016).

However, this study provides further insight of how adaptation in feeding occurs dependent on a long-term nutrition restriction. Here, I demonstrated that a long-lasting connectivity change further affects the valence of the MB188B DANs on the MB. These permanent structural modifications might ensure the persistence of the increase in food uptake under calorie restriction conditions.

4.3 Effect of dietary on behaviors

Flies show a wide range of behavioral adaptations, from the foraging behaviors to sleep regulation, from balancing the nutrition in the dietary to the decision making in oviposition site, etc. (Lihoreau et al., 2016; McDonald and Keene, 2010; Toates, 1986; Yang et al., 2008, see section 1.3).

In this study, a series of behavioral experiments were conducted in which flies were subjected to different caloric values of dietaries. The effects of different dietaries will be discussed in the following chapters.

4.3.1 State-dependent behaviors

It is no surprise that the flies tend to increase the food uptake when they are exposed to a low calorie dietary. The CAFE assay I performed revealed the same type of enhancement upon the calorie restriction in the flies (Carvalho et al., 2005). Flies deprived of a particular type of nutrients adjust to increase the uptake of the missing component (Ribeiro and Dickson, 2010; Vargas et al., 2010). In my recipes, each food type contains carbohydrate, thus preventing any bias in the food uptake, PER or appetitive memory formation experiments.

Flies fed with hypocaloric dietary must consume more amount of food to be able to get the same nutritional value as the other groups. During the feeding test, all fly groups were given the same nutritional value of food. However, still, an increase in food uptake was observed. Therefore, this elongation was concluded as an adaptation in feeding duration and amount.

Another interesting observation referred to the appetitive memory formation under the short starvation period (6h). Flies fed with isocaloric and hypocaloric flies failed to show a strong appetitive memory formation. However, under hypocaloric condition, an enhanced memory performance was observed. It has been shown that hunger gates the retrieval of the appetitive memory (Krashes et al., 2009). Therefore, the strong memory performance is concluded as an elevated hunger level and motivation for food uptake under short starvation period.

4.3.2 Odor and shock avoidance

It has been shown that the aversion to certain odors is inhibited in starved flies to contribute to the searching behavior of the animals (Ko et al., 2015; Root et al., 2011). In the odor avoidance tests performed in this study, the same decrease in aversion could be expected. However, no decrease in the aversion was prominent. There can be two reasons for this result. The first is that the odors used in the experiments were strongly aversive. The second is that the flies exposed to the hypocaloric conditions were not constantly hungry.

Additionally, risk taking of the flies was also shown to be enhanced among starved animals (Sih, 1980). However, when flies were tested under a calorie restriction condition, no impairment in shock avoidance was observed.

Strong avoidance against aversive odors and electric shock used in my experiments can also be shown as a proof that calorie restriction does not create constant starvation but adaptation to food uptake increase. On the other hand, since the odor and shock avoidance were not affected by dietary, change in appetitive memory formation can be concluded as state-dependent memory enhancement.

4.3.3 Locomotion

Finally, the activity of the flies was tested as the last behavior type. It is known that the flies demonstrate hyperactivity and an increase in the locomotion upon the starvation as well as the suppression of the sleep behavior (McDonald and Keene, 2010; Root et al., 2011). In the activity measurements, no hyperactivity or increase in arousal state was observed (Figure 3.3) that could be caused by the malnutrition or the starvation of the flies. Lack of hyperactivity, sleep impairment, or extended aroused state in the hypocaloric flies indicated that the flies were not suffering from malnutrition or constant starvation

So far, I discussed the effect of the calorie restriction on certain behaviors of the flies. I showed that the motivation for the food uptake is enhanced in the flies when the caloric value of the diet decreases for a long time. In the following chapters, structural changes in the MB188B DANs and their involvement in these feeding-related behavioral adaptations will be discussed.

4.4 Measures of the connectivity analysis

Mechanisms that involve structural modifications in the related circuitries behind adaptation to calorie restriction are ultimately aimed to be examined in this study.

The common methods used in the studies that examine and characterize the structural changes in certain neurons, are rather direct measurements and related to the physical properties of a single neuron such as the branch numbers, cell body size, axon length or if applicable the synaptic bouton number and size (Koon et al., 2011; Kremer et al., 2010; For mammalians: Lamprecht and LeDoux,

2004). However, these techniques remain insufficient when a cell population is investigated rather than a single cell. Additionally, the neurons, hence the neuronal arborizations in the *Drosophila* brain, are much smaller in size compared to the mammalian cells (Gao et al., 2019).

In this study, the reconstitution of the GFP technique, that is often referred to as the GRASP technique, is used as the first indication in cell connectivity (Pech et al., 2013). Here, it should be noted that the GRASP technique does not necessarily label only the synaptic connections. The proximity between two neurites can give rise to the reconstitution of spGFP that is tethered to the cell membranes independent of the active synaptic connections. Therefore, this technique is used initially as a primary indication of the increase or decrease in the connections. Following this technique, the connectivity and structural modifications are supported by further detailed experiments.

To eliminate the non-specific reconstitution of the splitGFP (spGFP) outside of the synaptic sites, a recently- developed synaptic GRASP (sybGRASP) (Macpherson et al., 2015), could also be utilized. Even though this GRASP technique is more confined in the synaptic areas, it is also activity-dependent. This means that the reconstitution of the splitGFP is affected by 2 parameters: 1) Structural modifications, and 2) functional modifications in the cells. Considering that the long term adaptation of the activity and structure of the MB188B DANs are counteracting with each other, I conclude that the sybGRASP technique is not suitable for this study (Figure 3.15).

The limitation in the structural plasticity is expected considering the solid brain circuitries of the adult fly. However, in this study, the plastic component of this solid wiring was shown as the MB188B DANs. Finding the plastic components of this solid wiring will enable us to understand where the adjusting points of the circuitries are located and if these adjustments can be tuned artificially whenever necessary.

4.5 Detailed characterization of the structural plasticity

In this chapter a detailed characterization of the structural modifications is provided. These modifications can also potentially elucidate the mechanisms of structural plasticity.

Prior to the structural plasticity characterization, decrease in GRASP signal can bring up the question if this decrease develops from malnutrition rather than a re-structuring phenomenon. The possibility of

poor re-wiring due to the lack of nutrition can be eliminated for two reasons: Firstly, the hypocaloric food is not introduced to the flies until the critical period is completed (Hensch, 2004). Secondly, the decreases in the protein levels are not observed in every protein type such as presynaptically localized sypGCaMP3. Additionally, if lack of nutrition caused the poor wiring, it should have been also observed in other DAN groups, which was not the case. Therefore, the apparent cause of the decrease in the GRASP signal is due to the decrease in postsynaptic homer-GFP protein level.

4.5.1 Postsynaptic structural plasticity

It is logical to think that re-structuring occurs on the synaptic sites to adjust the cell communication and following behavioral output in a long-lasting manner. Therefore, following the GRASP analysis, I demonstrated that the postsynaptic homer-GCaMP level decreases under calorie restriction.

The endogenous Drosophila homer protein is necessary for a behavioral plasticity in ethanol sensitivity (Urizar et al., 2007). Similar to this ethanol adaptation case, feeding adaptation can be achieved by the homer level regulation in the MB188B DANs, as well. Therefore, the first conclusion can be drawn that the structural modifications are pronounced on the postsynaptic sites.

The second conclusion can also be speculated on the long-lasting structural pruning based on a study done in the rats. The homer protein is known to interact with the postsynaptic protein Shank and form a scaffold to maintain the postsynaptic structure (Diagana et al., 2002; Tu et al., 1999). It has been shown that the level of the Homer is not regulated. However, its partner scaffold protein Shank is rather redistributed and adjusted in a presynaptic activity-dependent way in the postsynaptic density (Tao-Cheng et al., 2014). This indicates that the Homer protein regulation leads to rather long-lasting structural changes.

4.6 Structural plasticity of modulatory neurons in association to behavioral adaptations

The re-wiring of the modulatory neurons is proposed as a mechanism to adjust feeding-related behaviors that are pronounced after long- term calorie restriction exposure in adult *Drosophila* brain. I focused on the modulatory DANs innervating the MB. The integration of the hunger signal and the

effect of structural decrease on this integration is briefly discussed in section 4.2.4. Here, a detailed discussion is provided in terms of possible signaling integration in association to behavioral adaptation. It is well known that the DANs innervating proximal lobes of the MB such as γ1 and γ2 is involved in the aversive learning which requires experience-based sensory stimulus integration. Moreover, the optogenetic stimulation of these DANs induce strongly a pronounced memory formation and an underlying corresponding MBON response modulation (Aso et al., 2014a; Claridge-Chang et al., 2009). Similarly, the DANs that innervate the distal lobes such as γ4 and γ5 is also involved in strong modulation of sugar and thirst memory (Aso et al., 2010; Burke et al., 2012; Claridge-Chang et al., 2009; Liu et al., 2012; Perisse et al., 2013; Schroll et al., 2006).

However, the role of MB188B DANs, that innervate the γ3, γ4 and β'1 regions of the MB, are not shown to play any role in the context of memory formation. Additionally, the MB188B DANs are known to result in avoidance behavior upon stimulation. However, the valence encoded by these DANs remained unsolved (Aso et al., 2014). Finally, these DANs are not shown to lead a strong postsynaptic modulation in the learning process compared to its more proximal and more distal DAN populations (Louis et al., 2018).

In this study, the role of the MB188B DANs in food uptake was confirmed as a first approach to correlate structural modifications of these DANs with underlying feeding-related behaviors. Since, the inhibition of the MB188B DANs shows a behavioral effect, but not their activation, it is possible that these DANs are constantly active. Thus, the absence of the activity is informative about the hunger state. This phenomenon can be perhaps explained by potential oscillation of the MB188B DANs. The change in the oscillation (or complete suppression) could be an indicator of the internal state. In the literature, there are more examples of oscillatory DANs innervating the MB that are involved in food uptake behaviors. For instance, the frequency of certain oscillatory DANs is translated in terms of the energy level by Drosophila MB (Musso et al., 2015). Additionally, a group of oscillating γ3 innervating DANs is suppressed upon the sugar presentation to the fly.

If the oscillation of the MB188B DANs are responsible for encoding the energy level (or internal state) valence, the long-lasting (or even permanent) changes in the oscillation of these DANs can be achieved by the structural modifications. These changes can then result in the behavioral adaptation according to the food condition.

Another study showing the MB involvement in the foraging behavior suggests that flies lacking an intact MB shows less centrophobia (fear of freely exploring the center of an arena). The exploration rate of these flies increased when the MB is impaired (Besson and Martin, 2005). A similar study suggests that this enhancement in the exploratory behaviors develops from the downregulation of *Drosophila* Neuroligin protein Dnlg2 which is found in the synaptic structures of the MB. This protein is responsible for maintaining the structure of the synapses (Corthals et al., 2017). The same study also suggests that Dnlg2 knock-down in the MB results in a decrease in the connectivity between the MB and related neurons. This decrease in connectivity leads to an increase in exploratory behaviors quite similar to the hungry flies that have less centrophobia. As discussed above, here, I suggest that the decrease in the connectivity of these DANs, either on the MB or on the MB-related neurons enhances the foraging-related behaviors and ultimately the food uptake similar to Dnlg2 knock-down flies that has less connectivity to their MB.

Here, it is shown that the connectivity change in MB188B DANs occurs postsynaptically (Figure 3.11). Similar to this compartmentalized structural refinement, a branch-specific pruning in another DAN group (the DA-WED) and the involvement in the food uptake were also shown by Liu et al., 2017. These DANs are also involved in the motivation for particular nutrition seeking. Interesting enough, the structure of these DANs is compartmentalized in a way that certain branches are responsible for different nutrient types. Additionally, these branches are undergoing pruning when the animal needs to increase the uptake of a specific nutrient(Liu et al., 2017). However, what is remarkable about the structural refinements of the MB188B DANs shown in my study is that it occurs upon long term restriction unlike DA-WED. Additionally, these refinements are rather long-lasting.

All the arguments speculated above are rather an indirect explanation of how structural changes can modulate the feeding behavior. However, a direct evidence showing that the structural changes result in the enhancement of the food uptake was also presented (Figure 3.17). This evidence will be discussed extensively under section 4.7.

All in all, these arguments suggest that the MB188B DANs involve in the state-dependent foraging behavior. Structural modifications in these DANs can help the animal to adjust the corresponding behaviors according to the level of nutrition exposure in a long period.

4.7 Dynamics of functional and structural adaptation

So far the structural plasticity of the MB188B DANs leading behavioral plasticity in the foraging-related behavior in *Drosophila* is discussed. The next question is what causes these structural changes. Since functional adaptations occurred prior the structural adaptations, it is inevitable to consider that the functional and structural adaptations are dependent on each other. Thus, in this chapter, I argue the functional and structural adaptations in the course of the long term exposure and the possible mechanisms behind these modulations.

4.7.1 Synaptic plasticity leading to structural plasticity

Structural changes in adapting circuitries are mainly carried out by persisting synaptic plasticity. For instance, in a Hebbian learning paradigm, potentiation of the postsynaptic partners leads to synaptic strengthening and the generation of the synaptic varicosities on the presynaptic site (Kim et al., 2003). On the other hand, activity triggering pruning is also common for circuitry adjustments (Liu et al., 2017; Wong and Ghosh, 2002; Yuan et al., 2011). Elimination of specific branches in a DAN population upon increased cell activity can be mentioned as an example of this type of structural modification (Liu et al., 2017). Thus, in this section, activity induced structural plasticity (or vice versa) is recognized and subjected to discussion.

When the activity and structural plasticity of the MB188B DANs are measured at different time point during dietary, an early increase in the activity occurs upon calorie restriction in food (Figure 3.15). These results are the first indication of an increased cell activity leading to a decrease in connectivity. On the other hand, these late-emerging decreases in the connectivity could be a homeostatic response to the increase in the activity with the restriction of the caloric value. Another example of a homeostatic response that happens in the opposite direction, can be shown in the study of Pech et al., 2015. In this study, the increase in the response and volume are shown in the dendritic arborizations of KCs upon the decrease in the input from the presynaptic partners, the PNs.

If the activity-induced structural refinement is the case in the MB188B DANs, I speculate that the long-term artificial activation should lead to the same kind of decrease in these DANs. At this point, I took advantage of the optogenetic tools to artificially increase the activity and mimic the decrease in connectivity that occurs upon hypocaloric food exposure. However, artificial depolarization of these

DANs by light-inducible cation channels for a long period did not lead to the induction of structural plasticity (Figure 3.16). This failure does not necessarily mean that the increased activity does not lead to structural refinements. There can be several reasons why the functional plasticity could still be the mechanism behind the structural plasticity.

On the one hand, this type of depolarization may not be the real causative of the plasticity induction. Additionally, these results can give a hint about the cellular mechanism of the structural plasticity modulation. This means that the structural plasticity may not be modulated by ionotropic signal transduction mechanisms. Therefore, depolarizing these DANs with an cation channels may not result in structural plasticity.

On the other hand, the light stimulation frequency that I have used in my experiments is much smaller compared to the frequency of other oscillating DANs (Yamagata et al., 2016). If the MB188B DANs are oscillating the same way as speculated in section 4.7, the smaller light induction frequency might also fail to induce the structural plasticity.

The final reason could be the highly efficient optogenetic channels such as ChR-XXL. Therefore, the light stimulus could lead to a tetanus state where the neurons cannot be excited anymore. This high efficiency can even lead to the depletion of the synaptic vesicles. These two phenomena eventually result in the activity decrease in the long run instead of an increase. All these three reasons listed, could potentially prohibit the initiation of structural changes.

Contrary to the long-term depolarization, the artificial elevation in the cAMP level leads to a decrease in the connectivity of the MB188B DANs (Figure 3.16). Therefore, I conclude that the activity increased in the MB188B DANs following the onset of the hypocaloric diet, leads further increase in the cAMP level. This activity dependent cAMP increase induces the structural refinements in the long run. There are examples of the involvement of the cAMP pathway in regulating the experience-dependent modifications of the postsynaptic compartments, as in the case of MB188B DANs shown in this study (Yuan et al., 2011). For instance, in the study of Yuan et al., 2011, sensory input-induced refinement of the postsynaptic arbors in the visual system of the *Drosophila* larva was shown to be dependent on the cAMP increase. Therefore, I conclude that the experience-dependent activity increase of the MB188B DANs results in the structural modification via cAMP involved signaling pathways.

4.7.2 Role of reciprocal synapses in the synaptic and structural plasticity

Earlier, I discussed synaptic plasticity followed by the structural plasticity in the MB188B DANs. Another aspect of this type of plasticity is the role of reciprocal synapses on the regulation of the activity of the MB188B DANs.

The MB188B DANs apparently have reciprocal synapses with the KCs (or perhaps even with MBONs) (Figure 3.8) and the presence of the reciprocal synapses might have a role in the synaptic plasticity followed by structural plasticity. Regulation of the synaptic plasticity by reciprocal synapses is shown in other sensory modalities (e.g. Grimes et al., 2009) as well in the olfactory sensory system (e.g. Trombley and Shepherd, 1993) in vertebrates.

In the former study (Grimes et al., 2009), the reciprocal synapses are present in the amacrine cells that are connected to the rod bipolar cells in the visual system. These reciprocal synapses belong to the presynaptic partner and provide information about the activity of the postsynaptic partner. Thus, these synapses modulate the activity of the postsynaptic partner (red bipolar cells) by giving feedback to the presynaptic partners (amacrine cells).

In the latter study (Trombley and Shepherd, 1993), the reciprocal synapses are present in both postsynaptic compartments (dendro-dendritic reciprocal synapses) of the two communicating output neurons; mitral and tufted cells, in olfactory bulb. Trombley and Shepherd, 1993 speculated that the presence of reciprocal synapses between these cells tunes the olfactory information by lateral inhibition. It is also speculated that olfactory learning is modulated by NE (the mammalian equivalent of OA; Yang et al., 2015), which is achieved by the presence of these reciprocal synapses (Brennan et al., 1990; Trombley and Shepherd, 1993).

The mechanism explained in the latter study could be a possible working principle of the reciprocal synapses also in the case of the MB188B DANs. In both cases, the reciprocal synapses are included in the higher brain region of the olfactory processing and encode valence to this region (Trombley and Shepherd, 1993). These reciprocal synapses could modulate the downstream signaling by the input from the partners of the MB188B DANs as well as the MB188B DANs own activity.

It has been shown that the input from the MBONs on DANs is not necessary for DAN-dependent plasticity (Hige et al., 2015). Thus, the input obtained via the reciprocal synapses of the MB188B DANs most likely coming from the MB KCs or the MB188B DANs itself. Based on *trans*Tango experiments, the MB188B DANs appear to be postsynaptic to themselves (Figure 3.9). Therefore, this autoregulation mechanism is highly likely. Additionally, when the response profile of the MB188B DANs is examined closely, a late-evoked response in the γ3 regions might be an indication of in which compartment of the MB188B DANs, the reciprocal information flow can occur (Figure 3.12 and 13).

All in all, in this section, I argued that the long term calorie restriction is reflected in the synaptic activity of the MB188B DANs. Then, this activity increase in the MB188B DANs is followed by the structural refinements that are most likely achieved by the presence of the reciprocal synapses. The reciprocal synapses obtain the information either from the MB188B DANs themselves or the downstream neuron populations (most likely from KCs).

4.8 The possible molecular mechanisms underlying the structural plasticity induction

I demonstrated that the accumulated activity of the MB188B DANs over time based on the increase in the Ca^{2+} level (by CaLexA), occurs prior to the structural changes in the MB188B DANs (Figure 3.15). Above I argued that the elevation of Ca^{2+} via cation channel based optogenetic tools does not induce the structural plasticity. However, the elevation of cAMP resulted in this plasticity (Figure 3.16). Therefore, from now on the structural plasticity is referred to as "Ca^{2+} dependent cAMP-induced structural plasticity". In this chapter, I will discuss two possible cAMP involved molecular pathways as mechanisms behind the Ca^{2+} dependent cAMP-induced structural plasticity:

The first and most obvious mechanism leading to this Ca^{2+} dependent cAMP-induced structural plasticity is the communication with the AstA satiety neuropeptide (Figure 3.18). *Drosophila* has two AstA binding receptors, DAR1 and 2 and both of these receptors are GPCR which can lead to Ca^{2+} dependent cAMP modulation (Hergarden et al., 2012). AstA is also known to be inhibitory to the postsynaptic partner neurons like many of the other peptides (Hergarden et al., 2012; Lechner et al., 2002; Yamagata et al., 2016). Therefore, upon AstA downregulation, it can lead to more Ca^{2+} dependent cAMP elevation.

Following the same logic, it is also expected, the AstA release will be slower and overall much less under the hypocaloric condition compared to the other conditions. Therefore, this overall decrease in the AstA will lead to an increase in the activity of the MB188B DANs most possibly leading to further Ca^{2+} dependent cAMP increase in the cells. Then, in the long-term, either this increase itself or the feedback from the postsynaptic partners of the MB188B DANs will induce the Ca^{2+} dependent cAMP-induced structural plasticity (Figure 4.1).

The structural refinement could be also a compensatory mechanism against the increased activity of the MB188B DANs (see section 4.7.1). Here, an autoregulatory mechanism cannot be excluded since the MB188B DANs are also postsynaptic to themselves.

A second molecular mechanism dependent on cAMP increase in the MB188B DANs could be DA biosynthesis (Vié et al., 1999). I argued the possibility of the MB188B DANs oscillation. In such a case, DA release change is informative about the satiety state.

Flies needs to increase the food uptake to get the same amount of calories under the hypocaloric condition. In the case of long-term exposure to the hypocaloric conditions, the high frequency of food uptake must be ensured by the adaptation in DA synthesis. Therefore, a highly dynamic DA synthesis is necessary for more frequent food uptake.

It has been shown that the DA synthesis in the CNS of *Drosophila* is activated via the phosphorylation of the TH enzyme by cAMP-dependent protein kinase (PKA) in the absence of dopamine (Vié et al., 1999). Therefore, a more dynamic DA biosynthesis can be solved by the increase in the cAMP level in the long term. This phenomenon can also be part of the $Ca2^{+}$ dependent cAMP-induced structural plasticity.

In this section, I proposed two possible molecular mechanisms underlying the Ca^{2+} dependent cAMP-induced structural plasticity underlying the enhanced food uptake: The first mechanism is the cAMP elevation as a result of decreased AstA signaling. The second mechanism is the cAMP elevation-induced DA synthesis (and release). It should be noted that these two suggested mechanisms do not have to be mutually exclusive and can take place hand in hand.

4.9 Implementation of the structural adaptation in circuitry involved in motivational adaptation

Up until this point, the structural plasticity along with the involvement of this plasticity in the adaptation of feeding-related behaviors under calorie restriction condition were discussed. Then, I argued the possible molecular mechanisms that induce structural plasticity and how these mechanisms contribute to the feeding behavior of the flies in an adapted manner.

As final argumentation, I discuss the possible circuitry model where the structural refinement of the MB188B DANs could regulate the motivation-based behavioral adaptations dependent on the calorie restriction. As in the previous chapter, here again, the $Ca2^{+}$ dependent cAMP-induced structural plasticity will be taken as the core of the underpinning mechanism.

The compartmentalized manner of the structural plasticity is argued in section 4.7. However, in this circuitry model (Figure 4.1), I leave out the compartmentalized structural modifications and show the connectivity decrease as a whole for the simplicity of the illustration.

The first component of the circuitry was shown as the AstA neuropeptide (or the neuropeptide releasing neurons). The flies that are exposed to the low-calorie diet will extend the feeding time constantly to feel saturated. Since AstA is released upon satiation (Hergarden et al., 2012), this elongation will lead to cumulative AstA peptide decrease over time (Figure 4.1B). The reduction in the AstA will lead to a Ca^{2+}-dependent cAMP elevation in the MB188B DANs. The long term elevation of the cAMP, then, will give rise synaptic plasticity (most likely potentiation) followed by the structural depression in the long term (Figure 4.1B). The structural abolishment will be achieved by the postsynaptically localized Homer decrease as discussed in section 4.7.

This adaptation of the connectivity decrease then provides a more dynamic motivational increase for food uptake. Here, the adjective dynamic describes an early and fast occurrence of the hungriness. There can be two explanations for the food-seeking and uptake enhancement caused by the decrease in the postsynaptic site; 1) The effect of the AstA satiation signaling will be decreased leading to an increased food uptake. 2) When the decrease in the synaptic connection can be seen as the increase in the synaptic cleft between the MB188B DANs and KCs, the increase in the synaptic cleft will have the

same effect as in the study of Corthals et al., 2017 eventually leading to the exploring rate increase as an indication of motivation (Figure 4.1).

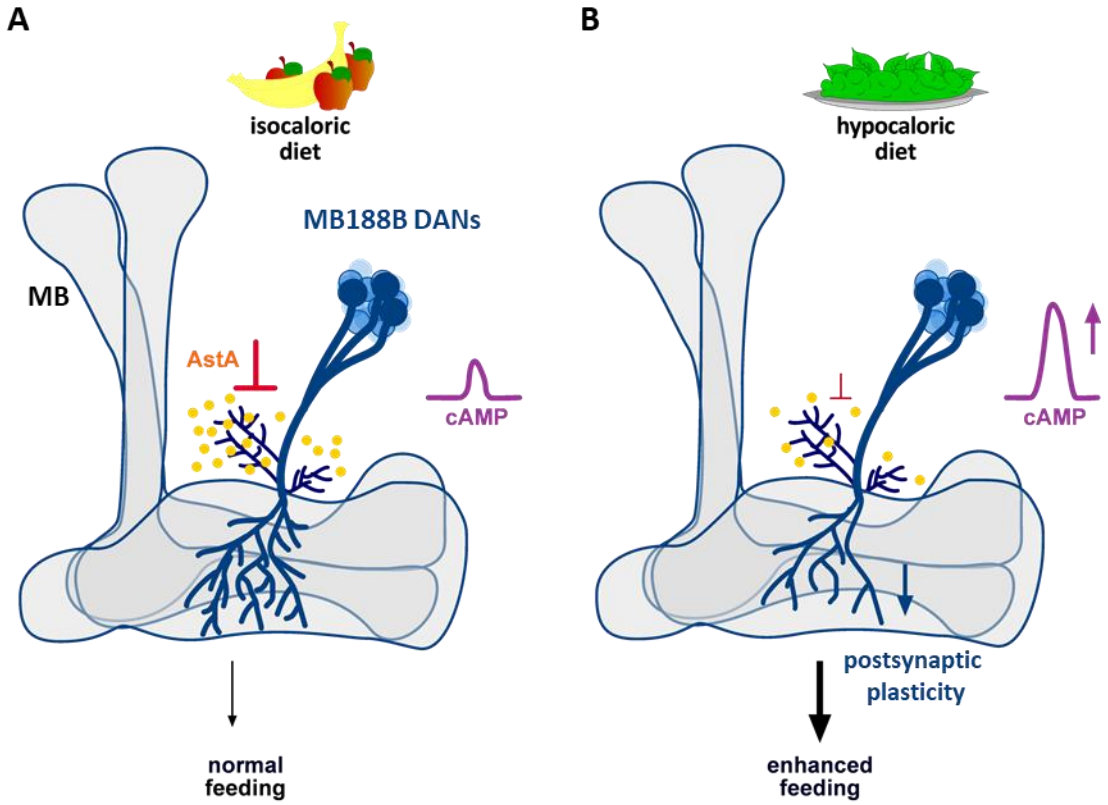

Figure 4.1 Illustration of the structural refinements of the MB188B DANs on the MB. **A** AstA-mediated feeding circuitry under isocaloric diet illustrated. The release of AstA keeps the cAMP level in certain level leading to the normal feeding related behaviors. **B** Hypocaloric diet case depicted. Decrease in nutritional value results in decrease in AstA signaling in the long run. Long-term cAMP elevation due to this decrease triggers the structural refinements. This situation yields in an enhanced motivation for food uptake.

It should be noted that the communication of the MB188B DANs to the other neuropeptides cannot be ruled out. For instance, I have shown that the MB188B DANs were not provided by SIFa peptide. However, SIFa could still be potentially the downstream of the MB188B DANs. Especially, the one-way involvement of the MB188B DANs and SIFa are considered feeding behaviors (Martelli et al., 2017).

4.10 Outlook

The study presented in this thesis demonstrates one of the few concepts how the compartmentalized structural plasticity is shaped by the changing environmental conditions in the fully developed adult

brain. It is demonstrated that certain dopaminergic neuron populations remain open to re-wiring in the adult *Drosophila* brain depending on the changes in the environmental factors.

DANs are shown to modify the valence of a stimulus in an experience-dependent way (Aso et al., 2010; Riemensperger et al., 2005; Schroll et al., 2006; Yamagata et al., 2016). Recently, the hunger state was also shown to be integrated in the MB via DANs (Krashes et al., 2009; Sayin et al., 2019; Tsao et al., 2018). This study also presents a group of DANs changing the internal state valence on the MB hunger signal. Even more interestingly, the structural changes in these DANs ensures the long-lasting valence changes. In order to understand to what degree the structural decrees in the investigated DAN population changes the valence, further translation in terms of activity modulation in downstream circuitry can be examined.

It has been shown that certain structural changes are responsible for behavioral plasticity in the developing Drosophila brain (Doll et al., 2017; Heisenberg et al., 1995; Koon et al., 2011). This study contributes to structural plasticity studies in a unique way since these re-structuring happens in fully developed brain. So far, the structural changes shown in the fully developed Drosophila brain was the age-related structural changes (Groh et al., 2012) . Some of this age-related structural plasticity examples was shown to be irreversible (Gupta et al., 2016). In this plasticity case, the reversibility of the structural decreases can also be further investigated.

Branch-specific structural plasticity is shown to underlie the active selection of a certain nutrient (Liu et al., 2017). In these DANs, the structural changes happen to be in a compartmentalized way as well. Additionally, this study suggests that the compartmentalized plasticity is achieved by reciprocal synapses, which is also a rather novel concept (Cervantes-Sandoval et al., 2017; Eichler et al., 2017). Seemingly, the MB188B DANs obtain information about their own activity and balance the homeostasis accordingly via these reciprocal synapses. Still, the branch specific structural plasticity can still be investigated in further detail by first questioning the homogenous structural decrease in these DANs.

Finally, this study provides a glimpse of the mechanisms triggering the structural changes. Thus, I could be able to induce the structural changes by imitating this mechanism artificially. The effect of this artificial induction can be studied further in terms of the communication with the other entities in the circuitry involved in the motivation increase for the food uptake such as the MB or MBONs.

Finally, to further support and elaborate the work presented here, the molecular mechanisms behind the structural modification can be investigated. In addition, a wide network is shown to communicate with the MB188B DANs that are re-wired, in the process of orchestrating the motivation enhancement for food uptake. The effect of this re-structuring can be studied in these component of the network as well.

5 Summary

All organisms have to adapt and adjust behaviors to changing environmental conditions. Foraging and feeding behaviors are one of the most adaptive behaviors when changes in nutrient sources occur. Neuronal and behavioral plasticity are not restricted to the developmental phase. An animal must adapt its feeding-related behaviors throughout its life-time to survive.

Drosophila melanogaster shows plasticity in adjusting food uptake dependent on the abundance of nutrient resources. It also adapts state-dependent behaviors like food uptake very similarly on mammals. An immense number of studies showed how internal state and state-dependent behaviors are controlled. However, adaptive mechanisms in the underlying neuronal networks dependent on the long term experience of food abundance remain unclear.

The involvement of the *Drosophila* mushroom bodies and related modulatory neurons, e.g. dopaminergic neurons, in experience-dependent behavioral adjustments is well established. Recently, their role in state-dependent foraging behaviors has also been shown. In this study, I addressed the mushroom body extrinsic dopaminergic neurons an element region involved in internal state regulation. Here I show an occurrence questioned the occurrence of structural plasticity in the adult fly brain that depends on the long-term experience of low or high caloric food value as a mechanism for long-lasting adaptation.

Parametric changes in the caloric value of the fly food were employed as experimental approach. Fully developed fruit flies were exposed to three different long-term dietaries; hypocaloric, isocaloric, and hypercaloric food. Nutritional decrease in the fly food elucidated enhanced feeding-related behaviors. In addition, a decrease in connectivity was also detected in a certain subset of dopaminergic neurons innervating the mushroom body. These neurons were shown to have reciprocal synapses in this study. Besides, structural refinements were shown to take place in postsynaptic sites.

An early activity increase was observed in these dopaminergic neurons upon calorie restriction. Artificially upregulating intrinsic cAMP levels could mimic the structural decrease in connectivity. Therefore, the mechanism behind the decrease in the connectivity under calorie restriction condition are considered to be activity-induced cAMP dependent. Furthermore, this study proved that this

artificial mimicking of the structural refinements led to increased feeding behavior similar to the experience hypocaloric food.

Finally, the information about the internal state was found to be relayed by a satiety peptide “Allatostatin A”. Disruption of Allatostatin A signaling resulted in a prevention of structural refinements. All in all, this study presents an experience-dependent structural modification accomplished by reciprocal synapses in the adult fly brain. Thereby, this study provides new insights into these types of refinements and shows that modulatory neurons in adult brains remain plastic to give rise to adaptive behavior. This plasticity can be induced by the external factors, i.e. nutrition restriction, and also by artificial mimicking whenever behavioral adjustments are necessary.

6 References

Al-Anzi, B., and Zinn, K. (2018). Identification and characterization of mushroom body neurons that regulate fat storage in Drosophila. Neural Development *13*, 18.

Al-Anzi, B., Armand, E., Nagamei, P., Olszewski, M., Sapin, V., Waters, C., Zinn, K., Wyman, R.J., and Benzer, S. (2010). The Leucokinin Pathway and Its Neurons Regulate Meal Size in Drosophila. Current Biology *20*, 969–978.

Alberch, P., Gould, S.J., Oster, G.F., and Wake, D.B. (1979). Size and Shape in Ontogeny and Phylogeny. Paleobiology *5*, 296–317.

Albertson, R., and Doe, C.Q. (2003). Dlg, Scrib and Lgl regulate neuroblast cell size and mitotic spindle asymmetry. Nature Cell Biology *5*, 166–170.

Alekseyenko, O.V., Chan, Y.-B., Li, R., and Kravitz, E.A. (2013). Single dopaminergic neurons that modulate aggression in Drosophila. PNAS *110*, 6151–6156.

Álvarez-Salvado, E., Licata, A.M., Connor, E.G., McHugh, M.K., King, B.M., Stavropoulos, N., Victor, J.D., Crimaldi, J.P., and Nagel, K.I. (2018). Elementary sensory-motor transformations underlying olfactory navigation in walking fruit-flies. ELife *7*, e37815.

Asano, S.M., Gao, R., Wassie, A.T., Tillberg, P.W., Chen, F., and Boyden, E.S. (2018). Expansion Microscopy: Protocols for Imaging Proteins and RNA in Cells and Tissues. Current Protocols in Cell Biology *80*, e56.

Aso, Y., Grübel, K., Busch, S., Friedrich, A.B., Siwanowicz, I., and Tanimoto, H. (2009). The mushroom body of adult Drosophila characterized by GAL4 drivers. J. Neurogenet. *23*, 156–172.

Aso, Y., Siwanowicz, I., Bräcker, L., Ito, K., Kitamoto, T., and Tanimoto, H. (2010). Specific dopaminergic neurons for the formation of labile aversive memory. Current Biology. *20*, 1445–1451.

Aso, Y., Herb, A., Ogueta, M., Siwanowicz, I., Templier, T., Friedrich, A.B., Ito, K., Scholz, H., and Tanimoto, H. (2012). Three Dopamine Pathways Induce Aversive Odor Memories with Different Stability. PLOS Genetics *8*, e1002768.

Aso, Y., Hattori, D., Yu, Y., Johnston, R.M., Iyer, N.A., Ngo, T.-T., Dionne, H., Abbott, L., Axel, R., Tanimoto, H., et al. (2014a). The neuronal architecture of the mushroom body provides a logic for associative learning. ELife *3*, e04577.

Aso, Y., Sitaraman, D., Ichinose, T., Kaun, K.R., Vogt, K., Belliart-Guérin, G., Plaçais, P.-Y., Robie, A.A., Yamagata, N., Schnaitmann, C., et al. (2014b). Mushroom body output neurons encode valence and guide memory-based action selection in Drosophila. ELife *3*, e04580.

Bailey, C.H., and Chen, M. (1988). Long-term sensitization in Aplysia increases the number of presynaptic contacts onto the identified gill motor neuron L7. PNAS *85*, 9356–9359.

Bailey, C.H., Kandel, E.R., and Harris, K.M. (2015). Structural Components of Synaptic Plasticity and Memory Consolidation. Cold Spring Harb Perspect Biol *7*, a021758.

Bargmann, C.I. (2012). Beyond the connectome: How neuromodulators shape neural circuits. BioEssays *34*, 458–465.

Barsh, G.S., and Schwartz, M.W. (2002). Genetic approaches to studying energy balance: perception and integration. Nat. Rev. Genet. *3*, 589–600.

Bernstein, J.G., Garrity, P.A., and Boyden, E.S. (2012). Optogenetics and thermogenetics: technologies for controlling the activity of targeted cells within intact neural circuits. Current Opinion in Neurobiology *22*, 61–71.

Berridge, C.W., and Waterhouse, B.D. (2003). The locus coeruleus–noradrenergic system: modulation of behavioral state and state-dependent cognitive processes. Brain Research Reviews *42*, 33–84.

Besson, M., and Martin, J.-R. (2005). Centrophobism/thigmotaxis, a new role for the mushroom bodies in Drosophila. J. Neurobiol. *62*, 386–396.

Biro, P.A., and Stamps, J.A. (2010). Do consistent individual differences in metabolic rate promote consistent individual differences in behavior? Trends in Ecology & Evolution *25*, 653–659.

van der Bliek, A.M., and Meyerowrtz, E.M. (1991). Dynamin-like protein encoded by the Drosophila shibire gene associated with vesicular traffic. Nature *351*, 411–414.

Brand, A.H., and Perrimon, N. (1993). Targeted gene expression as a means of altering cell fates and generating dominant phenotypes. Development *118*, 401–415.

Brembs, B., and Wiener, J. (2006). Context and occasion setting in Drosophila visual learning. Learn. Mem. *13*, 618–628.

Brennan, P., Kaba, H., and Keverne, E.B. (1990). Olfactory Recognition: A Simple Memory System. Science *250*, 1223–1226.

Brogiolo, W., Stocker, H., Ikeya, T., Rintelen, F., Fernandez, R., and Hafen, E. (2001). An evolutionarily conserved function of the Drosophila insulin receptor and insulin-like peptides in growth control. Current Biology *11*, 213–221.

Brown, M.R., Crim, J.W., Arata, R.C., Cai, H.N., Chun, C., and Shen, P. (1999). Identification of a Drosophila brain-gut peptide related to the neuropeptide Y family. Peptides *20*, 1035–1042.

Browne, L.B., and Evans, D.R. (1960). Locomotor activity of the blowfly as a function of feeding and starvation. Journal of Insect Physiology *4*, 27–37.

Buch, S., Melcher, C., Bauer, M., Katzenberger, J., and Pankratz, M.J. (2008). Opposing Effects of Dietary Protein and Sugar Regulate a Transcriptional Target of Drosophila Insulin-like Peptide Signaling. Cell Metabolism *7*, 321–332.

Budnik, V., and White, K. (1987). Genetic dissection of dopamine and serotonin synthesis in the nervous system of Drosophila melanogaster. Journal of Neurogenetics *4*, 309–314.

Budnik, V., Zhong, Y., and Wu, C.F. (1990). Morphological plasticity of motor axons in Drosophila mutants with altered excitability. J. Neurosci. *10*, 3754–3768.

Burke, C.J., and Waddell, S. (2011). Remembering Nutrient Quality of Sugar in Drosophila. Current Biology *21*, 746–750.

Burke, C.J., Huetteroth, W., Owald, D., Perisse, E., Krashes, M.J., Das, G., Gohl, D., Silies, M., Certel, S., and Waddell, S. (2012). Layered reward signaling through octopamine and dopamine in Drosophila. Nature *492*, 433–437.

Burke, M.K., Dunham, J.P., Shahrestani, P., Thornton, K.R., Rose, M.R., and Long, A.D. (2010). Genome-wide analysis of a long-term evolution experiment with Drosophila. Nature *467*, 587–590.

Campbell, R.A.A., Honegger, K.S., Qin, H., Li, W., Demir, E., and Turner, G.C. (2013). Imaging a Population Code for Odor Identity in the Drosophila Mushroom Body. J. Neurosci. *33*, 10568–10581.

Careau, V., Thomas, D., Humphries, M.M., and Réale, D. (2008). Energy metabolism and animal personality. Oikos *117*, 641–653.

Carvalho, G.B., Kapahi, P., and Benzer, S. (2005). Compensatory ingestion upon dietary restriction in Drosophila melanogaster. Nature Methods *2*, 813–815.

Cervantes-Sandoval, I., Phan, A., Chakraborty, M., and Davis, R.L. (2017). Reciprocal synapses between mushroom body and dopamine neurons form a positive feedback loop required for learning. ELife *6*, e23789.

Chen, F., Tillberg, P.W., and Boyden, E.S. (2015). Expansion microscopy. Science *347*, 543–548.

Chia, J., and Scott, K. (2020). Activation of specific mushroom body output neurons inhibits proboscis extension and sucrose consumption. PLoS ONE *15*, e0223034.

Chippindale, A.K., Leroi, A.M., Kim, S.B., and Rose, M.R. (2004). Phenotypic plasticity and selection in Drosophila life-history evolution. I. Nutrition and the cost of reproduction. In Methuselah Flies, (WORLD SCIENTIFIC), pp. 122–144.

Chung, B.Y., Ro, J., Hutter, S.A., Miller, K.M., Guduguntla, L.S., Kondo, S., and Pletcher, S.D. (2017). Drosophila Neuropeptide F Signaling Independently Regulates Feeding and Sleep-Wake Behavior. Cell Reports *19*, 2441–2450.

Claridge-Chang, A., Roorda, R.D., Vrontou, E., Sjulson, L., Li, H., Hirsh, J., and Miesenböck, G. (2009). Writing memories with light-addressable reinforcement circuitry. Cell *139*, 405–415.

Cognigni, P., Felsenberg, J., and Waddell, S. (2018). Do the right thing: neural network mechanisms of memory formation, expression and update in Drosophila. Current Opinion in Neurobiology *49*, 51–58.

Cohn, R., Morantte, I., and Ruta, V. (2015). Coordinated and Compartmentalized Neuromodulation Shapes Sensory Processing in Drosophila. Cell *163*, 1742–1755.

Corthals, K., Heukamp, A.S., Kossen, R., Großhennig, I., Hahn, N., Gras, H., Göpfert, M.C., Heinrich, R., and Geurten, B.R.H. (2017). Neuroligins Nlg2 and Nlg4 Affect Social Behavior in Drosophila melanogaster. Front. Psychiatry *8*.

Crittenden, J.R., Skoulakis, E.M., Han, K.A., Kalderon, D., and Davis, R.L. (1998). Tripartite mushroom body architecture revealed by antigenic markers. Learn. Mem. *5*, 38–51.

Davis, R.L. (1993). Mushroom bodies and drosophila learning. Neuron *11*, 1–14.

Dawydow, A., Gueta, R., Ljaschenko, D., Ullrich, S., Hermann, M., Ehmann, N., Gao, S., Fiala, A., Langenhan, T., Nagel, G., et al. (2014). Channelrhodopsin-2–XXL, a powerful optogenetic tool for low-light applications. PNAS *111*, 13972–13977.

Destexhe, A., and Marder, E. (2004). Plasticity in single neuron and circuit computations. Nature *431*, 789–795.

Dethier, V.G. (1976). The hungry fly: A physiological study of the behavior associated with feeding (Oxford, England: Harvard U Press).

Dethier, V.G., and Chadwick, L.E. (1948). Chemoreception in insects. Physiological Reviews *28*, 220–254.

Diagana, T.T., Thomas, U., Prokopenko, S.N., Xiao, B., Worley, P.F., and Thomas, J.B. (2002). Mutation of Drosophila homer Disrupts Control of Locomotor Activity and Behavioral Plasticity. J. Neurosci. *22*, 428–436.

Dietrich, M.O., Zimmer, M.R., Bober, J., and Horvath, T.L. (2015). Hypothalamic Agrp Neurons Drive Stereotypic Behaviors beyond Feeding. Cell *160*, 1222–1232.

Dolan, M.-J., Frechter, S., Bates, A.S., Dan, C., Huoviala, P., Roberts, R.J., Schlegel, P., Dhawan, S., Tabano, R., Dionne, H., et al. (2019). Neurogenetic dissection of the Drosophila lateral horn reveals major outputs, diverse behavioural functions, and interactions with the mushroom body. ELife *8*, e43079.

Doll, C.A., Vita, D.J., and Broadie, K. (2017). Fragile X Mental Retardation Protein Requirements in Activity-Dependent Critical Period Neural Circuit Refinement. Current Biology *27*, 2318-2330.e3.

Donoghue, P.C.J., and Dong, X. Embryos and Ancestors. 21.

Dubnau, J., Grady, L., Kitamoto, T., and Tully, T. (2001). Disruption of neurotransmission in Drosophila mushroom body blocks retrieval but not acquisition of memory. Nature *411*, 476–480.

Ebenman, B. (1992). Evolution in Organisms that change their niches during the life cycle. The American Naturalist *139*, 990–1021.

Edgecomb, R.S., Harth, C.E., and Schneiderman, A.M. (1994). Regulation of feeding behavior in adult Drosophila melanogaster varies with feeding regime and nutritional state. Journal of Experimental Biology *197*, 215–235.

Eichler, K., Li, F., Litwin-Kumar, A., Park, Y., Andrade, I., Schneider-Mizell, C.M., Saumweber, T., Huser, A., Eschbach, C., Gerber, B., et al. (2017). The complete connectome of a learning and memory centre in an insect brain. Nature *548*, 175–182.

Feinberg, E.H., VanHoven, M.K., Bendesky, A., Wang, G., Fetter, R.D., Shen, K., and Bargmann, C.I. (2008). GFP Reconstitution Across Synaptic Partners (GRASP) Defines Cell Contacts and Synapses in Living Nervous Systems. Neuron *57*, 353–363.

Fischer, J.A., Giniger, E., Maniatis, T., and Ptashne, M. (1988). GAL4 activates transcription in Drosophila. Nature *332*, 853–856.

Friggi-Grelin, F., Coulom, H., Meller, M., Gomez, D., Hirsh, J., and Birman, S. (2003). Targeted gene expression in Drosophila dopaminergic cells using regulatory sequences from tyrosine hydroxylase. Journal of Neurobiology *54*, 618–627.

Fujita, M., and Tanimura, T. (2011). Drosophila Evaluates and Learns the Nutritional Value of Sugars. Current Biology *21*, 751–755.

Gao, Q., Yuan, B., and Chess, A. (2000). Convergent projections of Drosophila olfactory neurons to specific glomeruli in the antennal lobe. Nat. Neurosci. *3*, 780–785.

Gao, R., Asano, S.M., Upadhyayula, S., Pisarev, I., Milkie, D.E., Liu, T.-L., Singh, V., Graves, A., Huynh, G.H., Zhao, Y., et al. (2019). Cortical column and whole-brain imaging with molecular contrast and nanoscale resolution. Science *363*.

Gilestro, G.F., Tononi, G., and Cirelli, C. (2009). Widespread Changes in Synaptic Markers as a Function of Sleep and Wakefulness in Drosophila. Science *324*, 109–112.

Givon, L.E., and Lazar, A.A. (2016). Neurokernel: An Open Source Platform for Emulating the Fruit Fly Brain. PLOS ONE *11*, e0146581.

Gordon, M.D., and Scott, K. (2009). Motor Control in a Drosophila Taste Circuit. Neuron *61*, 373–384.

Govorunova, E.G., Sineshchekov, O.A., Janz, R., Liu, X., and Spudich, J.L. (2015). Natural light-gated anion channels: A family of microbial rhodopsins for advanced optogenetics. Science *349*, 647–650.

Grigliatti, T.A., Hall, L., Rosenbluth, R., and Suzuki, D.T. (1973). Temperature-sensitive mutations in Drosophila melanogaster. Molec. Gen. Genet. *120*, 107–114.

Grimes, W.N., Li, W., Chávez, A.E., and Diamond, J.S. (2009). BK channels modulate pre- and postsynaptic signaling at reciprocal synapses in retina. Nature Neuroscience *12*, 585–592.

Groh, C., Lu, Z., Meinertzhagen, I.A., and Rössler, W. (2012). Age-related plasticity in the synaptic ultrastructure of neurons in the mushroom body calyx of the adult honeybee Apis mellifera. J. Comp. Neurol. *520*, 3509–3527.

Gupta, V.K., Pech, U., Bhukel, A., Fulterer, A., Ender, A., Mauermann, S.F., Andlauer, T.F.M., Antwi-Adjei, E., Beuschel, C., Thriene, K., et al. (2016). Spermidine Suppresses Age-Associated Memory Impairment by Preventing Adverse Increase of Presynaptic Active Zone Size and Release. PLOS Biology *14*, e1002563.

Hancock, C.E., Bilz, F., and Fiala, A. (2019). In Vivo Optical Calcium Imaging of Learning-Induced Synaptic Plasticity in Drosophila melanogaster. J Vis Exp.

Harris, K.P., Akbergenova, Y., Cho, R.W., Baas-Thomas, M.S., and Littleton, J.T. (2016). Shank Modulates Postsynaptic Wnt Signaling to Regulate Synaptic Development. J. Neurosci. *36*, 5820–5832.

Hattori, D., Aso, Y., Swartz, K.J., Rubin, G.M., Abbott, L.F., and Axel, R. (2017). Representations of Novelty and Familiarity in a Mushroom Body Compartment. Cell *169*, 956-969.e17.

Heisenberg, M. (2003). Mushroom body memoir: from maps to models. Nature Reviews Neuroscience *4*, 266–275.

Heisenberg, M., Borst, A., Wagner, S., and Byers, D. (1985). Drosophila Mushroom Body Mutants are Deficient in Olfactory Learning. Journal of Neurogenetics *2*, 1–30.

Heisenberg, M., Heusipp, M., and Wanke, C. (1995). Structural plasticity in the Drosophila brain. J. Neurosci. *15*, 1951–1960.

Hensch, T.K. (2004). Critical period regulation. Annu. Rev. Neurosci. *27*, 549–579.

Hergarden, A.C., Tayler, T.D., and Anderson, D.J. (2012). Allatostatin-A neurons inhibit feeding behavior in adult Drosophila. Proc. Natl. Acad. Sci. U.S.A. *109*, 3967–3972.

Hering, H., and Sheng, M. (2003). Activity-Dependent Redistribution and Essential Role of Cortactin in Dendritic Spine Morphogenesis. J. Neurosci. *23*, 11759–11769.

Hige, T. (2018). What can tiny mushrooms in fruit flies tell us about learning and memory? Neuroscience Research *129*, 8–16.

Hige, T., Aso, Y., Modi, M.N., Rubin, G.M., and Turner, G.C. (2015). Heterosynaptic Plasticity Underlies Aversive Olfactory Learning in Drosophila. Neuron *88*, 985–998.

Hochachka, P.W., and Somero, G.N. (2002). Biochemical Adaptation: Mechanism and Process in Physiological Evolution (Oxford University Press).

Huetteroth, W., Perisse, E., Lin, S., Klappenbach, M., Burke, C., and Waddell, S. (2015). Sweet Taste and Nutrient Value Subdivide Rewarding Dopaminergic Neurons in Drosophila. Current Biology *25*, 751–758.

Hull, C.L. (1951). Essentials of behavior (New Haven, CT, US: Yale University Press).

Inagaki, H.K., Panse, K.M., and Anderson, D.J. (2014). Independent, Reciprocal Neuromodulatory Control of Sweet and Bitter Taste Sensitivity during Starvation in Drosophila. Neuron *84*, 806–820.

Ismail, N., Robinson, G.E., and Fahrbach, S.E. (2006). Stimulation of muscarinic receptors mimics experience-dependent plasticity in the honey bee brain. Proc. Natl. Acad. Sci. U.S.A. *103*, 207–211.

Ja, W.W., Carvalho, G.B., Mak, E.M., Rosa, N.N. de la, Fang, A.Y., Liong, J.C., Brummel, T., and Benzer, S. (2007). Prandiology of Drosophila and the CAFE assay. PNAS *104*, 8253–8256.

Joiner, W.J., Crocker, A., White, B.H., and Sehgal, A. (2006). Sleep in Drosophila is regulated by adult mushroom bodies. Nature *441*, 757–760.

Jourjine, N., Mullaney, B.C., Mann, K., and Scott, K. (2016). Coupled Sensing of Hunger and Thirst Signals Balances Sugar and Water Consumption. Cell *166*, 855–866.

Keleman, K., Krüttner, S., Alenius, M., and Dickson, B.J. (2007). Function of the Drosophila CPEB protein Orb2 in long-term courtship memory. Nature Neuroscience *10*, 1587–1593.

Kennedy, J.S. (1987). Animal Motivation: The Beginning of the End? In Perspectives in Chemoreception and Behavior, R.F. Chapman, E.A. Bernays, and J.G. Stoffolano, eds. (New York, NY: Springer), pp. 17–31.

Kim, H., Kirkhart, C., and Scott, K. (2017). Long-range projection neurons in the taste circuit of Drosophila. ELife *6*, e23386.

Kim, J.-H., Udo, H., Li, H.-L., Youn, T.Y., Chen, M., Kandel, E.R., and Bailey, C.H. (2003). Presynaptic Activation of Silent Synapses and Growth of New Synapses Contribute to Intermediate and Long-Term Facilitation in Aplysia. Neuron *40*, 151–165.

Kim, Y.-C., Lee, H.-G., and Han, K.-A. (2007). D1 Dopamine Receptor dDA1 Is Required in the Mushroom Body Neurons for Aversive and Appetitive Learning in Drosophila. J. Neurosci. *27*, 7640–7647.

Kitamoto, T. (2001). Conditional modification of behavior in Drosophila by targeted expression of a temperature-sensitive shibire allele in defined neurons. Journal of Neurobiology *47*, 81–92.

Klapoetke, N.C., Murata, Y., Kim, S.S., Pulver, S.R., Birdsey-Benson, A., Cho, Y.K., Morimoto, T.K., Chuong, A.S., Carpenter, E.J., Tian, Z., et al. (2014). Independent optical excitation of distinct neural populations. Nature Methods *11*, 338–346.

Ko, K.I., Root, C.M., Lindsay, S.A., Zaninovich, O.A., Shepherd, A.K., Wasserman, S.A., Kim, S.M., and Wang, J.W. (2015). Starvation promotes concerted modulation of appetitive olfactory behavior via parallel neuromodulatory circuits. ELife *4*, e08298.

Koon, A.C., and Budnik, V. (2012). Inhibitory Control of Synaptic and Behavioral Plasticity by Octopaminergic Signaling. J. Neurosci. *32*, 6312–6322.

Koon, A.C., Ashley, J., Barria, R., DasGupta, S., Brain, R., Waddell, S., Alkema, M.J., and Budnik, V. (2011). Autoregulatory and paracrine control of synaptic and behavioral plasticity by octopaminergic signaling. Nature Neuroscience *14*, 190–199.

Krashes, M.J., and Waddell, S. (2008). Rapid Consolidation to a radish and Protein Synthesis-Dependent Long-Term Memory after Single-Session Appetitive Olfactory Conditioning in Drosophila. J. Neurosci. *28*, 3103–3113.

Krashes, M.J., Keene, A.C., Leung, B., Armstrong, J.D., and Waddell, S. (2007). Sequential Use of Mushroom Body Neuron Subsets during Drosophila Odor Memory Processing. Neuron *53*, 103–115.

Krashes, M.J., DasGupta, S., Vreede, A., White, B., Armstrong, J.D., and Waddell, S. (2009). A Neural Circuit Mechanism Integrating Motivational State with Memory Expression in Drosophila. Cell *139*, 416–427.

Kremer, M.C., Christiansen, F., Leiss, F., Paehler, M., Knapek, S., Andlauer, T.F.M., Förstner, F., Kloppenburg, P., Sigrist, S.J., and Tavosanis, G. (2010). Structural long-term changes at mushroom body input synapses. Curr. Biol. *20*, 1938–1944.

Krofczik, S., Khojasteh, U., de Ibarra, N.H., and Menzel, R. (2008). Adaptation of microglomerular complexes in the honeybee mushroom body lip to manipulations of behavioral maturation and sensory experience. Dev Neurobiol *68*, 1007–1017.

Lai, S.-L., and Lee, T. (2006). Genetic mosaic with dual binary transcriptional systems in Drosophila. Nature Neuroscience *9*, 703–709.

Laissue, P.P., and Vosshall, L.B. (2008). The olfactory sensory map in Drosophila. Adv. Exp. Med. Biol. *628*, 102–114.

Lamprecht, R., and LeDoux, J. (2004). Structural plasticity and memory. Nature Reviews Neuroscience *5*, 45–54.

Larsen, M.J., Burton, K.J., Zantello, M.R., Smith, V.G., Lowery, D.L., and Kubiak, T.M. (2001). Type A Allatostatins from Drosophila melanogaster and Diplotera puncata Activate Two Drosophila Allatostatin Receptors, DAR-1 and DAR-2, Expressed in CHO Cells. Biochemical and Biophysical Research Communications *286*, 895–901.

Lechner, H.A.E., Lein, E.S., and Callaway, E.M. (2002). A Genetic Method for Selective and Quickly Reversible Silencing of Mammalian Neurons. J. Neurosci. *22*, 5287–5290.

LeDue, E.E., Mann, K., Koch, E., Chu, B., Dakin, R., and Gordon, M.D. (2016). Starvation-Induced Depotentiation of Bitter Taste in Drosophila. Current Biology *26*, 2854–2861.

Lee, G., and Park, J.H. (2004). Hemolymph Sugar Homeostasis and Starvation-Induced Hyperactivity Affected by Genetic Manipulations of the Adipokinetic Hormone-Encoding Gene in Drosophila melanogaster. Genetics *167*, 311–323.

Lee, K.P., Kim, J.-S., and Min, K.-J. (2013). Sexual dimorphism in nutrient intake and life span is mediated by mating in Drosophila melanogaster. Animal Behaviour *86*, 987–992.

Lee, K.-S., You, K.-H., Choo, J.-K., Han, Y.-M., and Yu, K. (2004). Drosophila Short Neuropeptide F Regulates Food Intake and Body Size. J. Biol. Chem. *279*, 50781–50789.

Lewis, L.P.C., Siju, K.P., Aso, Y., Friedrich, A.B., Bulteel, A.J.B., Rubin, G.M., and Grunwald Kadow, I.C. (2015). A Higher Brain Circuit for Immediate Integration of Conflicting Sensory Information in Drosophila. Current Biology *25*, 2203–2214.

Li, Y., Zhou, Z., Zhang, X., Tong, H., Li, P., Zhang, Z.C., Jia, Z., Xie, W., and Han, J. (2013). Drosophila Neuroligin 4 Regulates Sleep through Modulating GABA Transmission. J. Neurosci. *33*, 15545–15554.

Lihoreau, M., Poissonnier, L.-A., Isabel, G., and Dussutour, A. (2016). Drosophila females trade off good nutrition with high-quality oviposition sites when choosing foods. Journal of Experimental Biology *219*, 2514–2524.

Lin, S., Senapati, B., and Tsao, C.-H. Neural basis of hunger-driven behaviour in Drosophila. Open Biology *9*, 180259.

Liu, C., Plaçais, P.-Y., Yamagata, N., Pfeiffer, B.D., Aso, Y., Friedrich, A.B., Siwanowicz, I., Rubin, G.M., Preat, T., and Tanimoto, H. (2012). A subset of dopamine neurons signals reward for odour memory in Drosophila. Nature *488*, 512–516.

Liu, L., Wolf, R., Ernst, R., and Heisenberg, M. (1999). Context generalization in Drosophila visual learning requires the mushroom bodies. Nature *400*, 753–756.

Liu, Q., Tabuchi, M., Liu, S., Kodama, L., Horiuchi, W., Daniels, J., Chiu, L., Baldoni, D., and Wu, M.N. (2017). Branch-specific plasticity of a bifunctional dopamine circuit encodes protein hunger. Science *356*, 534–539.

Louis, T., Stahl, A., Boto, T., and Tomchik, S.M. (2018). Cyclic AMP-dependent plasticity underlies rapid changes in odor coding associated with reward learning. PNAS *115*, E448–E457.

Luckinbill, L.S., Arking, R., Clare, M.J., Cirocco, W.C., and Buck, S.A. (1984). Selection for Delayed Senescence in Drosophila Melanogaster. Evolution *38*, 996–1003.

Macpherson, L.J., Zaharieva, E.E., Kearney, P.J., Alpert, M.H., Lin, T.-Y., Turan, Z., Lee, C.-H., and Gallio, M. (2015). Dynamic labelling of neural connections in multiple colours by trans-synaptic fluorescence complementation. Nature Communications *6*, 1–9.

Mann, K., Gordon, M.D., and Scott, K. (2013). A Pair of Interneurons Influences the Choice between Feeding and Locomotion in Drosophila. Neuron *79*, 754–765.

Mao, Z., and Davis, R.L. (2009). Eight different types of dopaminergic neurons innervate the Drosophila mushroom body neuropil: anatomical and physiological heterogeneity. Front. Neural Circuits *3*.

Marder, E. (2012). Neuromodulation of Neuronal Circuits: Back to the Future. Neuron *76*, 1–11.

Martelli, C., Pech, U., Kobbenbring, S., Pauls, D., Bahl, B., Sommer, M.V., Pooryasin, A., Barth, J., Arias, C.W.P., Vassiliou, C., et al. (2017). SIFamide Translates Hunger Signals into Appetitive and Feeding Behavior in Drosophila. Cell Rep *20*, 464–478.

Martin, J.R., Ernst, R., and Heisenberg, M. (1998). Mushroom bodies suppress locomotor activity in Drosophila melanogaster. Learn. Mem. *5*, 179–191.

Masuyama, K., Zhang, Y., Rao, Y., and Wang, J.W. (2012). Mapping Neural Circuits with Activity-Dependent Nuclear Import of a Transcription Factor. J Neurogenet *26*, 89–102.

McBride, S.M.J., Giuliani, G., Choi, C., Krause, P., Correale, D., Watson, K., Baker, G., and Siwicki, K.K. (1999). Mushroom Body Ablation Impairs Short-Term Memory and Long-Term Memory of Courtship Conditioning in Drosophila melanogaster. Neuron *24*, 967–977.

McDonald, D.M., and Keene, A.C. (2010). The sleep-feeding conflict: Understanding behavioral integration through genetic analysis in Drosophila. Aging (Albany NY) *2*, 519–522.

McGuire, S.E., Le, P.T., and Davis, R.L. (2001). The Role of Drosophila Mushroom Body Signaling in Olfactory Memory. Science *293*, 1330–1333.

Melcher, C., and Pankratz, M.J. (2005). Candidate Gustatory Interneurons Modulating Feeding Behavior in the Drosophila Brain. PLOS Biology *3*, e305.

Min, K.-J., and Tatar, M. (2006). Restriction of amino acids extends lifespan in Drosophila melanogaster. Mechanisms of Ageing and Development *127*, 643–646.

Mobbs, D., Trimmer, P.C., Blumstein, D.T., and Dayan, P. (2018). Foraging for foundations in decision neuroscience: insights from ethology. Nature Reviews Neuroscience *19*, 419–427.

Mohammad, F., Stewart, J.C., Ott, S., Chlebikova, K., Chua, J.Y., Koh, T.-W., Ho, J., and Claridge-Chang, A. (2017). Optogenetic inhibition of behavior with anion channelrhodopsins. Nat. Methods *14*, 271–274.

Murakami, M., Kashiwadani, H., Kirino, Y., and Mori, K. (2005). State-Dependent Sensory Gating in Olfactory Cortex. Neuron *46*, 285–296.

Musso, P.-Y., Tchenio, P., and Preat, T. (2015). Delayed Dopamine Signaling of Energy Level Builds Appetitive Long-Term Memory in Drosophila. Cell Reports *10*, 1023–1031.

Nagel, G., Szellas, T., Huhn, W., Kateriya, S., Adeishvili, N., Berthold, P., Ollig, D., Hegemann, P., and Bamberg, E. (2003). Channelrhodopsin-2, a directly light-gated cation-selective membrane channel. PNAS *100*, 13940–13945.

Ni, J.D., Gurav, A.S., Liu, W., Ogunmowo, T.H., Hackbart, H., Elsheikh, A., Verdegaal, A.A., and Montell, C. (2019). Differential regulation of the Drosophila sleep homeostat by circadian and arousal inputs. ELife *8*, e40487.

Nicolaï, L.J.J., Ramaekers, A., Raemaekers, T., Drozdzecki, A., Mauss, A.S., Yan, J., Landgraf, M., Annaert, W., and Hassan, B.A. (2010). Genetically encoded dendritic marker sheds light on neuronal connectivity in Drosophila. Proc Natl Acad Sci U S A *107*, 20553–20558.

OROZCO-terWENGEL, P., Kapun, M., Nolte, V., Kofler, R., Flatt, T., and Schlötterer, C. (2012). Adaptation of Drosophila to a novel laboratory environment reveals temporally heterogeneous trajectories of selected alleles. Molecular Ecology *21*, 4931–4941.

Owald, D., Felsenberg, J., Talbot, C.B., Das, G., Perisse, E., Huetteroth, W., and Waddell, S. (2015). Activity of Defined Mushroom Body Output Neurons Underlies Learned Olfactory Behavior in Drosophila. Neuron *86*, 417–427.

Partridge, L., and Farquhar, M. (1981). Sexual activity reduces lifespan of male fruitflies. Nature *294*, 580–582.

Partridge, L., Green, A., and Fowler, K. (1987). Effects of egg-production and of exposure to males on female survival in Drosophila melanogaster. Journal of Insect Physiology *33*, 745–749.

Pech, U., Dipt, S., Barth, J., Singh, P., Jauch, M., Thum, A.S., Fiala, A., and Riemensperger, T. (2013). Mushroom body miscellanea: transgenic Drosophila strains expressing anatomical and physiological sensor proteins in Kenyon cells. Front Neural Circuits *7*, 147.

Pech, U., Revelo, N.H., Seitz, K.J., Rizzoli, S.O., and Fiala, A. (2015a). Optical dissection of experience-dependent pre- and postsynaptic plasticity in the Drosophila brain. Cell Rep *10*, 2083–2095.

Pech, U., Revelo, N.H., Seitz, K.J., Rizzoli, S.O., and Fiala, A. (2015b). Optical Dissection of Experience-Dependent Pre- and Postsynaptic Plasticity in the Drosophila Brain. Cell Reports *10*, 2083–2095.

Perisse, E., Yin, Y., Lin, A.C., Lin, S., Huetteroth, W., and Waddell, S. (2013). Different Kenyon Cell Populations Drive Learned Approach and Avoidance in Drosophila. Neuron *79*, 945–956.

Pitman, J.L., McGill, J.J., Keegan, K.P., and Allada, R. (2006). A dynamic role for the mushroom bodies in promoting sleep in Drosophila. Nature *441*, 753–756.

Pitman, J.L., DasGupta, S., Krashes, M.J., Leung, B., Perrat, P.N., and Waddell, S. (2009). There are many ways to train a fly. Fly *3*, 3–9.

Pool, A.-H., and Scott, K. (2014). Feeding regulation in Drosophila. Current Opinion in Neurobiology *29*, 57–63.

Potter, C.J., Tasic, B., Russler, E.V., Liang, L., and Luo, L. (2010). The Q System: A Repressible Binary System for Transgene Expression, Lineage Tracing, and Mosaic Analysis. Cell *141*, 536–548.

Qin, H., Cressy, M., Li, W., Coravos, J.S., Izzi, S.A., and Dubnau, J. (2012). Gamma Neurons Mediate Dopaminergic Input during Aversive Olfactory Memory Formation in Drosophila. Current Biology *22*, 608–614.

Ribeiro, C., and Dickson, B.J. (2010). Sex Peptide Receptor and Neuronal TOR/S6K Signaling Modulate Nutrient Balancing in Drosophila. Current Biology *20*, 1000–1005.

Riemensperger, T., Völler, T., Stock, P., Buchner, E., and Fiala, A. (2005). Punishment Prediction by Dopaminergic Neurons in Drosophila. Current Biology *15*, 1953–1960.

Riemensperger, T., Issa, A.-R., Pech, U., Coulom, H., Nguyễn, M.-V., Cassar, M., Jacquet, M., Fiala, A., and Birman, S. (2013). A Single Dopamine Pathway Underlies Progressive Locomotor Deficits in a Drosophila Model of Parkinson Disease. Cell Reports *5*, 952–960.

Rohwedder, A., Wenz, N.L., Stehle, B., Huser, A., Yamagata, N., Zlatic, M., Truman, J.W., Tanimoto, H., Saumweber, T., Gerber, B., et al. (2016). Four Individually Identified Paired Dopamine Neurons Signal Reward in Larval Drosophila. Current Biology *26*, 661–669.

Root, C.M., Ko, K.I., Jafari, A., and Wang, J.W. (2011). Presynaptic Facilitation by Neuropeptide Signaling Mediates Odor-Driven Food Search. Cell *145*, 133–144.

Roy, B., Singh, A.P., Shetty, C., Chaudhary, V., North, A., Landgraf, M., VijayRaghavan, K., and Rodrigues, V. (2007). Metamorphosis of an identified serotonergic neuron in the Drosophila olfactory system. Neural Dev *2*, 20.

Rubin, G.M. (1985). P transposable elements and their use as genetic tools in drosophila. Trends in Neurosciences *8*, 231–233.

Rulifson, E.J., Kim, S.K., and Nusse, R. (2002). Ablation of Insulin-Producing Neurons in Flies: Growth and Diabetic Phenotypes. Science *296*, 1118–1120.

Sayin, S., De Backer, J.-F., Siju, K.P., Wosniack, M.E., Lewis, L.P., Frisch, L.-M., Gansen, B., Schlegel, P., Edmondson-Stait, A., Sharifi, N., et al. (2019). A Neural Circuit Arbitrates between Persistence and Withdrawal in Hungry Drosophila. Neuron *104*, 544-558.e6.

Scholz, M., Dinner, A.R., Levine, E., and Biron, D. (2017). Stochastic feeding dynamics arise from the need for information and energy. PNAS *114*, 9261–9266.

Schoofs, A., Hückesfeld, S., Schlegel, P., Miroschnikow, A., Peters, M., Zeymer, M., Spieß, R., Chiang, A.-S., and Pankratz, M.J. (2014). Selection of Motor Programs for Suppressing Food Intake and Inducing Locomotion in the Drosophila Brain. PLOS Biology *12*, e1001893.

Schroll, C., Riemensperger, T., Bucher, D., Ehmer, J., Völler, T., Erbguth, K., Gerber, B., Hendel, T., Nagel, G., Buchner, E., et al. (2006). Light-Induced Activation of Distinct Modulatory Neurons Triggers Appetitive or Aversive Learning in Drosophila Larvae. Current Biology *16*, 1741–1747.

Schulz, R.A., Chromey, C., Lu, M.F., Zhao, B., and Olson, E.N. (1996). Expression of the D-MEF2 transcription in the Drosophila brain suggests a role in neuronal cell differentiation. Oncogene *12*, 1827–1831.

Schwaerzel, M., Heisenberg, M., and Zars, T. (2002). Extinction Antagonizes Olfactory Memory at the Subcellular Level. Neuron *35*, 951–960.

Shao, L., Saver, M., Chung, P., Ren, Q., Lee, T., Kent, C.F., and Heberlein, U. (2017). Dissection of the Drosophila neuropeptide F circuit using a high-throughput two-choice assay. PNAS *114*, E8091–E8099.

Shinomiya, K., Matsuda, K., Oishi, T., Otsuna, H., and Ito, K. (2011). Flybrain neuron database: a comprehensive database system of the Drosophila brain neurons. J. Comp. Neurol. *519*, 807–833.

Sigrist, S.J., Reiff, D.F., Thiel, P.R., Steinert, J.R., and Schuster, C.M. (2003). Experience-Dependent Strengthening of Drosophila Neuromuscular Junctions. J. Neurosci. *23*, 6546–6556.

Sih, A. (1980). Optimal behavior: can foragers balance two conflicting demands? Science *210*, 1041–1043.

Singh, A.P., VijayRaghavan, K., and Rodrigues, V. (2010). Dendritic refinement of an identified neuron in the Drosophila CNS is regulated by neuronal activity and Wnt signaling. Development *137*, 1351–1360.

Stierl, M., Stumpf, P., Udwari, D., Gueta, R., Hagedorn, R., Losi, A., Gärtner, W., Petereit, L., Efetova, M., Schwarzel, M., et al. (2011). Light Modulation of Cellular cAMP by a Small Bacterial Photoactivated Adenylyl Cyclase, bPAC, of the Soil Bacterium Beggiatoa. J. Biol. Chem. *286*, 1181–1188.

Strausfeld, N.J., Hansen, L., Li, Y., Gomez, R.S., and Ito, K. (1998). Evolution, Discovery, and Interpretations of Arthropod Mushroom Bodies. Learn. Mem. *5*, 11–37.

Symons, D. (1990). Adaptiveness and adaptation. Ethology and Sociobiology *11*, 427–444.

Talay, M., Richman, E.B., Snell, N.J., Hartmann, G.G., Fisher, J.D., Sorkaç, A., Santoyo, J.F., Chou-Freed, C., Nair, N., Johnson, M., et al. (2017). Transsynaptic Mapping of Second-Order Taste Neurons in Flies by trans-Tango. Neuron *96*, 783-795.e4.

Tanaka, N.K., Tanimoto, H., and Ito, K. (2008). Neuronal assemblies of the Drosophila mushroom body. J. Comp. Neurol. *508*, 711–755.

Tang, S., and Guo, A. (2001). Choice Behavior of Drosophila Facing Contradictory Visual Cues. Science *294*, 1543–1547.

Tao-Cheng, J.-H., Thein, S., Yang, Y., Reese, T.S., and Gallant, P.E. (2014). Homer is concentrated at the postsynaptic density and does not redistribute after acute synaptic stimulation. Neuroscience *266*, 80–90.

Technau, G.M. (1984). Fiber Number in the Mushroom Bodies of Adult Drosophila melanogaster depends on Age, Sex and Experience. Journal of Neurogenetics *1*, 113–126.

Technau, G., and Heisenberg, M. (1982). Neural reorganization during metamorphosis of the corpora pedunculata in Drosophila melanogaster. Nature *295*, 405–407.

Tempel, B.L., Bonini, N., Dawson, D.R., and Quinn, W.G. (1983). Reward learning in normal and mutant Drosophila. PNAS *80*, 1482–1486.

Tessier, C.R., and Broadie, K. (2008). Drosophila fragile X mental retardation protein developmentally regulates activity-dependent axon pruning. Development *135*, 1547–1557.

Thorpe, W.H. (1956). Learning and instinct in animals (Cambridge, MA, US: Harvard University Press).

Tian, L., Hires, S.A., Mao, T., Huber, D., Chiappe, M.E., Chalasani, S.H., Petreanu, L., Akerboom, J., McKinney, S.A., Schreiter, E.R., et al. (2009). Imaging neural activity in worms, flies and mice with improved GCaMP calcium indicators. Nature Methods *6*, 875–881.

Toates, F.M. (1986). Motivational Systems (CUP Archive).

Tolman, E.C. (1949). Purposive Behavior in Animals and Men (University of California Press).

Tripodi, M., Evers, J.F., Mauss, A., Bate, M., and Landgraf, M. (2008). Structural Homeostasis: Compensatory Adjustments of Dendritic Arbor Geometry in Response to Variations of Synaptic Input. PLOS Biology *6*, e260.

Trombley, P.Q., and Shepherd, G.M. (1993). Synaptic transmission and modulation in the olfactory bulb. Current Opinion in Neurobiology *3*, 540–547.

Tsao, C.-H., Chen, C.-C., Lin, C.-H., Yang, H.-Y., and Lin, S. (2018). Drosophila mushroom bodies integrate hunger and satiety signals to control innate food-seeking behavior. ELife *7*, e35264.

Tu, J.C., Xiao, B., Naisbitt, S., Yuan, J.P., Petralia, R.S., Brakeman, P., Doan, A., Aakalu, V.K., Lanahan, A.A., Sheng, M., et al. (1999). Coupling of mGluR/Homer and PSD-95 complexes by the Shank family of postsynaptic density proteins. Neuron *23*, 583–592.

Tully, T., and Quinn, W.G. (1985). Classical conditioning and retention in normal and mutantDrosophila melanogaster. J. Comp. Physiol. *157*, 263–277.

Ukani, N.H., Yeh, C.-H., Tomkins, A., Zhou, Y., Florescu, D., Ortiz, C.L., Huang, Y.-C., Wang, C.-T., Turkcan, M.K., Liu, T., et al. (2019). The Fruit Fly Brain Observatory: From Structure to Function. BioRxiv 580290.

Urizar, N.L., Yang, Z., Edenberg, H.J., and Davis, R.L. (2007). Drosophila Homer Is Required in a Small Set of Neurons Including the Ellipsoid Body for Normal Ethanol Sensitivity and Tolerance. J. Neurosci. *27*, 4541–4551.

del Valle Rodríguez, A., Didiano, D., and Desplan, C. (2012). Power tools for gene expression and clonal analysis in Drosophila. Nature Methods *9*, 47–55.

Vargas, M.A., Luo, N., Yamaguchi, A., and Kapahi, P. (2010). A Role for S6 Kinase and Serotonin in Postmating Dietary Switch and Balance of Nutrients in D. melanogaster. Current Biology *20*, 1006–1011.

Vasmer, D. (2017). Morphological Analysis of Kenyon Cells of the Drosophila Mushroom Bodies.

Vié, A., Cigna, M., Toci, R., and Birman, S. (1999). Differential Regulation of Drosophila Tyrosine Hydroxylase Isoforms by Dopamine Binding and cAMP-dependent Phosphorylation. J. Biol. Chem. *274*, 16788–16795.

Vosshall, L.B. (2000). Olfaction in Drosophila. Current Opinion in Neurobiology *10*, 498–503.

Waddell, S. (2013). Reinforcement signalling in Drosophila; dopamine does it all after all. Curr. Opin. Neurobiol. *23*, 324–329.

Waddell, S. (2016). Neural Plasticity: Dopamine Tunes the Mushroom Body Output Network. Curr. Biol. *26*, R109-112.

Waddell, S., Armstrong, J.D., Kitamoto, T., Kaiser, K., and Quinn, W.G. (2000). The amnesiac Gene Product Is Expressed in Two Neurons in the Drosophila Brain that Are Critical for Memory. Cell *103*, 805–813.

Wagh, D.A., Rasse, T.M., Asan, E., Hofbauer, A., Schwenkert, I., Dürrbeck, H., Buchner, S., Dabauvalle, M.-C., Schmidt, M., Qin, G., et al. (2006). Bruchpilot, a protein with homology to ELKS/CAST, is required for structural integrity and function of synaptic active zones in Drosophila. Neuron *49*, 833–844.

Wang, Q.-P., Lin, Y.Q., Zhang, L., Wilson, Y.A., Oyston, L.J., Cotterell, J., Qi, Y., Khuong, T.M., Bakhshi, N., Planchenault, Y., et al. (2016). Sucralose Promotes Food Intake through NPY and a Neuronal Fasting Response. Cell Metabolism *24*, 75–90.

Wang, Z., Singhvi, A., Kong, P., and Scott, K. (2004). Taste representations in the Drosophila brain. Cell *117*, 981–991.

Werner, E.E. (1992). Individual Behavior and Higher-Order Species Interactions. The American Naturalist *140*, S5–S32.

Wolf, R., Wittig, T., Liu, L., Wustmann, G., Eyding, D., and Heisenberg, M. (1998). Drosophila Mushroom Bodies Are Dispensable for Visual, Tactile, and Motor Learning. Learning & Memory *5*, 166–178.

Wong, R.O.L., and Ghosh, A. (2002). Activity-dependent regulation of dendritic growth and patterning. Nat. Rev. Neurosci. *3*, 803–812.

Wu, Q., Wen, T., Lee, G., Park, J.H., Cai, H.N., and Shen, P. (2003). Developmental Control of Foraging and Social Behavior by the Drosophila Neuropeptide Y-like System. Neuron *39*, 147–161.

Yamagata, N., Hiroi, M., Kondo, S., Abe, A., and Tanimoto, H. (2016). Suppression of Dopamine Neurons Mediates Reward. PLoS Biol *14*.

Yang, C., Belawat, P., Hafen, E., Jan, L.Y., and Jan, Y.-N. (2008). Drosophila Egg-Laying Site Selection as a System to Study Simple Decision-Making Processes. Science *319*, 1679–1683.

Yang, Z., Yu, Y., Zhang, V., Tian, Y., Qi, W., and Wang, L. (2015). Octopamine mediates starvation-induced hyperactivity in adult Drosophila. Proc. Natl. Acad. Sci. U.S.A. *112*, 5219–5224.

Yeh, E., Gustafson, K., and Boulianne, G.L. (1995). Green fluorescent protein as a vital marker and reporter of gene expression in Drosophila. Proc. Natl. Acad. Sci. U.S.A. *92*, 7036–7040.

Youn, H., Kirkhart, C., Chia, J., and Scott, K. (2018). A subset of octopaminergic neurons that promotes feeding initiation in Drosophila melanogaster. PLOS ONE *13*, e0198362.

Yu, Y., Huang, R., Ye, J., Zhang, V., Wu, C., Cheng, G., Jia, J., and Wang, L. (2016). Regulation of starvation-induced hyperactivity by insulin and glucagon signaling in adult Drosophila. ELife *5*, e15693.

Yuan, Q., Xiang, Y., Yan, Z., Han, C., Jan, L.Y., and Jan, Y.N. (2011). Light-Induced Structural and Functional Plasticity in Drosophila Larval Visual System. Science *333*, 1458–1462.

Zandawala, M., Yurgel, M.E., Texada, M.J., Liao, S., Rewitz, K.F., Keene, A.C., and Nässel, D.R. (2018). Modulation of Drosophila post-feeding physiology and behavior by the neuropeptide leucokinin. PLOS Genetics *14*, e1007767.

Zariwala, H.A., Borghuis, B.G., Hoogland, T.M., Madisen, L., Tian, L., De Zeeuw, C.I., Zeng, H., Looger, L.L., Svoboda, K., and Chen, T.-W. (2012). A Cre-dependent GCaMP3 reporter mouse for neuronal imaging in vivo. J. Neurosci. *32*, 3131–3141.

Zhang, Y., Guo, H., Kwan, H., Wang, J.-W., Kosek, J., and Lu, B. (2007). PAR-1 Kinase Phosphorylates Dlg and Regulates Its Postsynaptic Targeting at the Drosophila Neuromuscular Junction. Neuron *53*, 201–215.

Zhang, Y.Q., Rodesch, C.K., and Broadie, K. (2002). Living synaptic vesicle marker: Synaptotagmin-GFP. Genesis *34*, 142–145.

7 Appendix

7.1 Abbreviations

3-Oct	3-Octanol
4HT	4 hydroxy tempo
AcX	Acrylol-X
AKH	adipokinetic hormone
AL	anetnnal lobe
AMP	adenosine monophosphate
APS	amonium per sulfate
AstA	allatostatin A
ATR	all-trans retinal
AV	apple vinegar
AZ	active zone
bPAC	bacterial photoactivated adenylyl cyclase
Brp	burchpilot
BS	blocking solution
BSA	bovine serum albumin
CaCl2	calcium chloride
CAFE	capillary feeder
CaM	calmodulin
cAMP	cyclic AMP
ChR	channelrhodopsin
CNS	central nervous system
CS	conditioned stimulus
DA	dopamine
DACA	*drosophila* circadian analysis
DAN	dopaminergic Neuron
DenMark	dendritic marker
DILP	*drosophila* insulin-like peptide
Dlg	disclarge
DMSO	dimethyl sulfoxide

dNPF	*drosophila* neuropeptide F
EDTA	ethylenediaminetetraacetic acid
FMRP	fragile X mental retardation protein
GECI	genetically encoded Ca^{2+} indicators
GFP	green fluorescent protein
GPCR	G-protein Coupled receptor
GRASP	GFP reconstitution across synaptic partner
gtACR	*Guillardia theta* anion channelrhodopsin
HCl	hydrochloric acid
Hz	herz
IHC	immunohistochemistry
KC	kenyon cell
KCl	potassium chloride
LexAop	LexA operator
LH	lateral horn
LK	leucokinin
MB	mushroom body
MBON	mushroom body output neuron
MBS	MES buffered saline
MCH	4-methylcyclohexamide
MES	2-(N-Morpholino)ethanesulfonic acid
MgCl2	magnesium chloride
MIP	myoinhibitory peptides
NaCl	sodium chloride
NaH_2PO_4	monosodium phosphate
NaOH	sodium hydroxide
NE	norepinephrine
NPF	neuropeptide F
NPY	neuropeptide Y
OA	octopamine
PAM	protocerebral anterior medial
PBS	phosphate buffered saline
PBS-T	PBS-Trition X 100

PER	proboscis extension reflex
PFA	paraformaldehyde
PKA	protein kinase A
PN	projection neuron
PN	projection neurons
PPL	protocerebral poterior lateral
QUAS	QF upstream activating sequence
RFP	red fluorescent protein
ROI	region of interest
RT	room temperature
SD	standard deviation
SEM	standard error of mean
SEZ	sub-esophageal zone
Shi^{ts}	$shibire^{temperature\ sensitive}$
SIFa	SIFamide
sNPF	short neuropeptide F
spGal4	split Gal4
spGFP	splitGFP
syb	synaptobrevin
syp	synaptophysin
TEMED	tetramethylethylenediamine
TF	transcription factor
TH	tyrosine hydroxylase
ts	temperature sensitive
US	unconditioned stimulus

Acknowledgements

Initially, I would like to thank Prof. Dr. André Fiala for giving me the chance to work on this project and his supervision. This project would not be possible without his guidance and intellectual contributions. Additionally, this project was supported by the Volkswagen-Foundation (Niedersächsisches vorab; VWZN3014) and the Deutsche Forschungsgemeinschaft (SFB 889/2; 6700413) funds that is granted to Prof. Dr. André Fiala.

I also wanted to thank all the scientists contributed this study intellectually and physically by supplying materials. One of these scientist (and also my former second-supervisor) is Dr. Thomas Riemensperger. I always appreciate our scientific discussions and also his emotional support during the difficulties I encountered. Other scientist contributed to this study were undoubtably my thesis committee members; Prof Dr. Martin Göpfert and Prof. Dr. Thomas Dresbach. I am thankful for their critical comments during our meetings. I am also thankful them for always making me feel their support as a PhD student. I also would like to thank other examination board members; Prof. Dr. Carolin Wichmann, Dr. Jan Clemens, and Prof. Dr. Ralf Heinrich, for accepting to review my work and give their valuable idea on it. I would like to further thank Dr. Bart Guerten for his intellectual support, allowing me to use his experimental tools and set ups in my behavioral test, and helping me with the data analysis of some behavioral experiments. He was ready to help me whenever I needed without any doubt. Last but not least, I would like to thank Prof. Dr. Hiromu Tanimoto and Prof. Dr. Christian Wegener for the supplying the transgenic fly lines and antibodies. There are a number of scientist with whom I had fruitful scientific discussions about my projects during conferences and meetings. I would like to thank them all for their critics and intellectual contributions as well.

I would like to thank the current lab members; Dr. Annekathrin Widmann, Clare Hancock and Yazid El Yazid Rachad, for providing such a friendly and supporting environment. My colleagues were also there for me for intellectual contributions during working hours, and friendly supports outside of the work. I am especially thankful for Anne's energy and will to help, and for Clare's sense of humor and friendship. The other current lab members and also unknown heroes; Annegret Lattner and Jutta Böker, also deserve great appreciations. Jutta Böker was like a fairy making every lab equipment and solutions available with her magic wand. Also, Annegret Lattner was making every complicated paperwork possible to handle and always in time with a fantastic discipline. These two heroes always provided great positive energy under all conditions.

I should not skip the former lab members and also close friends of mine; Dr. Florian Bilz, Dr. Carlotta Martelli. Florian was always there to support me when I was experiencing the same kind of obstacles as a PhD student. I also appreciate his friendship and help outside of the work. Moreover, Carlotta was also one of my friends/colleagues who was always understanding and supporting. Especially as a woman scientist, she was one of my role models. As the last former lab members, I should also thank the students I supervised. They also supported my journey of PhD by learning and practicing together with me.

I would like to thank my family whose contributions were not smaller than my colleagues and friends. They always supported my work even though they wanted me closer. I appreciate my family for making my choices their priorities. Especially, the support of my father and my sister for me to be a scientist should be recognized.

I would like to thank my close friends Burak Bali and Serdar Capar who are also a scientist like myself. Their friendship and scientific supports kept (and are still keeping) me motivated since our Bachelor study together, even from other edges of the world.

Finally, my deepest and the most special thanks are for Haiko Poppinga who is not only my life partner, but also my closest friend, my colleague and my eternal love. If I can stand my ground and have hopes on humanity, it is all thanks to Haiko. Also, his intellectual and emotional support during my PhD journey was priceless.

Büşra Çoban-Poppinga

Home address:	Hermann-Rein Str. 8A, 37075 Göttingen / GERMANY
E mail:	busracoban29@gmail.com
Family status:	married
Nationality:	Turkish

Education

2016 - 2020	**Ph.D.** – Molecular Neurobiology of Behavior, Georg-August University of Göttingen, Sensory and Motor Neuroscience Doctoral Program
2013 - 2015	**M.Sc.** – Molecular Biology and Genetics, Bogazici University (study language-English)
2008 - 2013	**B.Sc.** – Molecular Biology and Genetics, Bogazici University (study language-English)

Laboratory experience

2016 February –	Ph.D. student of Prof. Dr. Andre Fiala's lab on *"Optophysiological analysis of experience-dependent plasticity in the Drosophila brain"* at Georg-August University, Göttingen
2013 September – 2015 August	Master student of Associated Professor Dr. Stefan H. Fuss's lab on "*Selective neurogenesis in zebrafish olfactory epithelium*" at Bogazici University, Istanbul
2014 June – 2014August	Summer school intern student of Dr Hokto Kazama on "*The circuit formation of olfactory sensory system in Drosophila antennal lobe*" at Riken Brain Science Institute, Tokyo
2012 February – 2013 September	Undergraduate researcher of Assistant Professor Dr. Stefan H. Fuss's lab on "*Mechanism of odorant receptor gene choice in zebrafish and neurogenesis in the olfactory epithelium"* at Bogazici University, Istanbul
2011 August	Undergraduate researcher of Professor Takashi Fujita's molecular genetics lab on "*Innate immune system against double stranded RNA viruses*" at The Institute for Virus Research of Kyoto University, Kyoto.

Awards & scholarships

2013 September – 2015 August	Graduate Science Scholarship by the Scientific and Technological Research Council of Turkey (TUBİTAK)

Posters & Talks

2014, 15-22 July	"Disentangling Mental Disorders from Genes to Circuits" at Riken BSI, Tokyo **(poster presentation)**
2014, 4-7 September	Turkish- German Molecular Neuroscience Workshop at Bogazici University, Istanbul **(as part of organization team)**
2014, 26-28 September	EMBO workshop, Decoding Neural Circuit Structure and Functions at Bogazici University, Istanbul **(poster presentation)**
2017, 11-12 May	16th meeting on "Development and Plasticity of the Nervous System of Insects", Marburg **(as speaker)**
2017, 2-4 June	Learning & Memory: a Synthesis of Bees and Flies, Aspet **(as speaker)**
2018, 27-29 March	ANN – Arthropod Neuroscience Network – Spring Meeting,2018, Altleiningen **(as speaker)**
2018, 3-7 September	17th European Drosophila Neurobiology Conference – Neurofly 2018, Krakow **(poster presentation)**
2019, 20-23 March	13th Göttingen Meeting of the German Neuroscience Society, Göttingen **(poster presentation)**
2019, 19-23 October	SFN – Society for Neuroscience 2019, San Diego **(poster presentation)**

Publications

2017	Niens, J., Reh, F., **Çoban, B**., Cichewicz, K., Eckardt, J., Liu, Y.-T., Hirsh, J., and Riemensperger, T.D. (2017). Dopamine Modulates Serotonin Innervation in the Drosophila Brain. Front. Syst. Neurosci. 11.